Bolted Flanged Connections with Full Face Gaskets

Kamal Naser

A Thesis
in
The Department
of
Mechanical Engineering

Presented in Partial Fulfilment of the Requirements
for the Degree of Master of Applied Science at
Concordia University
Montreal, Quebec, Canada

March 1995

ISBN 0-612-01355-3

Canada

TO

MY PARENTS, ALICE AND FAHIM, WHO ARE ALWAYS THEIR FOR ME.
AND MY WIFE , EMAN, FOR HER SUPPORT AND ENCOURAGEMENT.

ABSTRACT

Bolted flanged connections with full face gaskets were very popular when pipe and pressure vessel flanges were made in cast iron only. It was felt that such gaskets were necessary to limit the deflection of flanges made of brittle material. When steel replaced cast iron as the preferred material for piping and pressure vessel construction, full face gasketed flanges became unpopular, for the simple reason that metallic or composite gaskets could not be used for large seating areas because of limited bolt area in standard flanges.

Full face gasketed bolted flanged connections nevertheless remained popular, in particular, among low pressure applications in water works, paper mills, food industry, also for non-circular flanges which are difficult to seal with ring or strip gaskets.

In spite of the continuous use of such flanges, no design rules are contained in the ASME Boiler and Pressure Vessel Code.

In this thesis, full face gasketed bolted flanged connections are analyzed by implementing a design method that is similar to the ASME Code design method used in ring flanges. Results of the analysis are compared with existing simplified design procedures and with results from a series of experiments made on three different test pressure vessels. A finite element analysis is performed to explore the effect of a number of design parameters and results are used to propose a new design method for such flanges.

ACKNOWLEDGEMENTS

The author wishes to express his sincere appreciation to his supervisor, Dr. A. E. Blach, for his continuous support and guidance throughout the course of this research.

The author also wishes to thank faculty and staff of the mechanical engineering department at Concordia University, as well as his colleagues for all the help received.

TABLE OF CONTENTS

LIST OF FIGURES

LIST OF TABLES

NOMENCLATURE

a	Area
A	Flange outside diameter
A_b	Bolt area provided
b	Width of full face gasket
b	Effective width of ring gasket
B	Flange inside diameter
C	Bolt circle diameter
C_1 ... C_{15}	Dimensionless coefficients
D	Bolt hole diameter, flexural rigidity
D	Flexural rigidity
E	Modulus of elasticity, or Joint efficiency
E	Welding efficiency
E_G	Gasket modulus
F	Flange rotation force
g	Hub thickness
G	Effective gasket diameter
h_d	Moment arm for hydrostatic end force
h_g	Moment arm for gasket force, operation
h_{gs}	Moment arm for gasket force, bolt -up
h_t	Moment arm for hydrostatic force under gasket
H_d	Hydrostatic end force
H_g	Gasket compression force, operation
H_{gs}	Gasket compression force, gasket seating
H_t	Hydrostatic force under gasket
k	Constant related to stiffness
K	Ratio of outside to inside diameter of flange ring
K_1 ... K_5	Dimensionless coefficients

Continue Nomenclature

$\begin{Bmatrix} L_1 \\ . \\ . \\ L_g \end{Bmatrix}$	Dimensionless coefficients
M	Discontinuity moment
M1	Net total flange moment
M_B	Moment component due to bolt force
M_d	Moment due to hydrostatic end force
M_g	Moment due to gasket compression, operation
M_{gs}	Moment due to gasket compression in gasket seating
M_O	Flange operating moment
M_R	Radial flange moment
M_T	Moment due to hydrostatic force under the gasket
m	Gasket maintenance factor
n	Number of bolts
P	Internal pressure
Q	Discontinuity force
r	Radial coordinate
R	Radius
S_b	Allowable bolt stress, operation
S_{H1}	Longitudinal hub stress
S_{H2}	Tangential hub stress
S_R	Radial flange stress
S_T	Tangential flange stress
t	Flange thickness
t_G	Gasket thickness
u_S	Radial displacement, shell
u_f	Radial displacement, flange
V	Volume
W	Total bolt load on flange
W_{m1}	Bolt load, operation
W_{m2}	Bolt load, gasket seating
X	Radial coordinate
x_o	Location of centroid of differential area
x_1	Location of centroid of unit sector

y	Gasket seating stress
Y	Code flange parameter
Z	Axial coordinate
α	Gasket constant
β	Shell constant
γ	Flange constant
δ	Gasket displacement at outer edge
ϵ	Strain
ζ	Moment arm coefficient
θ	Rotation
θ_S	Shell rotation
θ_f	Flange rotation
υ	Poisson's ratio
σ	Stress
σ_g	Gasket compressive stress

CHAPTER ONE

INTRODUCTION

1.1 Scope of Work

Bolted flanged connections are widely employed in pressure containing apparatus, such as pressure vessels and pipes. They provide a convenient method of joining together pieces of equipment.

The analysis and design of bolted flange connections are governed by various pressure vessel rules and standards. In north America, for example, the ASME Boiler and Pressure Vessel Code is used. The code contains extensive procedures on the design of pressure vessel components, including rules for the design of a number of different circular and non-circular bolted flanges. The ASME Boiler and Pressure Vessel Code includes design procedures for ring type flanges and flanges with metal-to-metal contact beyond the bolt circle. No rules are provided for Flat Faced Flanges with Full Face Gaskets.

The objective of this thesis is to investigate the problem of full face gasketed bolted flanged connections, to evaluate the methods of analysis used at present, and to produce a simplified design method, which is based on the ASME Code criteria for flange design.

In order to do so the ASME Code method is briefly introduced, and related to the design problem of full face gasketed flanges. An analytical solution that is based on the theory of shells and plates is employed and verified through finite element analysis. Experimental testing is then employed to further verify the results. Finally a simplified design method that follows the analytical solution is presented.

1.2 Literature Review

A survey of the literature on bolted flanged connections gives little of interest prior to the first quarter of the present century. Before that time flanges were designed by a rule of thumb based on a good grade of grey cast iron from patterns that adhered dimensionally to traditional practice. What little analysis one finds was approximations from simple beam theory.

1.2.1 Early Methods

In 1891 Bach [1]*, in Germany, proposed the earliest method of calculations, to receive wide attention. In 1905, in the United States, the "Locomotive" Method [2], generally accredited to Dr. A.D.Risteen, was introduced. Bach's method assumes that bending is taking place on a section along a diameter of the flange. Circumferential stresses are then calculated by dividing the external moment by the section modulus of the whole section. The Locomotive method, on the other hand, considers the flange to be made up of sectors bent along a circumferential part of the hub. Both of these methods are based on the flexure of beams, and only tangential stresses are calculated.

* Numbers in square brackets [ ] refer to references.

An extension of Bach's method was proposed by Crocker [3]. In this method it is assumed that, for ring flanges, the ring is fixed at the base of the hub. It is equivalent to a cantilever beam with the load being distributed along a width equal to the circumference. This gives radial stresses near the hub, by dividing the bolt moment (W. a), by the section modulus ;

$Z' = \pi D.t^2/6$, as shown in Figure 1.

1.2.2 **Exact Methods**

None of the foregoing methods took into account all the conditions present in the flange, and only in 1927 Waters and Taylor [4] presented the first exact method based on the theory of a beam on an elastic foundation and the deflection of flat circular plates. A schematic diagram is shown in Figure 2. This method is based on a discontinuity analysis between a cylindrical shell and a flat circular plate with a central hole. It was the first instance in which the stress conditions in the three principal directions, tangential, radial and axial were explored. This method was included in the ASME Code [5] in 1934.

Timoshenko [6] later proposed a simplified version of this method in which he applied the theory of ring bending to the flange, as shown in Figure 2. This theory is based on the assumption that the flange thickness is

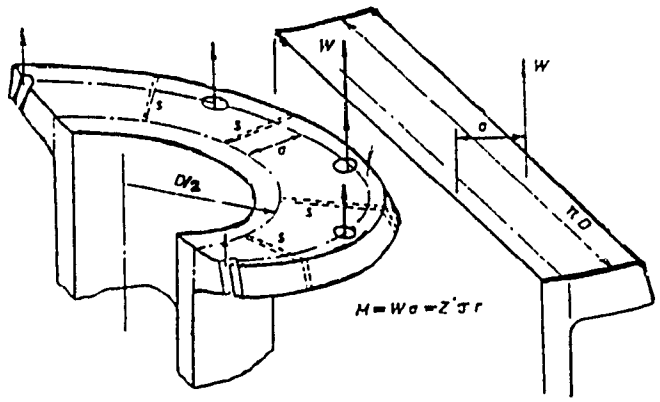

Figure 1: Beam Theory & Flange Design (Bach [1] & Crocker [3])

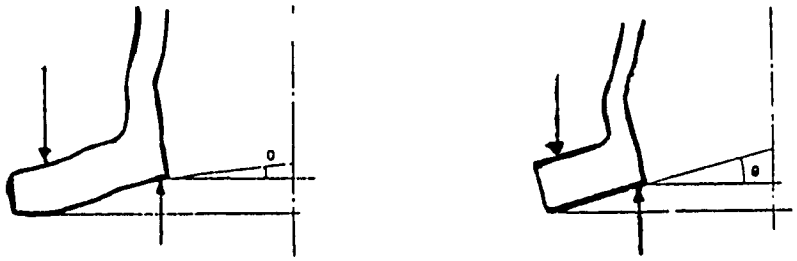

Plate Theory
Water & Taylor [4]

Ring Theory
Timoshenko[6]

Figure 2: Discontinuity Analysis

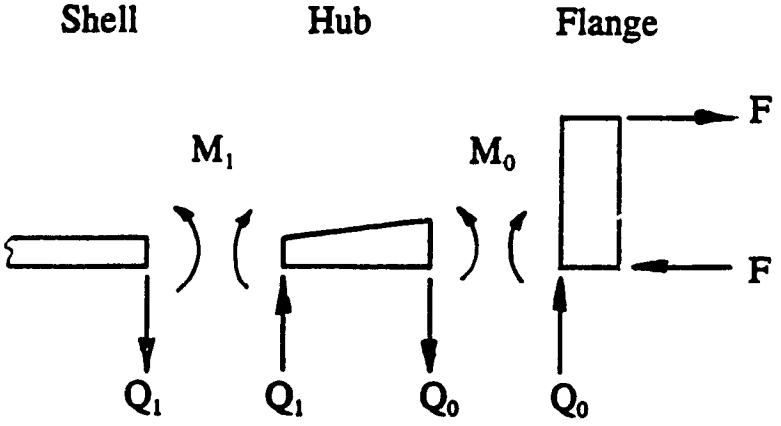

Figure 3: Taper Hub Analysis

much heavier than the thickness of the connecting hub, hence the rotation of a circular ring may advantageously be used instead of the more complex plate bending formulation. Timoshenko's method has been used in the British standard B.S.10 for low pressure mild steel flanges connected to thin pipes.

Later contributions by Wahl and Lobo [7] on ring flanges and Holmberg and Axelsen [8] on ring and hub flanges, paved the way to a better understanding of flange behaviour.

1.2.3 **Development of the ASME Code Method**

The development of fusion welding as a joining method in the process industry established the need for flanges that could be butt welded to the end of a pipe. Higher operating pressures led to the development of tapered hub weld neck flanges. This prompted Waters, Wesstrom, Rossheim, Williams [9] [10] to modify the original work done by Waters and Taylor, and to publish their well known method "The Taylor Forge method". The refined method consisted of a complete elastic analysis of the pipe, hub, and flange ring assembly, as shown in Figure 3. This method was included in the ASME Boiler and Pressure Vessel Code in 1938 and 1942. The method in the 1938 ASME Boiler Code left the determination of gasket loads to the designer. In 1942 gasket loading constants were included as described by

Rossheim and Markl [11], which completed the ASME Code Method as the valuable design method that is still used in boiler and pressure vessel codes of many industrialized countries

1.2.4 Other Elastic Methods

Based on the ASME Code method, Schwaigerer and Kobitzsch [12] added the effects of bolt strains during gasket seating, Wesstrom and Bergh [13] included the effect of the radial displacement of the flange ring due to internal pressure, and Kraus [14] [15] included the effect of bolt holes on stresses.

1.2.5 Elasto-Plastic Analysis

Lake and Boyd [16] suggested a method that includes plastic analysis in the design of hubs. Schwaigerer [17][18][19][20], based his design on the concept of a plastic hinge. He used a plastic collapse moment at a critical section between the flange and hub to govern the design of the flange. The German Standard, DIN 2505, was based on Schwaigerer's work [17]. It also addresses in detail the tightness of the joint.

1.2.6 **Flat Faced Flanges**

Flat faced flanges with full contact across the flange face were recognized early to minimize bending. This is especially important in cast iron, glass, and ceramic flanges. The arrival of the O-Ring and other self energizing gaskets simulated interests in flanges with metal-to-metal contact over most of the flange surface.

1.2.7 **Flat Face Flanges with Metal Contact Beyond the Bolt Circle**

Several papers were published on the subject. In 1968 Schneider [21] published his general method for flanges with metal-to-metal contact beyond the bolt circle. Waters [22] [23] suggested simplifications to Schneider's work that led to the adoption of this method by the ASME Code , covering the formerly called "Part B" flanges. At present this method can be found in Appendix "Y" of this Code.

1.2.8 **Flat Face Flanges with Full Face Gaskets**

This type of flanges is used widely in low pressure applications, for circular and non-circular flanges. Not many methods exist to treat flanges of this type because of the complexity to predict gasket reactions. In 1951 the Taylor-Forge & Pipe Works Inc. [24] produced a design method that

prompted some attention. In this method it is assumed that the full face gasket can be replaced by two ring gaskets, one inside, one outside the bolt circle, both gaskets under uniform compression. A systematic computational procedure is included, that follows the nomenclature of the ASME Code. Schwaigerer [20] applied a simplified method based on plastic-elastic analysis, where he included the uneven compression effects of the gasket. Later in 1986 Blach and Bazergui [25] published a detailed method that includes a linear uneven gasket compression based on the Taylor Forge method [9][10], using a beam on an elastic foundation for the pipe and the deflection of a circular plate with centre hole for the flange ring. Blach also compared his results with those of the Taylor Forge [24] method showing the later to be very conservative. In 1985 Blach [26] published a paper on reducing flanges and on non-circular flanges with full face gaskets.

1.3 Summary

Although many papers were published on the subject of flange design, not many have addressed the design of flat faced flanges with full face gaskets. The ASME Boiler and Pressure Vessel Code, mandatory for the design of pressure vessels in many industrialized countries, contains rules for the design of flanges with ring gaskets in Section VIII, Division 1, Appendix 2, and also for flanges with metal-to-metal contact beyond the bolt circle in Appendix Y. No rules exist at present for flanges with full face gaskets.

CHAPTER TWO

THEORY AND ANALYSIS

2.1 General Review of Flanges

2.1.1 Flange Types

To understand the theory behind flange design it is important to distinguish between the different types and to put into context the factors that most influence the strength and integrity of the flanged joint. Flanges used in pressure vessels are classified in the ASME Boiler and Pressure Vessel Code [27] as per the location and type of the gasket, shown in Figure 4. In flanges per Appendix 2, called "Raised Face" or "Ring" flanges, the gasket ring is located inside the bolt circle. Flanges with self energizing gaskets such as "O" rings, have metal-to-metal contact outside the bolt circle and are included in the non-mandatory Appendix "Y". One other class of flanges exist for which the ASME Code contains no rules for their design. These are flanges with full face gaskets, that is gaskets covering the entire face of the flange. Flanges are also divided into loose, integral and optional flanges following the method of attachment between the flange and shell, as shown in Figure 5.

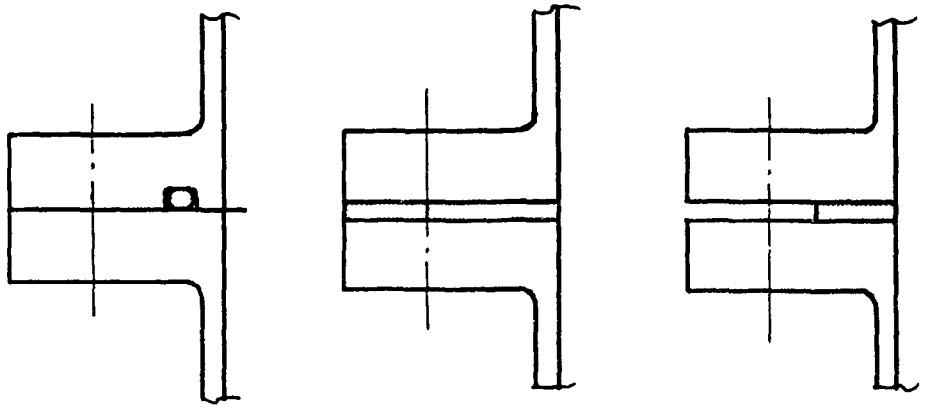

O-Ring Gasket Ring Gasket Full Face Gasket

Figure 4: Flange Types Based on Gasket Location

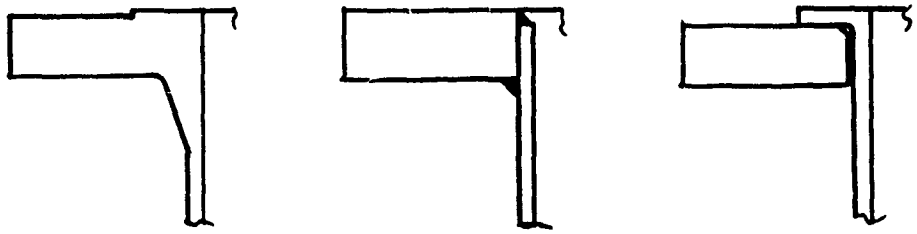

Taper Hub Flange Ring Flange Loose Flange

Figure 5: Flange Types Based on Hub-Flange Attachment

2.1.2 **Advantages and Disadvantages**

Ring Flanges tend to rotate about the gasket as a pivot. One way to describe a ring flange is shown in Figure 6. This ability to rotate freely about the gasket causes high longitudinal bending stresses in the hub and high tangential stresses in the flange. Comparison of ring flanges without hubs and hubbed flanges indicate that hubbed flanges are stiffer and give better support to the connecting pipe and thus reduce considerably both the maximum longitudinal and hoop stresses in the hub. The stiffening effect of the hub, studied by Waters [9], is found also to cause a reduction in the angle of rotation of the flange, which in turn reduces the tangential stress and increases the radial stress in the flange ring. Ring flanges, because of smaller gaskets, require less bolt area and can be used for higher pressure applications. Pressure-temperature rating for standard flanges with ring gaskets can be found in standard ASME / ANSI B 16.5.

Flanges having self-energizing gaskets, like O-rings, eliminate the rotation and thus minimize the stress, their disadvantage, though, is the limited material choice for gaskets and the required accuracy in the design of the groove.

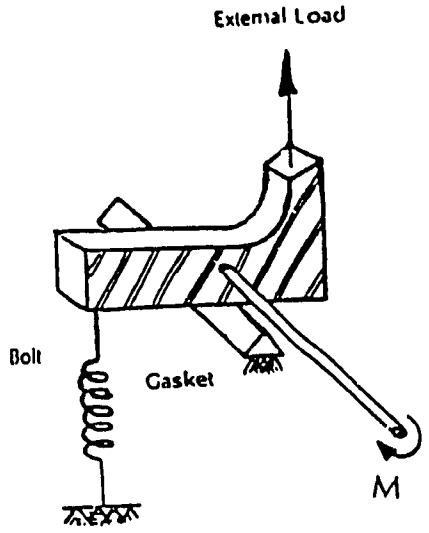

Figure 6: Symbolized Ring Type Flange Segment

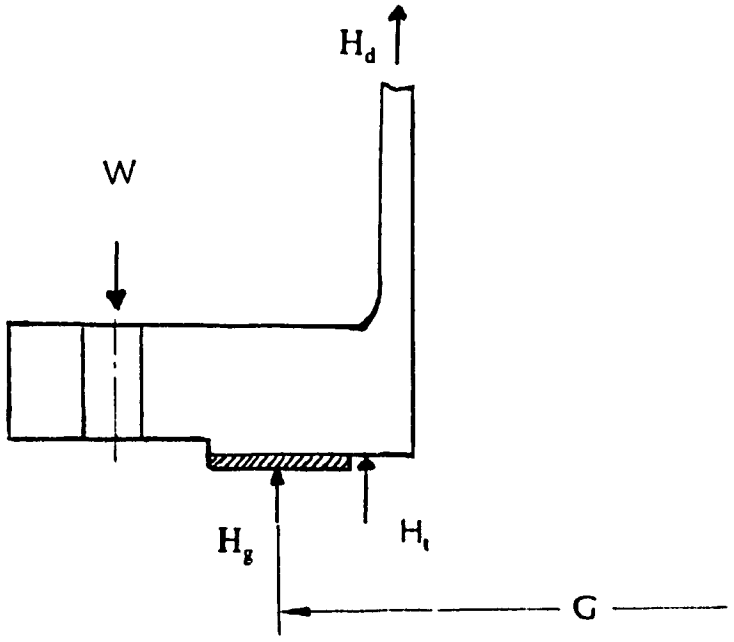

Figure 7: Forces Acting on Ring Type Flange

Flanges with full face gaskets, like flanges with self energizing gaskets, tend to resist rotation and thus reduce stresses in hub and flange. They are easy to fabricate, however, their disadvantage is that they require a large bolting area to seat the very wide gasket. Only relatively soft gaskets are used, hence they are applied in low pressure applications only.

2.2 The ASME Code Design Method for Flanges with Ring Gaskets

The ASME Boiler and Pressure Vessel Code [27], Section VIII, Division 1, has given the design engineer a systematic and simplified way of calculation that allows for a safe flange design. It is therefore important to review briefly the design approach used in the code and to be able to build a design method following the same nomenclature. It is equally important, though, to recognize that standardization follows not only experience, but also has to keep in step with new scientific methods and engineering developments. Based on the work of Waters [4] and the so-called Taylor-Forge method [9], [10], a set of rules for the design of bolted flange connections for ring type flanges were published in the ASME Code and, except for minor revisions and additions, they are still in use.

The design method is based on the theory of thin elastic plates and the theory of a beam on an elastic foundation where the later is used to calculate the stresses existing in the hub. The Code design is based on the following:

1- Operating condition: The conditions required to resist the hydrostatic end force tending to part the joint , and also to maintain sufficient compression on the gasket to assure a tight joint.

2- Gasket seating: The condition when the gasket is seated (initially compressed) is purely a function of the gasket properties and the contact area, and bolt cross section area.

2.2.1 **Gasket Seating (Pre-Load)**

The bolt load depends on both the effective area of the gasket, $G\pi b$ and the seating contact stress "y" which is the minimum stress in the gasket required to prevent leakage. The minimum bolt load required for this condition is found by multiplying the effective gasket contact area by the gasket seating factor $W_{m2}= \pi.G.b.y$, where G is the gasket effective diameter.

2.2.2 **Operating Conditions**

The bolt load for the operating condition must be equal to the total hydrostatic pressure force acting on the flange, given by $G^2P\pi/4$ and a

multiple of the force on the gasket due to internal pressure, given by, $2b\pi GmP$, where "b" is the gasket width. The equation for the operating bolt load is:

$$W_{m1} = H + H_p = G^2P\pi/4 + 2b\pi GmP$$

The multiple of the pressure on the gasket given in the second term of the equation is a function of the maintenance gasket stress constant "m". This maintenance gasket constant is used to maintain the gasket stress during operating conditions. The ratio between contact pressure and contained pressure must be greater than unity. Both the seating and maintenance stresses are experimentally determined gasket properties and were described initially by Rossheim and Markl [11]. A modified list of the original "m" and "y" factors are included in the current ASME Code.

2.2.3 **Flange Dimensions and ASME Design Equations**

After having made the choice of gasket and the bolting required to maintain a sealed joint, the designer then turns to the problem of flange dimensions required to withstand the bolt load with stresses which are within allowable limits. The outside diameter of the flange must be large enough to seat the bolts with some manufacturing tolerance to spare. The next step is to determine the lever arms of the various forces shown in Figure 7. The

stress in the flange is then determined for both the operating and gasket seating conditions, and the more severe will control the design. At this point the designer has all the information necessary to determine the flange and hub thickness in accordance with stress formulas given in the Code [27].

This is a cut and try process in which the designer varies the ring thickness, hub diameter and height until he or she achieves a combination which gives stresses in the flange and hub within limits specified in the Code, with reasonable economy of materials. The formulas given in the Code were developed based on the following simplifying assumptions:

1) Complete elastic behaviour under axisymmetric loading.
2) The flange is assumed to follow thin plate theory, loaded by a force couple acting on the inside and outside diameter of the flange, and uniformly distributed.
3) Neglect the radial displacement of the flange ring at the junction.
4) The bolt load is assumed to be constant all through the operation.
5) The location of the bolt circle and the moment arms are assumed not to be effected by rotation.
6) Bolt holes effects are neglected.

2.2.4 Comments on the ASME Code Design Procedure

Despite the fact that the code method avoids defining the gasket load, the implication is there. The "m" and "y" factors provide minimum indication of the actual behaviour of the gasket. It is understood that the gasket contact surface should not be less than "m" times the internal pressure nor so great that an ultimate compression of the gasket is reached that may cause crushing of the gasket. Since the gasket in ring flanges covers a small portion of the flange, it is assumed that the gasket compression is constant and the gasket reaction moment arm remains constant. In the design of full face gasketed flanges, although the same design approach is taken, a more elaborate gasket reaction force is needed.

2.3 Flanges with Full Face Gaskets

For many years flat face flanges with gaskets extending to the outer periphery of the flange, called also "rigid flanges", have been used in industry. Due to the large area of the gasket much higher bolting pressure is required and consequently such flanges are used with soft gaskets such as synthetic rubber or compressed asbestos. They are also usually limited to straight hubs and are often cut from steel plate and welded directly to the pressure vessel shell.

The ASME Code states that such flanges may be used provided they are designed in accordance with good engineering practice. Until now no design criteria have yet been recognized. Any development in design codes or any unconventional design of bolted flange connections require a thorough analysis of all the underlying elements that constitute the flange, including assumptions made to put the said flange design problem in a mathematically sound easily to handle model.

There are three separate elements in a bolted flange connection. they shall be considered in the following order :

Gasket, bolting and finally, flange design.

A well designed flange joint must hold the joint tight at all times without over stressing the three elements that constitute it.

2.3.1 **Gaskets and Their Behaviour**

Gasket selection for full face flanges is confined to relatively soft elastomeric compounds or compressed mineral fibre compositions that require low unit joint compression to keep them tight. The main difference between full face gaskets and ring gaskets in a bolted connection is the resistance to rotation of the flange produced by the uneven compression of the gasket.

It is assumed that a gasket which has yielded during initial bolt loading

is most likely a relatively inflexible component, compared to the axial flexibility of bolts. This assumption means that, as the internal pressure load is applied, the bolt load remains unchanged while the gasket load is redistributed to resist the overall external moment. Since the flange can only supply a resisting bending moment necessary to keep the system in equilibrium and no force loads, it is evident that the gasket load must always be equal to the algebraic sum of the bolt load and the pressure load. Having assumed that the external moment is restrained almost exclusively by a redistribution of the gasket pressures, it is necessary to determine possible redistribution patterns. Three critical stages for the bolted flange probable gasket compression are shown in Figure 8. Stage (a) shows full compression during initial bolt up. Stage (b) assumes zero gasket compression at the flange inside diameter. Stage (c) assumes initial joint separation, and the possibility of leakage. The following analysis will consider only case (a) pre-load, and (b) operating since they assure a tight joint, while case (c) may cause leaks through the bolts and will not therefore be considered.

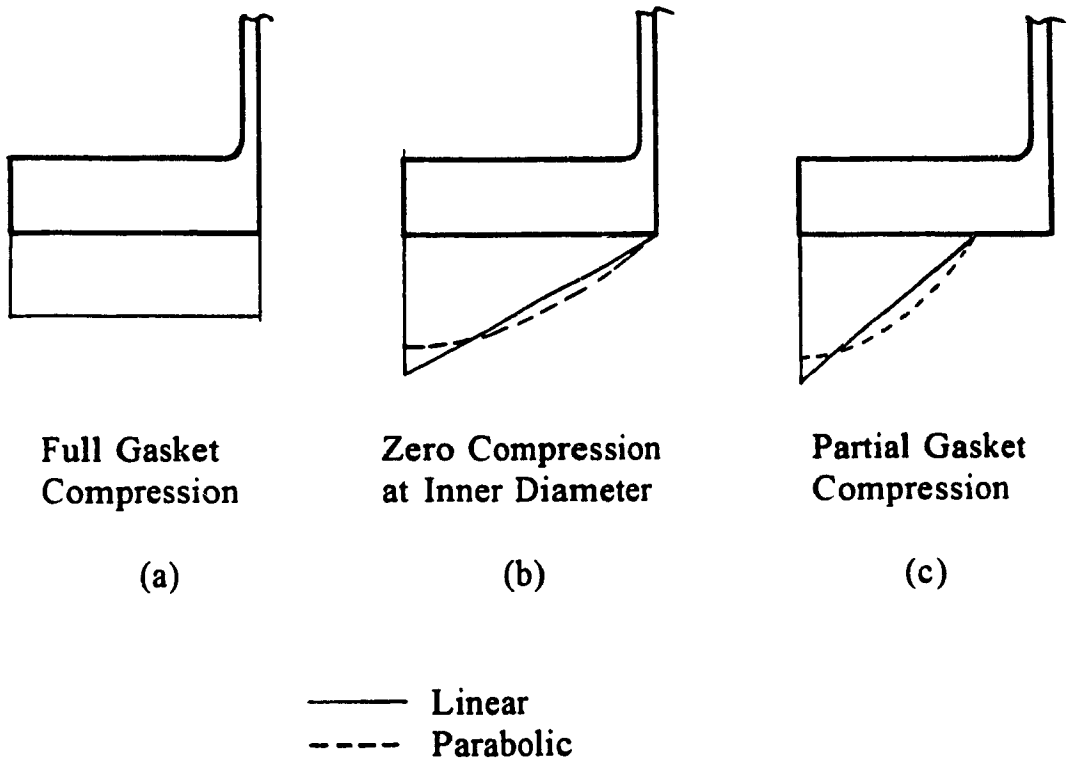

Figure 8: Suggested Gasket Compression Force Distribution

2.3.2 **Gasket Force Distribution Profiles**

Since gasket behaviour is complex and there are no accurate methods for actually measuring the gasket distribution pressure, assumptions must be made to simplify it. Two force distributions are assumed, one is linear and the other is parabolic.

2.3.2.1 Gasket Compression Force in Bolt-Up Condition (Seating)

The bolt circle is larger than the mean gasket diameter which will cause limited rotation of the flange. The rotation, however, is small and will be neglected, and uniform compression of the gasket during bolt-up is assumed. The gasket compression force passes through the flange centroid and is equal to the bolt load. The proposed compression profile is shown in a broken line, in Figure 8(a).

2.3.2.2 Gasket Compression in Operating Conditions

The linear gasket behaviour was addressed by Blick [28], Schwaigerer [19], and Blach [26]. It assumes that during operating pressure conditions, the flange goes through a rigid body rotation. The gasket will compress in the triangular form shown as a thin line in Figure 8(b). Although a linear force distribution is fairly true for thick, short flanges [29], it proved to be sensitive for relatively thin flanges. If the stiffness of the flange ring is low, solid rotation is accompanied by limited bending of the flange face. The gasket compression follows the deformed flange face, and the centre of gasket pressure shifts. To accommodate for this change, Blach, Naser [30] suggested a simple parabolic distribution, shown as a broken line in Figure 8(b).

2.3.2.3 **Gasket Unit Compression " σ_g"**

To calculate the gasket unit stress, the reader must keep in mind that the gasket is pre-stressed in seating conditions (bolt up), the pre-stress value "σ_g" is assumed uniform. As pressure is introduced, the flange rotates and the amount of gasket compression released at the inside diameter of the flange is gained at the outside. The compression (energy) lost on one side of the gasket is gained on the other side. The amount of compression at the outer periphery of the flange will be ($2\sigma_g$) for a triangular distribution. Similar analogy can be followed for a parabolic distribution, where the compression stress at the outer periphery is taken as (σ_g).

2.3.3 **Bolting**

Recommended bolts for medium to low pressure applications are either SA-307 or SA-325, since they provide an optimum balance between high strength, moderate ultimate elongation and low cost. The bolt material is heat treated (Quenched and Tempered) and made of medium carbon steel.

After establishing the size and shape of the gasket, and selecting the contact pressure, bolt loads can be calculated as per the ASME Code for gasket seating and operating conditions. Selection of bolt size and spacing can follow the recommended ASME and ANSI Standards. It is recommended

to use several slender bolts instead of few heavier ones, since larger number of bolts result in better uniform load distribution on the gasket. Pre-loading is of great importance in bolted flange connections, it is usually recommended to tighten the bolt slightly beyond its allowable stress. It is also recommended to use hard plain washers under the bolt head and nut. The washer serves primarily as a bearing surface and distributes the bolt load over a larger area.

2.4 Summary

The chapter has discussed the theory behind flange design by taking the ASME Code method as the basis for the design of flat faced full face gasketed circular flanges. A review of the different types of flanges and how they compare with full faced flanges is also given. The parts that constitute the full face flange and how they influence its design are discussed.

The next chapter includes a detailed analysis of the geometry and forces that act on the flange ring.

CHAPTER THREE

ANALYTICAL DESIGN ANALYSIS

3.1 Flange Geometry

3.1.1 Centroid of Unit Sector

Due to axial symmetry, the complete flange ring can be replaced by a unit sector, shown in Figure 9.

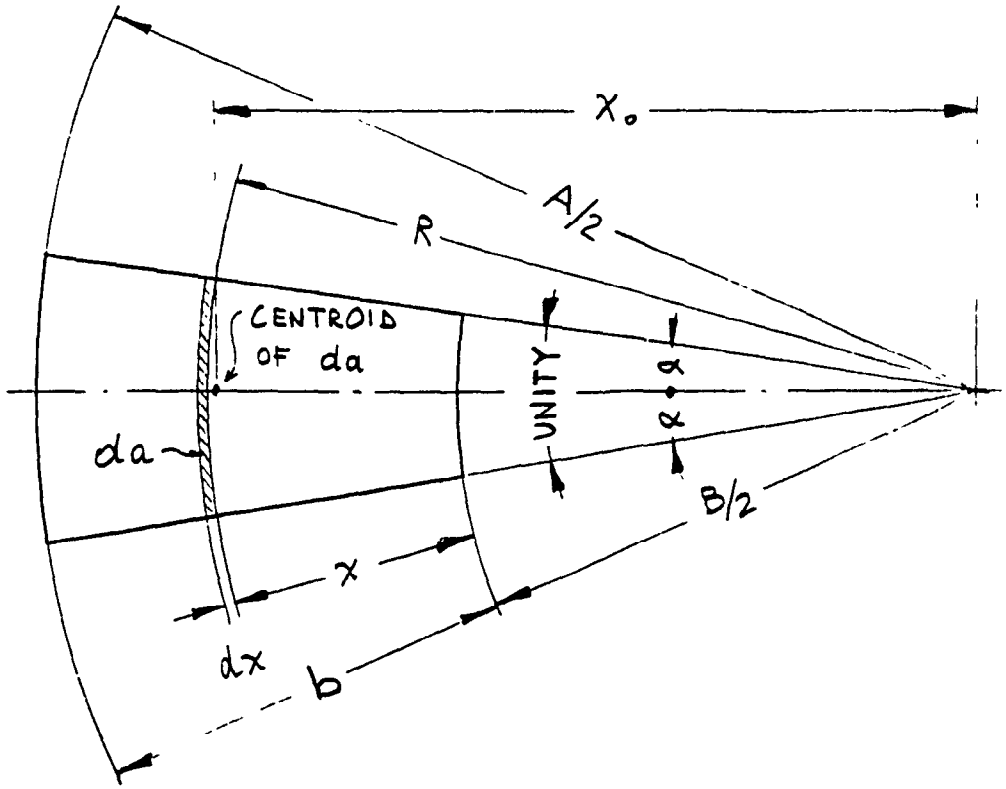

Figure 9: Flange Unit Sector

The centroid of the unit sector "x_1" can be located as follows:

From Figure 9, defining "x_0", the centroid of a circular arc

$$x = R\cdot\cos(\phi)\cdot d\phi \qquad dA = R\cdot(2\cdot\alpha)\cdot dx$$

$$x_o = \left(\frac{2\cdot\alpha\cdot R^2}{2\cdot\alpha\cdot R}\right)\cdot\frac{\int_{-\alpha}^{\alpha}\cos(\phi)\,d\phi\cdot dx}{\int_{-\alpha}^{\alpha}d\phi\,dx}$$

$$x_o = \frac{R\cdot\sin(\alpha)}{\alpha} \qquad (1)$$

where,

$b = 1/2\ (A-B)$ and $\alpha = 1/B$

"da" is the differential area of the unit sector "a",

$$da = 2\cdot R\cdot\alpha\cdot dx \qquad da = 2\cdot\alpha\cdot\left(\frac{B}{2}+x\right)\cdot dx$$

$$a = 2\cdot\alpha\cdot\int_{0}^{b}\left(\frac{B}{2}+x\right)dx$$

$$a = 2\cdot\alpha\cdot\left(B\cdot\frac{b}{2}+\frac{b^2}{2}\right)$$

$$a = \alpha\cdot b\cdot(B+b)$$

and, integrating over the sector area

$$x_1 = \frac{1}{a} \cdot \int_0^b x_o \, da$$

$$x_1 = \frac{1}{a} \cdot \int_0^b 2 \cdot \sin\alpha \cdot \left(\frac{B}{2} + x\right)^2 dx$$

$$x_1 = \frac{2 \cdot \sin(\alpha)}{\alpha \cdot b \cdot (B + b)} \cdot \left(B^2 \cdot \frac{b}{4} + B \cdot \frac{b^2}{2} + \frac{b^3}{3}\right)$$

$$x_1 = B \cdot \frac{\sin(\alpha)}{3 \cdot \alpha} \cdot \left(1 + \frac{K^2}{K + 1}\right) \qquad (2)$$

where,

$$K = A/B$$

3.1.2 The Gasket Effective Diameter

The effective diameter "G" is located at the centroid of the unit sector,

$$G = 2x_1$$

$$G = \frac{B \cdot 2 \cdot \sin\alpha}{3 \cdot \alpha} \cdot \left(1 + \frac{K^2}{K + 1}\right)$$

$$G = 2 \cdot \frac{B^2}{3} \cdot \sin\left(\frac{1}{B}\right) \cdot \left(1 + \frac{K^2}{K - 1}\right) \qquad (3)$$

3.2 Forces Acting on the Flange

3.2.1 Hydrostatic End Force "H_d"

This force "H_d" is assumed to act on the inside diameter of the flange, Its moment arm "h_d" can be seen in Figure 10.

$$H_d = \frac{\pi}{4} \cdot P \cdot B^2 \tag{4}$$

$$h_d = \frac{1}{2} \cdot (G - B - g) \tag{5}$$

3.2.2 Hydrostatic Force Acting Under the Gasket "H_t"

As in the design of flanges with ring gaskets in the ASME Code, it is assumed that some fluid leaks under the uneven compression of the gasket face causing an additional hydrostatic force, acting somewhere between the inside diameter of the flange and the effective gasket diameter. However in flat face full gasket flanges, this force can act only inside the bolt circle and can be calculated as follows:

$$H_t = \frac{\pi}{4} \cdot \left[(C - D)^2 - B^2 \right] \cdot P \tag{6}$$

The moment arm is

$$h_t = \frac{1}{4} \cdot (2G - B - C + D) \tag{7}$$

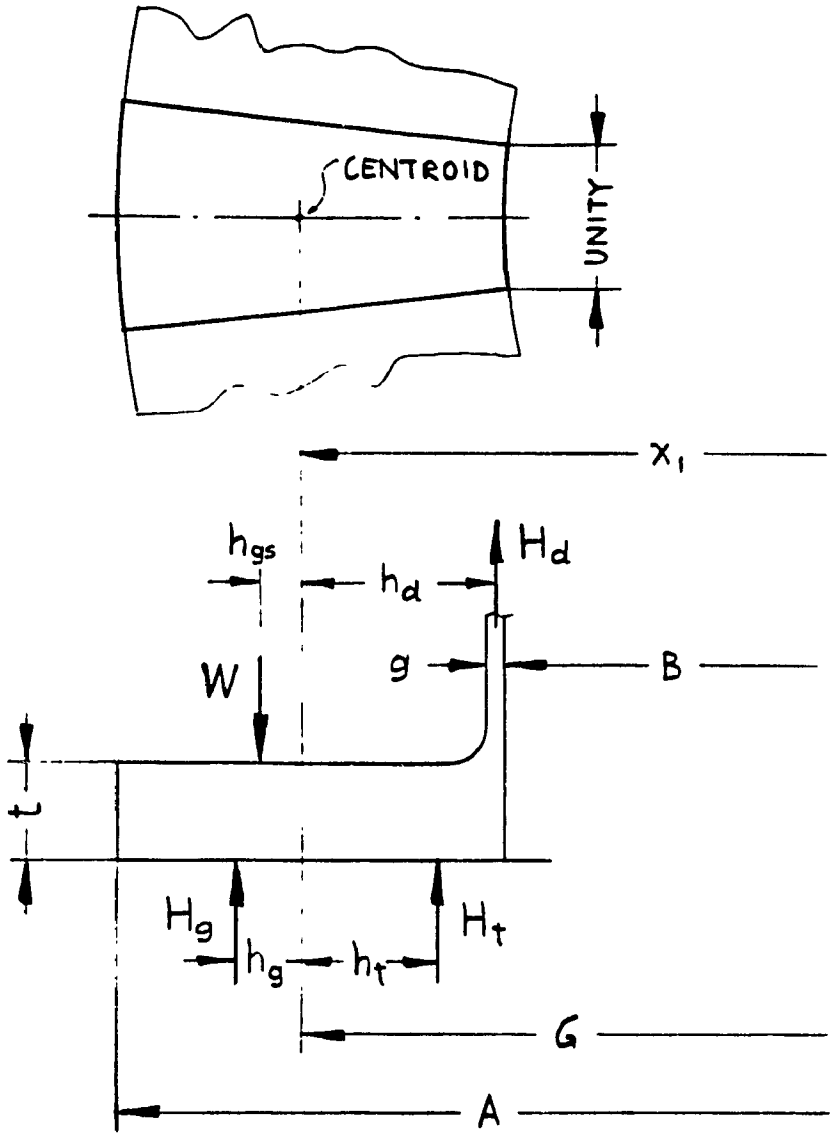

Figure 10: Forces Acting on Flat Face Full Gasket Flanges

3.2.3 **Total Gasket Load "H_g"**

It was assumed that the gasket exclusively resists the flange external moment by a redistribution of the compression pressure "σ_g". For this case, a value for the total gasket force H_g can be calculated by relating it to "σ_g" for different pressure distribution patterns that may exist in both, gasket seating and operating conditions.

3.2.3.1 **Gasket Force During Bolt Up**

For the bolt up condition, the flange is assumed not to rotate, which means that the gasket is compressed uniformly. Since the gasket compression force is the only force reacting to the bolt load, they are numerically equal and so it is simply taken as the total bolt area times the maximum allowable stress of the bolt material [23]. The seating gasket load is thus,

$$H_{gs}=A_b\ S_a \tag{8}$$

The moment arm "h_{gs}" is the distance between the bolt circle and the effective diameter "G", from which

$$h_{gs}=1/2\ (C-G) \tag{9}$$

3.2.3.2 **Gasket Load During Operating Conditions**

The gasket reaction force "H_g", causes a moment "M_g" that resists the flange rotation.The line of action of the gasket reaction "H_g" is assumed to pass through the centroid of the gasket compression sectorial wedge profile. The Gasket load "H_g" can be found for previously proposed linear and parabolic gasket compression profiles. A linear profile implies a solid body rotation of the flange, while a parabolic profile takes flange bending into account.

3.2.3.3 **Triangular Gasket Force Distribution**

The line of action of the gasket force " H_g" passes through the centroid of the gasket compression force profile. The moment arm "h_g" for a triangular gasket force, is the distance between the centroid of a triangular sectorial wedge and the centroid of the sector of unit width located at "G/2". The centroid of the triangular sectorial wedge can then be found from Figure 11(a), by first calculating the volume of gasket compression sectorial wedge "V" [29]: From Equ. 1,

$$x_o = \frac{\sin(\alpha)}{\alpha} \cdot \left(\frac{B}{2} + x\right)$$

$$dV = (2 \cdot R \cdot \alpha) \cdot \frac{2 \cdot x \cdot \sigma_g}{b} \cdot dx$$

$$dV = 2\cdot\alpha\cdot\frac{\sigma_g}{b}\cdot\left(B\cdot x + 2\cdot x^2\right)\cdot dx$$

$$V = \frac{2\cdot\alpha\cdot\sigma_g}{b}\cdot\int_0^b \left(B\cdot x + 2\cdot x^2\right) dx$$

$$V = \frac{\sigma_g\cdot b}{3}\cdot(1 + 2\cdot K) \qquad (10)$$

Centroid of sectorial wedge x_1 ,

$$x_1 = \frac{1}{V}\cdot\int x_o\, dV$$

$$x_1 = \frac{1}{V}\cdot\int_0^b \frac{4\cdot\alpha\cdot\sigma_g}{b}\cdot\frac{\sin\alpha}{\alpha}\cdot\left(\frac{B}{2} - x\right)^2\cdot x\, dx$$

$$x_1 = \frac{B^2}{4}\cdot\sin\left(\frac{1}{B}\right)\cdot\left(1 + \frac{3\cdot K^2}{1 - 2\cdot K}\right) \qquad (11)$$

where K=A/B . The moment arm h_g can now be found:

$$h_g = x_1 - \frac{G}{2}$$

$$h_g = \frac{B^2}{4}\cdot\sin\left(\frac{1}{B}\right)\cdot\left(1 + 3\cdot\frac{K^2}{1 + 2\cdot K}\right) - \frac{G}{2} \qquad (12)$$

From Figure 11(a) and Equ. (10), the gasket load H_g as a function of "V" is:

$$\frac{Hg}{\pi\cdot G} = \frac{\sigma_g\cdot b}{3}\cdot(1 + 2\cdot K) \qquad (13)$$

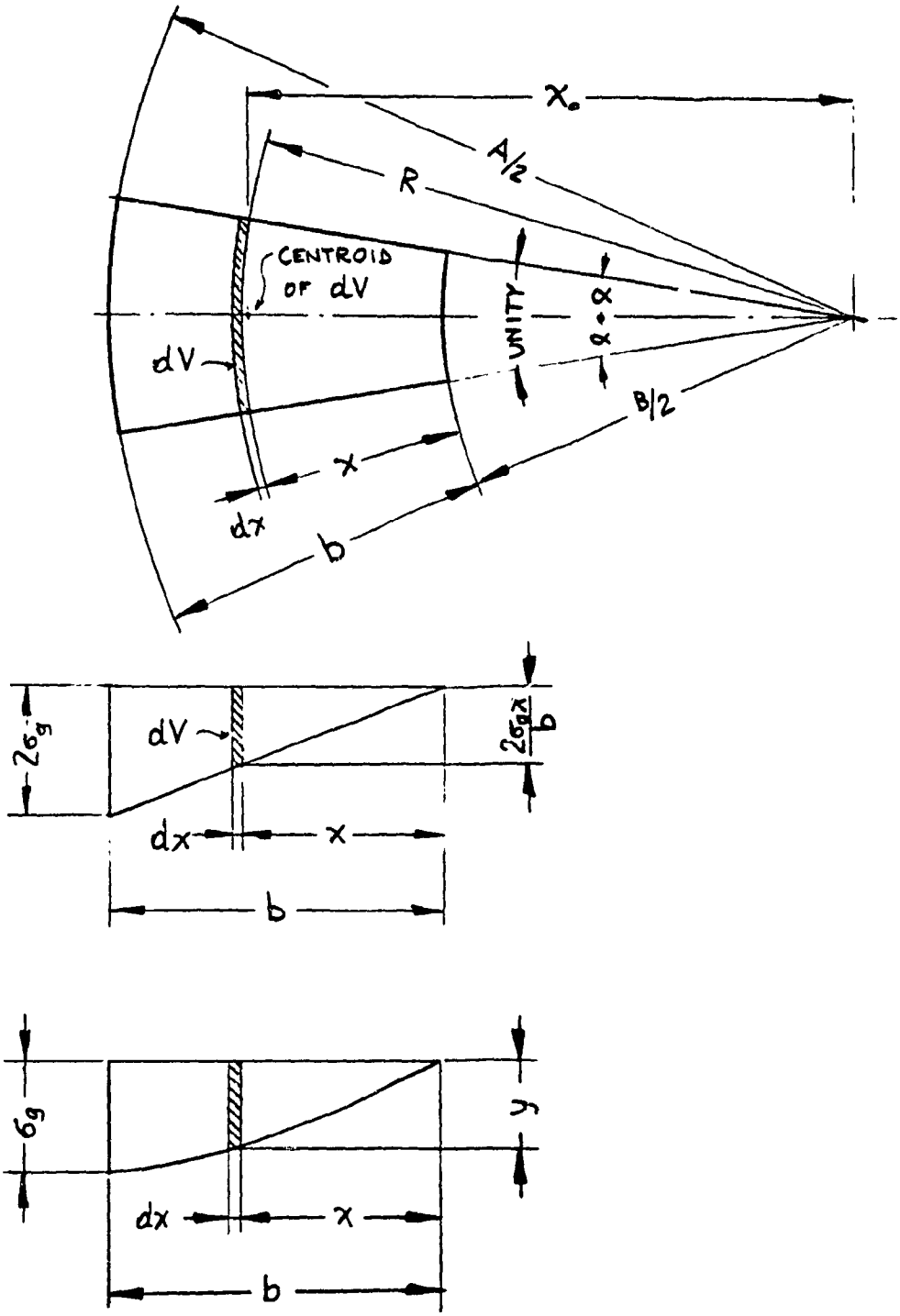

Figure 11: Location of Centroid of Gasket Compression Force

3.2.3.4 **Parabolic Gasket Force Distribution**

The triangular gasket compression distribution, discussed earlier, is a first degree polynomial which accounts for linear gasket behaviour. It is a fairly accurate presumption provided that the flange remains straight during solid body rotation, commonly seen in thick and narrow flanges.

In the case of relatively thin wide flanges where the flange face may bend, the linear triangular force does not account for the actual curvature of the flange face. The actual behaviour is therefore approximated by a second degree polynomial function, provided as a parabolic force distribution acting on the gasket side of the flange, shown in Figure 11(b). The total gasket load "Hg", from the parabolic distribution, acting at its centroid, can be calculated by assuming a parabola of the following form,

$$y = \frac{\sigma_g}{b^2} \cdot \left(2 \cdot b \cdot x - x^2\right) \tag{14}$$

$$R = \frac{B}{2} + x$$

$$x_0 = R \cdot \frac{\sin(\alpha)}{\alpha}$$

$$b = \frac{B}{2} \cdot (K - 1)$$

where,

$$K = A/B$$

The volume of the compression force"dV" is

$$dV = 2R\cdot\alpha\cdot y\cdot dx$$

from Equ. 14, substitute for "y"

$$dV = \frac{2\cdot\alpha\cdot\sigma_g}{b^2}\cdot\left(B\cdot b\cdot x - \frac{B\cdot x^2}{2} + 2\cdot b\cdot x^2 - x^3\right)\cdot dx$$

$$V = \frac{2\cdot\alpha\cdot\sigma_g}{b^2}\cdot\int_0^b\left(B\cdot b\cdot x - \frac{B\cdot x^2}{2} + 2\cdot b\cdot x^2 - x^3\right)dx$$

$$V = \frac{2\cdot\alpha\cdot\sigma_g}{b^2}\cdot\left(\frac{B\cdot b^3}{2} - \frac{B\cdot b^3}{6} + \frac{2\cdot b^4}{3} - \frac{b^4}{4}\right)$$

Rearranging and substituting for K=A/B this becomes:

$$V = \frac{\sigma_g\cdot b}{12}\cdot(3 + 5\cdot K) \qquad (15)$$

The centroid "x_1" of the volume sectorial wedge is

$$x_1 = \frac{1}{V}\cdot\int x_o\, dV$$

$$x_1 = \frac{1}{V}\cdot\int_0^b\left[\frac{\sin(\alpha)}{\alpha}\cdot\left(\frac{B}{2} + x\right)\right]\cdot\left[\frac{2\cdot\alpha\cdot\sigma_g}{b^2}\cdot\left(B\cdot b\cdot x - B\cdot\frac{x^2}{2} + 2\cdot b\cdot x^2 \quad x^3\right)\right]dx$$

Integrate the above equation and arrange

$$x_1 = \frac{\sigma_g}{V} \cdot 2 \cdot \frac{\sin(\alpha)}{b^2} \cdot \left(\frac{B^2 \cdot b^3}{4} + \frac{2 \cdot B \cdot b^4}{3} - \frac{B^2 \cdot b^3}{12} + \frac{b^5}{2} - \frac{B \cdot b^4}{4} - \frac{b^5}{5} \right)$$

$$x_1 = \frac{6 \cdot \left(2 \cdot \sin(\alpha) \cdot \sigma_g \cdot b\right)}{\sigma_g \cdot \alpha \cdot b \cdot (4 \cdot B + 5 \cdot b)} \cdot \left(\frac{B^2}{4} + \frac{2 \cdot B \cdot b}{3} - \frac{B^2}{12} + \frac{b^2}{2} - \frac{B \cdot b}{4} - \frac{b^2}{5} \right)$$

$$x_1 = \frac{12}{60} \cdot \frac{\sin(\alpha)}{\alpha} \cdot \frac{10 \cdot B^2 + 25 \cdot B \cdot b + 18 \cdot b^2}{4 \cdot B + 5 \cdot b}$$

$$x_1 = B^2 \cdot \frac{\mathrm{Sin}(\alpha)}{5} \cdot \left(\frac{2 + 3.5 \cdot K + 4.5 \cdot K^2}{1.5 + 2.5 \cdot K} \right)$$

Substituting for $\alpha = 1/B$, "x_1" then becomes:

$$x_1 = \frac{B^2}{5} \cdot \sin\left(\frac{1}{B}\right) \cdot \left(\frac{4 + 7 \cdot K + 9 \cdot K^2}{3 + 5 \cdot K} \right) \qquad (16)$$

The moment arm of the parabolic gasket reaction "h_g" is

$$h_g = x_1 - \frac{G}{2}$$

$$x_1 = \frac{B^2}{5} \cdot \mathrm{Sin}\left(\frac{1}{B}\right) \cdot \left(\frac{4 + 7 \cdot K + 9 \cdot K^2}{3 + 5 \cdot K} \right) - \frac{G}{2} \qquad (17)$$

From Figure 11(b) the gasket load H_g related to the volume of the parabolic sectorial wedge given in Equ.15 is

$$\frac{Hg}{\pi \cdot G} = \sigma_g \cdot b \cdot \frac{3 + 5 \cdot K}{12} \qquad (18)$$

3.3 Flange Angle of Rotation Due to Gasket Compression

As the flange rotates, it causes a deformation of the gasket accompanied by uneven compression. If, for simplification, this uneven compression is assumed either triangular or parabolic, it is then possible to relate the angle of rotation of the flange to the uneven compression force of the gasket.

Assuming the gasket to be completely elastic, the gasket compression force will be proportional to its displacement "δ", thus

$$\sigma_g = (\delta . E_g) / t_g \qquad (19)$$

where, E_g is the gasket modulus and t_g is it's original thickness.

If the gasket rotates about its centroid that is located at "b/2", the angle of rotation "θ" can be found as follows [29] (see Figure 12):

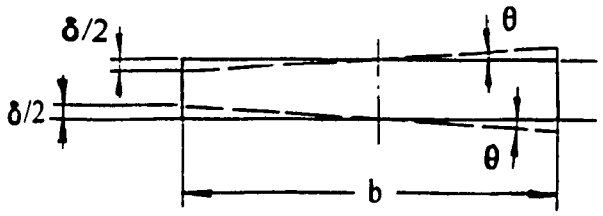

Figure 12: Flange Rotation and Gasket Compression

$$\theta = \delta / b \qquad (20)$$

Substitute for δ in Equ.(19),

$$\theta = \sigma_g \,.b.\, t_g / E_g \tag{21}$$

For a triangular force distribution substitute "σ_g" from Equs. (13) & (21)

$$\theta = \left(\frac{3}{1 + 2\cdot K}\right)\cdot\left[\left(Mgt_g\right)\cdot\left(\pi\cdot G\cdot E\cdot b^2\cdot h_g\right)^{-1}\right] \tag{22}$$

For a parabolic gasket distribution substitute "σ_g" from Equs. (19) & (21)

$$\theta = \left(\frac{12}{3 + 5\cdot K}\right)\cdot\left[Mgt_g\cdot\left(\pi\cdot G\cdot E\cdot b^2\cdot h_g\right)^{-1}\right] \tag{23}$$

3.4 Moments Acting on the Flange Ring

3.4.1 External Moments

In the operating conditions, the flange ring is subjected to an external moment "M_o" acting about its effective gasket diameter "G", from Figure 10,

$$\begin{aligned} M_o &= H_d\ h_d\ +\ H_t\ h_t\ +\ W_{gs}\ -\ H_g\ h_g \\ &= M_d + M_t + (\ H_d + H_t + \ H_g\ )\ h_{gs} - \ M_g \\ &= M_d + M_t + (\ H_d + H_t\ )\ h_{gs} - \ (1 - \ h_{gs} / h_g\ )\ M_g \\ &= M_d + M_t + M_b - \mu\, M_g \end{aligned} \tag{24}$$

where,

$$M_b = \ (\ H_d + H_t\ )\ h_{gs} \tag{25}$$

$$\mu \ = \ 1 - \ h_{gs} / h_g$$

3.4.2 **Discontinuity Moments and Force**

Discontinuity moment "M" and force "Q" are accounted for by the sudden change in cross section at the shell flange junction and tend to resist rotation caused by the external moment "M_o". The discontinuity force, when applied at the junction, causes meridional moment equal to Q.(t/2). Both "M" and Q.(t/2) are moments per unit circumference acting on the shell-flange junction.

3.5 **Summary**

The analytical analysis, based on a fully symmetric structure, defines the flange geometry, and all forces and moments acting on the flanged ring. The analysis also formulates the gasket reaction force based on linear and parabolic distribution profiles and produces a relationship between the flange angle of rotation and the gasket compression. The next chapter will discuss a method that applies plate and shell equations to the solution of the flanged structure.

CHAPTER FOUR

SOLUTION OF THE FLANGED STRUCTURE PROBLEM

4.1 General

Factors that most influence the flanged structure have been defined. They include the flange geometry and all the forces that act on it. In this chapter equations for the shell and ring are developed and solved for the unknowns. The flanged structure is a statistically indeterminate problem having the following unknowns: M, Q, H_g. From continuity at the junction and rotation caused by gasket compression the solution for the three unknowns can be found.

4.2 The Shell

4.2.1 General

The membrane action of the shell is incapable of withstanding any bending moments. Loads are carried by internal forces induced in the surface of the shell, called membrane stresses. In most cases, though, shells are subjected to external moments, so the membrane theory is not sufficient to solve the problem. A more complex theory that is based on the principles of a semi-infinite beam on an elastic foundation can be applied to find deflections and rotations of shells.

During seating of the flange, the shell is subjected to a discontinuity moment and shear which causes only bending stresses. When the vessel is pressurized (operating conditions) the shell is subjected to membrane forces caused by the uniform internal pressure. Membrane stresses must then be superimposed to the bending stresses.

4.2.2 Shell Equations

Shell equations have been derived in many reference books, the fourth order differential equation for circular cylindrical shell loaded symmetrically is given by Timoshenko [31],

$$D\left(d^4u/dx^4\right) + \left(E.g/a^2\right) u = Z \tag{26}$$

$$\beta^4 E.g / B^2 D = 12\,(1-\upsilon^2) / B^2 g^2 \tag{27}$$

$$d^4u/dx^4 + 4\,\beta^4\, u = Z/D \tag{28}$$

where,

$$D = E\,g^3 / 12(1-\upsilon^2) \quad \text{and} \quad \beta^4 = 6(1-\upsilon^2) / B.g^2 \tag{29}$$

which is the same equation obtained for a bar supported by a continuous elastic foundation and submitted to the action of a load of intensity Z. The general solution of Equ. (28) is well known,

$$u_S = e^{\beta\cdot x}\cdot\left(C_1\cdot\cos(\beta\cdot x) + C_2\cdot\mathrm{Sin}(\beta\cdot x)\right) + e^{-\beta\cdot x}\cdot\left(C_3\cdot\cos(\beta\cdot x) + C_4\cdot\mathrm{Sin}(\beta\cdot x)\right) + f(x) \tag{30}$$

During flange seating the vessel walls are subjected to a bending moment "M" and a shearing force "Q", both uniformly distributed at x=0. There is no pressure distributed over the shell surface, and so f(x)=0. Since the forces "M" and "Q" applied at the end produce local bending that tends to die as the distance from the edge is increased the first two terms of the equation vanish, and C1= C2=0, so we obtain

$$u_s = e^{\beta \cdot x} \cdot (C_3 \cdot \cos(\beta \cdot x) + C_4 \cdot \mathrm{Sin}(\beta \cdot x)) \tag{31}$$

The two constants can be determined from the boundary conditions,

$$M_{x=o} = M \qquad \text{and} \qquad Q_{x=o} = Q$$

Substituting back into Equ.(31) to get the constants of integration

$$C_3 = \frac{1}{2 \cdot \beta^3 \cdot D} \cdot (Q + \beta \cdot M) \tag{32}$$

$$C_4 = \frac{M}{2 \cdot \beta^2 \cdot D} \tag{33}$$

The final expression for "u_s" is,

$$u_s = \frac{e^{-\beta \cdot x}}{2 \cdot \beta^3 \cdot D} \cdot (\beta \cdot M \cdot (\sin(\beta x) - \cos(\beta x)) - Q \cdot \cos(\beta x)) \tag{34}$$

The deflection at the shell flange junction ($\beta x=0$) is then found,

$$u_s = 1/(2\ \beta^3 D)\ .\ (\ \beta\ M + Q\ ) \tag{35}$$

The rotation is,

$$\theta_s = 1/(2\ \beta^2 D)\ .\ (2\ \beta\ M + Q\ ) \tag{36}$$

Using k, the spring constant of shell

$$k = 4\ E\ g\ /\ B^2$$

$$u_s = 2\ Q\ \beta/\ k\ -\ 2\ M\ \beta^2\ /\ k \tag{37}$$

$$\theta_s = 4\ M\ \beta^3/\ k\ -2\ Q\ B^2\ /\ k \tag{38}$$

The effect of the internal pressure on the radial displacement "u_s"

$$u_s = (2\text{-}\nu)\ B^2\ P\ /\ 8.E.g \tag{39}$$

add it to the bending effects,

$$u_s = \frac{6\cdot(1-\nu^2)\cdot Q}{E\cdot g^3\cdot\beta^3} - \frac{6\cdot(1-\nu^2)\cdot M}{E\cdot g^3\cdot\beta^2} + \frac{(2\ \nu)\cdot B^2}{8\cdot E\cdot g}\cdot P \tag{40}$$

$$\theta_s = \frac{M\cdot B^2\cdot\beta^4}{E\cdot g\cdot\beta} - Q\cdot B^4\cdot B^2 \tag{41}$$

$$\theta_s = \frac{12\cdot(1-\nu^2)\cdot M}{E\cdot g^3\cdot\beta} - \frac{6\cdot(1-\nu^2)\cdot Q}{E\cdot g^3\cdot\beta^2} \tag{42}$$

4.3 Plate Theory Applied to Flange Design

4.3.1 General

The flange ring may be treated as a flat circular plate with a central hole subjected to external bending moments that cause it to rotate. From the point of view of plate theory, some typical flanges are in fact thick plates. However, for practical reasons it is customary to treat flanges in theoretical analysis and even in experimental research as thin plates. Consequently, the typical mathematical models assumed in engineering practice as the basis for bolted flange connections, are based on the assumptions of thin plate theory, or what is the so-called Kirchhoff's Theory. Solutions supplied by the thick plate theory are not yet practical.

Common mathematical models in the field of linear thin plate theory as applied to the flange problem can be based on the following assumptions [31]:

1- The material is linearly elastic, homogeneous and isotropic.

2- The flange ring is initially flat.

3- The plate thickness is small compared to other dimensions.

4- Deformation exists such that straight lines originally normal to the middle surface remain straight and normal to that surface.

5- The stress component normal to the middle surface is small to the ones parallel and thus can be neglected in relations between stress and strain.

6- Strains in the middle surface are small compared to strains resulting from bending (neglect stretching of middle surface).

7- Bolt holes effects are neglected

8- Bolt loads are uniformly distributed along the bolt circle

4.3.2 **Plate Equations**

The general differential equation for a symmetrically loaded circular plate is derived in many books [31][32],

$$\frac{d}{dr}\left[\frac{1}{r}\frac{d}{dr}\left(r\frac{dz}{dr}\right)\right] = \frac{Q_o}{D} \qquad (43)$$

where "Qo" is the shear force per unit length of circumference and "D" is the flexural rigidity of the plate $D = E.t^3/12(1-\upsilon^2)$. The plate differential equation can be applied to the flange problem, and the solution can be simplified by replacing the moment on the flange by a twisting couple located at the inside and outside diameter of the flange. This implies that the effect of the external moment on the flange, which is equal to the product of the bolt load and lever arm, is the same in all cases regardless of the location of the bolt circle. This assumption may not appear rational but studies were made that indicate this is true. Equations by Holmberg and

Axelson [8] enable a study of the effect of applying external loads at various diameters and it has shown that points of application can be varied over wide limits without effecting the results to any particular extent. This assumption has been used in most major flange theories including the present ASME Code rules for flanges with ring gaskets [27]. The rotation of a circular plate with central hole subjected to a twisting couple, can then be solved by substituting $Q_o=F/2\pi.x$, and integrating Equ. (43),

$$\theta \quad \frac{-F\cdot x}{8\cdot\pi\cdot D}\cdot(2\cdot\ln(x) - 1) + C_1\cdot\frac{x}{2} + C_2\cdot\frac{1}{x} \tag{44}$$

where "F" is the twisting couple acting on the inside and outside of the flange ring. The boundary conditions for a plate with edges free to rotate are zero radial (M_r) and tangential (M_t) moments at the inner and outer edge of the plate.

$$M_r = 0 \quad \text{and} \quad M_t = 0$$

$$M_r = D(d\theta/dx + \upsilon\theta/x) \tag{45}$$

$$M_t = D(\theta/x + \upsilon d\theta/dx) \tag{46}$$

Evaluating C1, C2 and substituting back into θ gives,

$$\theta = F\cdot\frac{x}{4\cdot\pi\cdot D}\left\{\frac{K^2\cdot\ln(K)}{K^2 - 1}\left[1 + \frac{1+\nu}{1-\nu}\cdot\left(\frac{B}{2\cdot x}\right)^2\right\} - \ln\left(\frac{2\cdot x}{B}\right) + \frac{1}{1+\nu}\right] \tag{47}$$

The total couple acting on the flange ring "M1" is given by,

$$M1 = \frac{A - B}{2} \cdot \frac{F}{B \cdot \pi}$$

$$M1 = \frac{K - 1}{2 \cdot \pi} \cdot F \tag{48}$$

The rotation at the inside diameter of the flange "θ_f" as a function of "M1",

$$\theta_f = \frac{3 \cdot B \cdot M1}{E \cdot t^3 \cdot (K - 1)} \cdot \left[2 \cdot (1 + \nu) \cdot \left(\frac{K^2 \cdot \ln(K)}{K^2 - 1} \right) + 1 \quad \nu \right] \tag{49}$$

The flange parameter "Y", which is used in the ASME Code, can be applied

$$Y = \frac{1}{K - 1} \cdot \left[\frac{3}{\pi} \cdot (1 - \nu) + \frac{6}{\nu} \cdot (1 + \nu) \cdot \left(\frac{K^2 \cdot \ln(K)}{K^2 - 1} \right) \right] \tag{50}$$

from which

$$\theta_f = \frac{B \cdot \pi \cdot Y \cdot M1}{E \cdot t^3} \tag{51}$$

From Figure 12, the net moment per unit length transferred to the inside diameter of the flange ring "M1" is

$$M1 = \frac{Mo}{B \cdot \pi} - M - Q \cdot \frac{t}{2} \tag{52}$$

The radial displacement of the flange "U_f" is found using the theory of thick walled cylinder Blach [29], Timoshenko [33],

$$U_f = B \cdot j \cdot \frac{P}{2 \cdot E} - B \cdot A \cdot \frac{Q}{2 \cdot t \cdot E} \tag{53}$$

$$j = A^2 + \frac{B^2}{A^2} - B^2 + \nu \tag{54}$$

Having found all the equations required for each part of the bolted flange connection, it is now necessary to relate them to solve for the unknown discontinuity moment "M", shear "Q", and gasket moment "Mg".

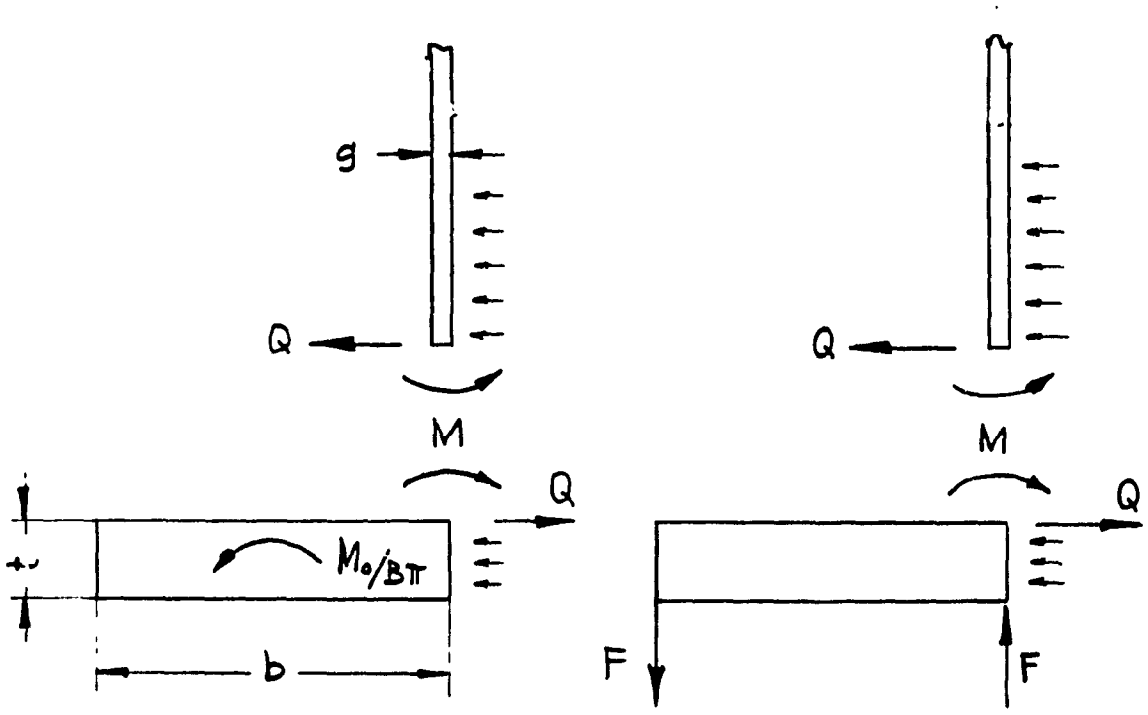

Figure 13: Flange-Shell Junction

4.4 **Compatibility:**

In order to seek an acceptable solution to the stress distribution in the flange and shell, it must insure a piece wise-continuous-deformation of the whole structure, that is the stress distribution and the resulting deflection must be compatible with boundary conditions and a continuous distribution of deformation. This, in turn, insures the requirement of continuity at the flange-shell junction for both rotation and displacement, hence deflections and rotations must be equated.

Assuming the same modulus of elasticity for both shell and flange, rotations Equs. (40), (53) and displacements Equs. (42), (51) are equated:

$$\frac{6\cdot\left(1-\nu^2\right)\cdot Q}{E\cdot g^3\cdot\beta^3}-\frac{6\left(1-\nu^2\right)}{E\cdot g^3\cdot\beta^2}+\frac{(2-\nu)\cdot B^2\cdot P}{8\cdot E\cdot G}=\frac{B\cdot j\cdot P}{2\cdot E}-\frac{B\cdot j\cdot Q}{2\cdot t\cdot E} \tag{55}$$

$$\frac{12\cdot\left(1-\nu^2\right)\cdot M}{E\cdot g^3\cdot\beta}-\frac{6\cdot\left(1-\nu^2\right)\cdot Q}{E\cdot g^3\cdot\beta^2}=\frac{Y\cdot B\cdot\pi}{E\cdot t^3}\cdot\left(\frac{Mo}{B\cdot\pi}-M-Q\cdot\frac{t}{2}\right) \tag{56}$$

$$M = C7\ \beta\ Mo - C8\ P/\beta^2 \tag{57}$$

$$Q = C9\ \beta^2\ Mo + C10\ P/\beta \tag{58}$$

where C7,C8,C9,C10 are dimensionless coefficients, listed in Appendix "A".

The external Moment "Mo" contains the unknown gasket moment "M". This is a statically indeterminate problem with two equations and three unknowns M, Q, M. To arrive at an additional equation, analysis of the rotation of the flange based on gasket reaction profiles, can be implemented.

4.4.1 **Triangular Gasket Distribution**

The flange rotation based on a triangular gasket compression Equ.(22) can be equated to the rotation of the ring Equ.(51). This gives,

$$\frac{B\cdot\pi\cdot Y\cdot M1}{E\cdot t^3} = \frac{3}{1+2\cdot K}\cdot\frac{Mg\cdot tg}{\pi\cdot Eg\cdot G\cdot b^2\cdot hg} \tag{59}$$

from which

$$Mg = C14\cdot(Md + Mt + Mb) + C15\cdot\frac{P}{\beta^3} \tag{60}$$

4.4.2 **Parabolic Distribution**

Following the same steps as used in the triangular distribution but using Equ.(23) instead, the flange rotation based on a parabolic gasket reaction profile is equated to flange rotation due to ring bending.

$$\frac{B\cdot\pi\cdot Y\cdot M1}{E\cdot t^3} = \frac{12}{3+5\cdot K}\cdot\frac{Mg\cdot tg}{\pi\cdot Eg\cdot G\cdot b^2\cdot hg} \tag{61}$$

The above equation can then be solved for "Mg",

$$Mg \quad C14\cdot(Md + Mt + Mb) + C15\cdot\frac{P}{\beta^3} \tag{62}$$

were C14 and C15 are parabolic dimensionless coefficients, given in Appendix "A".

4.5 Simplifying Assumptions

The flange ring is usually of substantial thickness when compared to the shell. It will resist the expansion of the shell, and the radial displacement of the flange can be neglected. This assumption is valid and has been applied [33].

Let " U_{ζ}" in equation (40) be equal to zero,

$$\frac{6\cdot(1-\nu^2)\cdot Q}{E\cdot g^3\cdot\beta^3} - \frac{6\cdot(1-\nu^2)}{E\cdot g^3\cdot\beta^2} + \frac{(2-\nu)\cdot B^2\cdot P}{8\cdot E\cdot G} = 0 \tag{63}$$

assume also that

$$(1-\upsilon^2) = 1/2(2-\upsilon)$$

Substitute back into Equ.(63)

$$\beta\cdot M - Q = \frac{g^3\cdot\beta^3\cdot B^2\cdot P}{24} \tag{64}$$

The above assumptions simplify the expressions in the previous articles, and a new set of equations and dimensionless coefficients is defined. Following the same steps, the flange rotation is equated with the shell rotation and solved for "M" and "Mg" [29],

$$M = \frac{1}{K1 - K2}\left[\frac{Mo}{B\cdot\pi} - \left(\beta\cdot\frac{t}{2} - K2\right)\frac{g^2\cdot\beta^2\cdot B^2\cdot P}{24}\right] \tag{65}$$

$$Mg = K4\cdot(Md + Mt + Mb) + K5\cdot g^2\cdot B\cdot P \tag{66}$$

A list of the new coefficients "K" is given in Appendix "A". Details of the derivation of the equations can be found in [29], where it was referred to as the Simplified Method of Solution.

4.5.1 **Effects of Internal Pressure on Flange Neglected**

Most methods of design analysis for flanges with ring gaskets neglect the effect of internal pressure on flange stresses, with little error. For full face gasketed flanges this is not the case, since internal pressure causes bending moments that affect the gasket moment "Mg".

Blach [29] suggested that it is possible to neglect the internal pressure only when computing flange moments and stresses, but include pressure effects in computing direct shell stresses.

This means it is possible to neglect the pressure term in Equ.(64) and a very simple relation between "M" and "Q" is obtained

$$\beta.M = Q \tag{67}$$

which, if substituted into Equ (42), results in the following shell rotation:

$$\theta_s = \frac{6\left(1 - \nu^2\right)}{E \cdot g^3 \cdot \beta} \tag{68}$$

Repeating the same steps as before, the following moment equations are derived:

$$M = \frac{Mo}{(L1 + L2) \cdot B \cdot \pi} \tag{69}$$

$$Mg = L4 \cdot (Md + Mt + Mb) \tag{70}$$

New coefficients "L" are given in Appendix "A", for both triangular and parabolic solutions.

4.6 Ring Theory Applied to Flat Faced Flanges

4.6.1 Design Equations

To simplify the tedious work involved in plate theory, Timoshenko[33] proposed a method that applies the theory of a narrow ring . In this section Timoshenko's method will be applied to the design of flat face flanges with full face gaskets. It is assumed that under the action of forces, the cross section of the ring is rotated without distortion. Denoting the angle "θ" as the angle of rotation, the radial displacement of any point "a" distance "z" from the middle surface of the ring is (z.θ), shown in Figure 14, from which,

$\epsilon = (\theta z)/x$ and $\sigma_t = E\theta z/x$

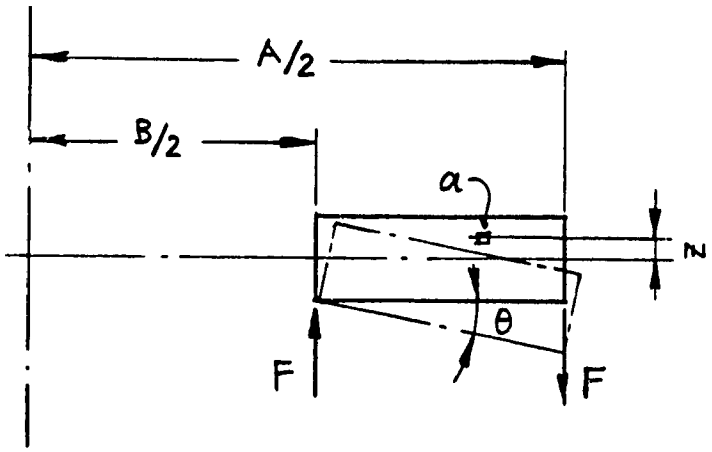

Figure 14: Ring Theory

It is explained that the stress $\sigma_t = E\theta z/x$, varies directly with the distance "z", therefore all the stresses over the cross section can be reduced to a couple "M1", acting at the centroid, in a plane perpendicular to the "x" axes. The magnitude of this couple is:

$$M1 = \int_{b}^{a} \int_{-t/2}^{t/2} E \cdot z \cdot \frac{\theta}{x} \, dx \, dz$$

$$M1 = \frac{E \cdot \theta \cdot t^3}{12} \cdot \ln(K) \tag{71}$$

Where

$$K = A/B$$

The same theory can be applied to a narrow ring twisted by moments uniformly distributed along the edge, after transforming "M1" to the inside diameter of the ring.

$$M1 = \frac{E \cdot \theta \cdot t^3}{6 \cdot B} \cdot \ln(K) \tag{72}$$

Since the flange is assumed to go through a rigid rotation, a triangular gasket force distribution is used. Following assumptions used in plate theory and simplifications described in sections (4.5 & 4.5.1), the solution of the unknowns, M, Mg and Q can be found as follows, From Equ.(68),

$$\theta = \frac{6 \cdot (1 - \nu^2) \cdot M}{E \cdot g^3 \cdot \beta}$$

Neglecting $(1- \upsilon^2)$, and substituting for "θ" in Equ.(72),

$$M1 = \frac{M \cdot \ln(K)}{B \cdot \beta} \cdot \frac{t^3}{g^3} \tag{73}$$

$$M1 = \frac{Mo}{\pi \cdot B} - M - Q \cdot \frac{t}{2}$$

$$\frac{M \cdot \ln(K)}{B \cdot \beta} = \frac{Mo}{\pi \cdot B} - M\left(1 + \beta \cdot \frac{t}{2}\right)$$

$$\frac{Mo}{\pi \cdot B} = M \cdot \left[\left(1 + \beta \cdot \frac{t}{2}\right) + \frac{\ln(K)}{\beta \cdot B} \cdot \frac{t^3}{g^3}\right]$$

$$M = \frac{Mo}{(L1 + L2)\cdot B\cdot \pi} \tag{74}$$

Applying Equ.(67), and substituting back into Equ.(52)

$$M1 = \frac{Mo}{\pi\cdot B} - \left(1 + \beta\cdot\frac{t}{2}\right)\cdot M$$

$$M1 = \frac{Mo}{\pi\cdot B} - \frac{L1}{L1 + L2}\cdot\frac{Mo}{\pi\cdot B}$$

$$M1 = \frac{L2\cdot Mo}{(L1 + L2)\cdot B\cdot \pi} \tag{75}$$

If flange rotation due to gasket compression force Equ.(22), is used

$$\frac{3}{1 + 2\cdot K}\cdot\frac{6\cdot M_g\cdot\left(t_g\right)}{G\cdot\pi\cdot E_g\cdot b^3} = \frac{6\cdot M1\cdot B}{E\cdot t^3\cdot \ln(K)}$$

$$\left(\frac{3}{1 + 2\cdot K}\right)\cdot\frac{t_g}{E_g}\cdot M_g = \frac{Mo}{\ln(K)}\cdot\left(\frac{L2}{L1 + L2}\right)$$

$$M_o = \left(\frac{L1 + L2}{L2}\right)\cdot\alpha\cdot L3\cdot Mg \tag{76}$$

where the following non-dimensional parameters are defined.

$$L6 = 1 + \beta \cdot \frac{t}{2}$$

$$L7 = \frac{\ln(K)}{B \cdot \beta} \cdot \frac{t^3}{g^3}$$

$$L8 = \frac{t^3}{b^3} \cdot \ln(K)$$

$$\alpha = \frac{3}{1 - 2 \cdot K} \cdot \frac{tg}{Eg} \cdot \frac{E}{G}$$

Substituting for Mo, from Equ.(25)

$$Mg = \frac{Md - Mt - Mb}{\mu + \alpha \cdot L3 \cdot \frac{L1 - L2}{L2}} \qquad (77)$$

4.7 Stresses

Stresses in the flange and shell are caused by both membrane forces and bending moments caused by pressure and flange rotation respectively.

4.7.1 Shell Stresses

The longitudinal shell stress at the junction "Sh1" is found by combining the membrane stress caused by the internal pressure and the bending stress caused by the discontinuity moment "M" at the junction.

$$Sh1 = (PB/4g) + (6M/g^2) \qquad (78)$$

The tangential (hoop) stress in the shell "Sh2"is found by combining the pressure stress (PB/2g) and the Poisson effect of the longitudinal discontinuity stress ($6.\upsilon.M/g^2$) to the direct extension shear stress [($\beta B/g$)(βM-Q)], which gives

$$Sh2 = \frac{P \cdot B}{2 \cdot g} + 6 \cdot \nu \cdot \frac{M}{g^2} + \beta \cdot \frac{B}{g} \cdot (\beta M - Q) \tag{79}$$

In applying the simplification of Article (4.5), the last term of this equation reduces to ($\beta B/g$)($g^2\beta^3 BP/24$) and Equ.(78) becomes

$$Sh2 = \frac{P \cdot B}{2 \cdot g} \cdot \left(1 - g^2 \cdot \beta^4 \cdot \frac{B^2}{12}\right) + 6 \cdot \nu \cdot \frac{M}{g^2} \tag{80}$$

If the internal pressure is also neglected as shown in Article (4.5.1), then the last term of Equ.(79) vanishes, and the tangential stress becomes

$$Sh2 = \frac{P \cdot B}{2 \cdot g} + 6 \cdot \nu \cdot \frac{M}{g^2} \tag{81}$$

The tangential stress is reduced at the junction due to the influence of the flange ring which prevents extension of the shell.

4.7.2 **Flange Stresses**

Radial stresses in the flange are caused by discontinuity moment applied at the junction. The radial bending stress is found by dividing the moment "M", by the section modulus ($t^2/6$),

$$S = 6M/t^2 \quad (82)$$

From Equ.(51) the tangential stress caused by flange rotation is:

$$S_T = YM1/t^2B$$

For integral ring flanges the ASME Code applies the following equation

$$S_T = YMo/t^2B - ZS_R$$

where, $Z = (K^2+1) / (K^2-1)$

For loose type flanges the Code uses the following equation:

$$S_T = YMo/t^2B \quad (83)$$

which may be applied in the case of flat faced full face flanges.

4.8 Results of Analytical Analysis

Results of analytical methods are plotted in Figures 15 through 21 for three vessels A, B , C, having different K values (1.175, 1.416, 1.5) based on three different analytical solution procedures. Comparing these methods it is seen that the ring theory, section (4.6), gives results that are similar to a triangular gasket distribution in plate theory given in Article (4.4.1) and they both have results that are less than the experimentally measured data. The parabolic gasket force distribution gives the safest results for all the vessels and gasket types. It will be the only method considered for later design work.

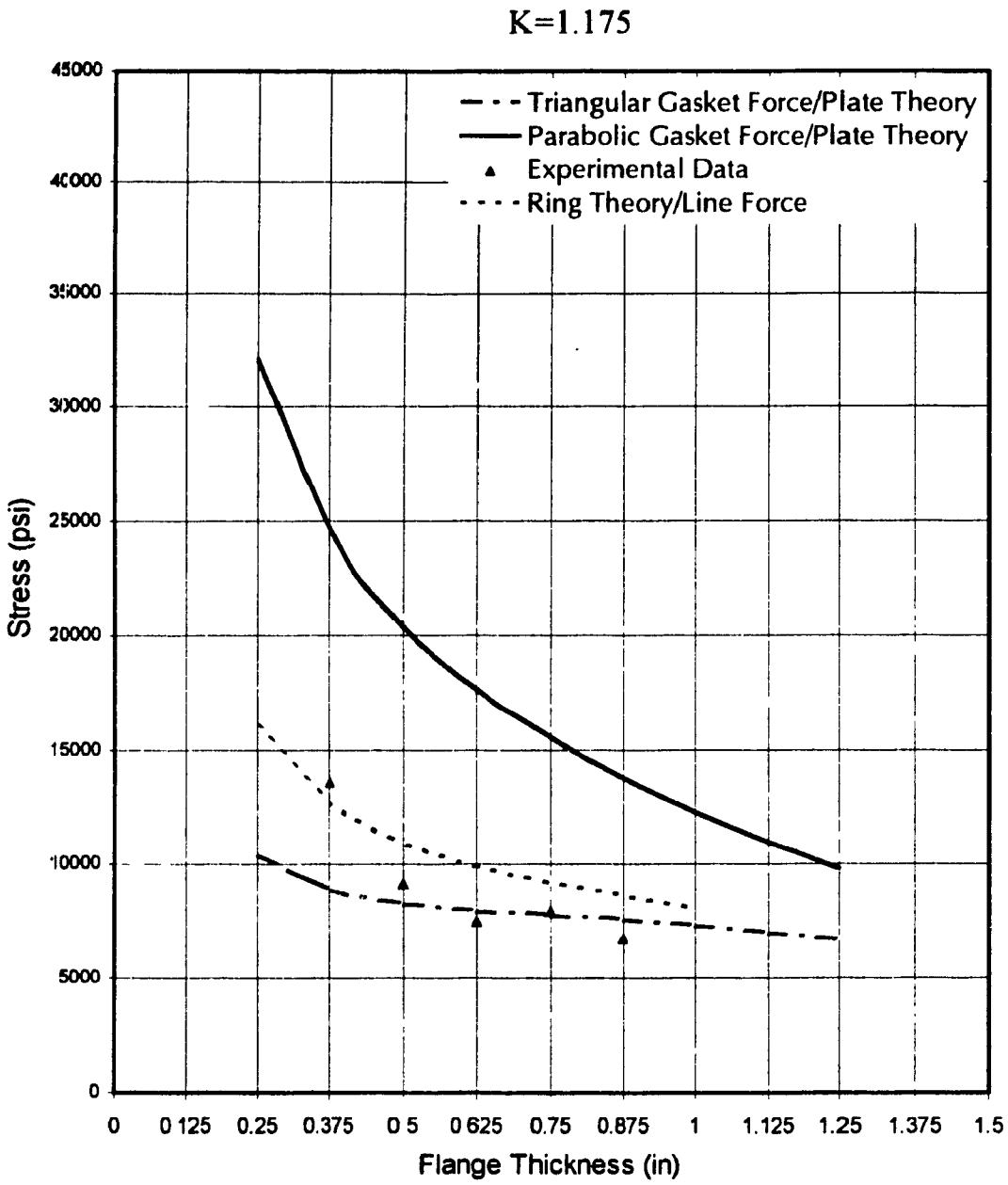

Figure 15: Maximum Tangential Flange Stress vs Flange Thickness for Flange Connection With "1/16in" Full Face Asbestos Gasket Results From Theoretical & Experimental Data

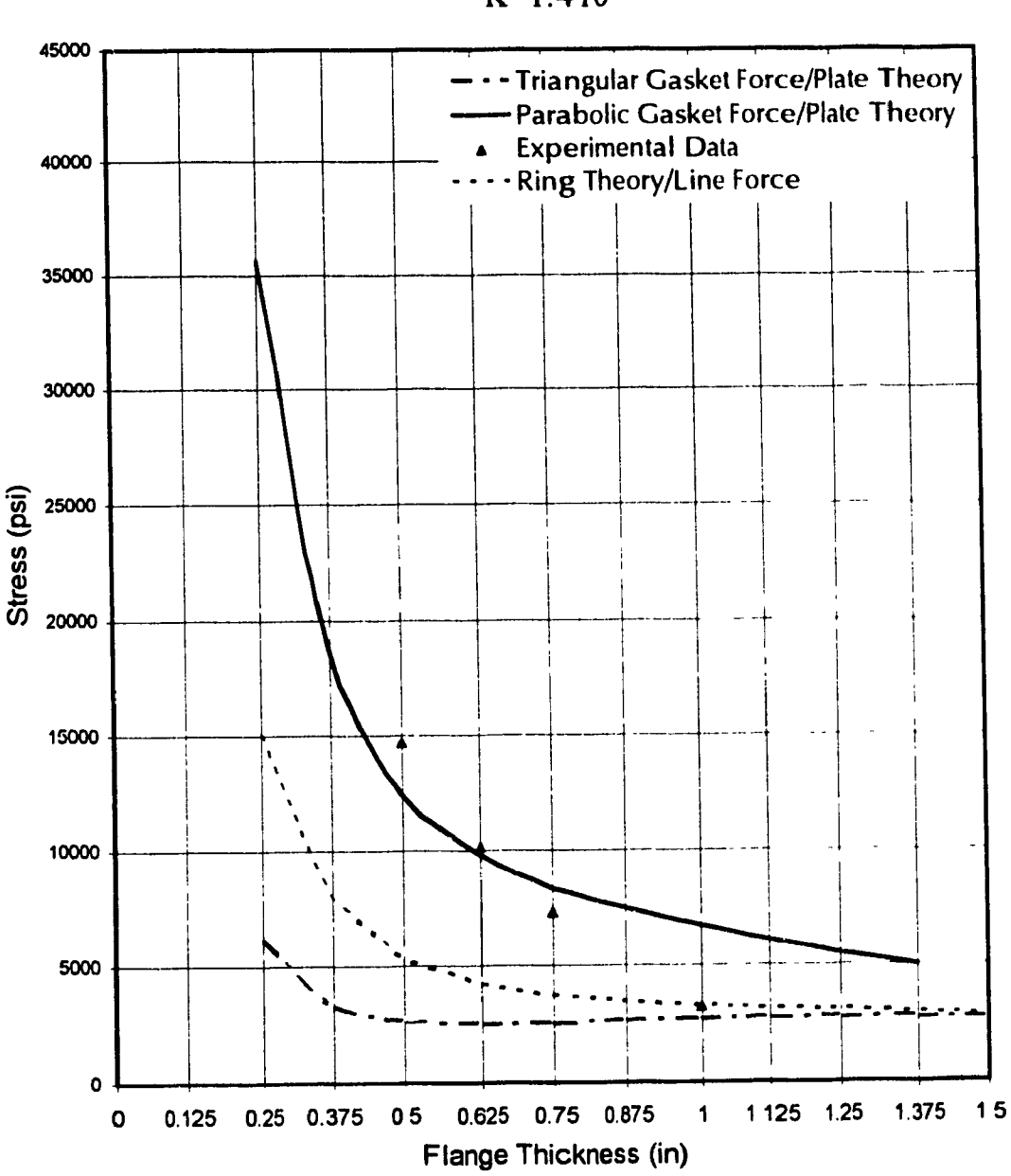

Figure 16: Maximum Tangential Flange Stress vs Flange Thickness Flange Connection With "1/16in" Full Face Rubber Gasket Results From Theoretical & Experimental Data

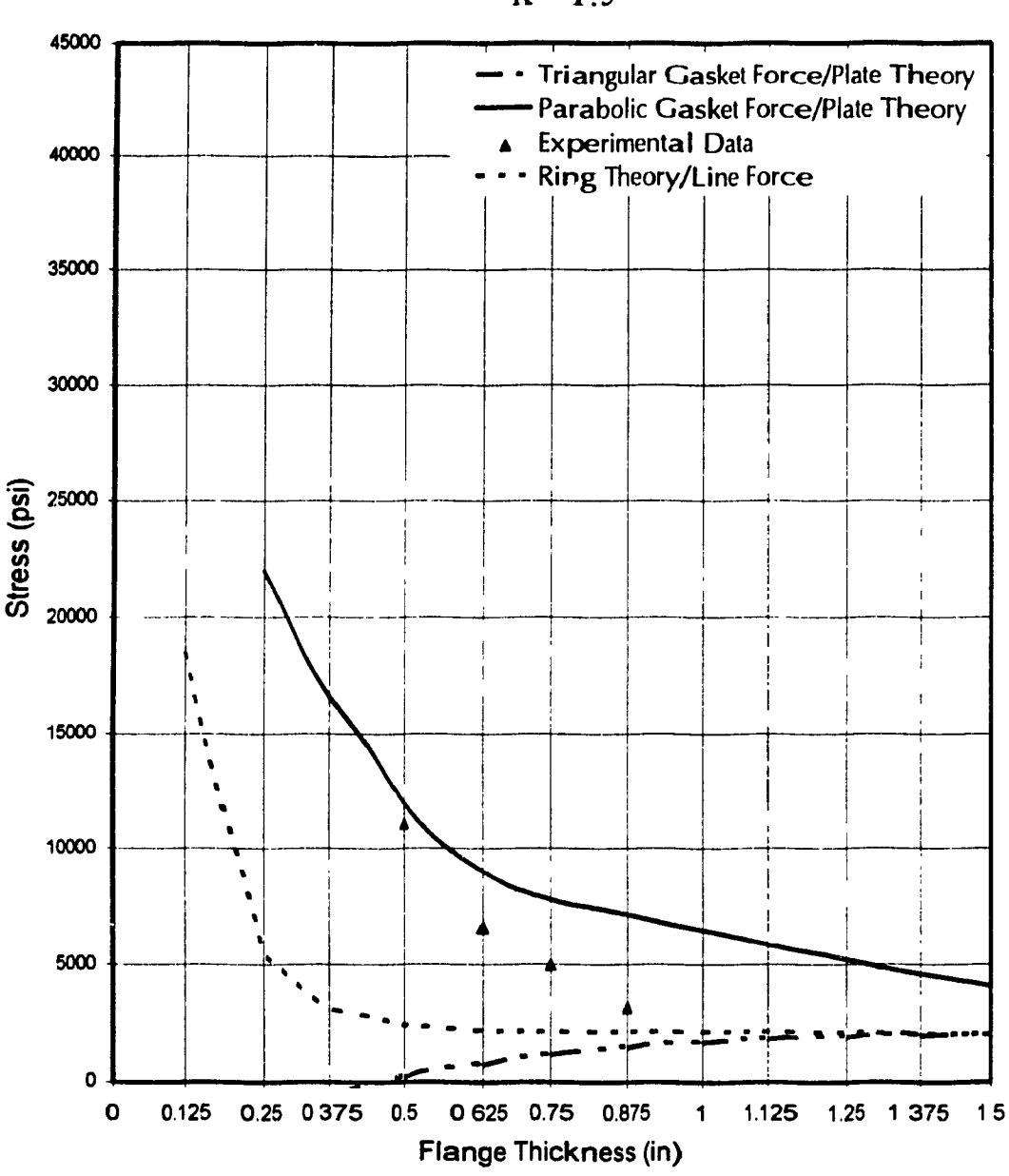

Figure 17: Maximum Tangential Flange Stress vs Flange Thickness Flange Connection With "1/16in" Full Face Asbestos Gasket Results From Theoretical & Experimental Data

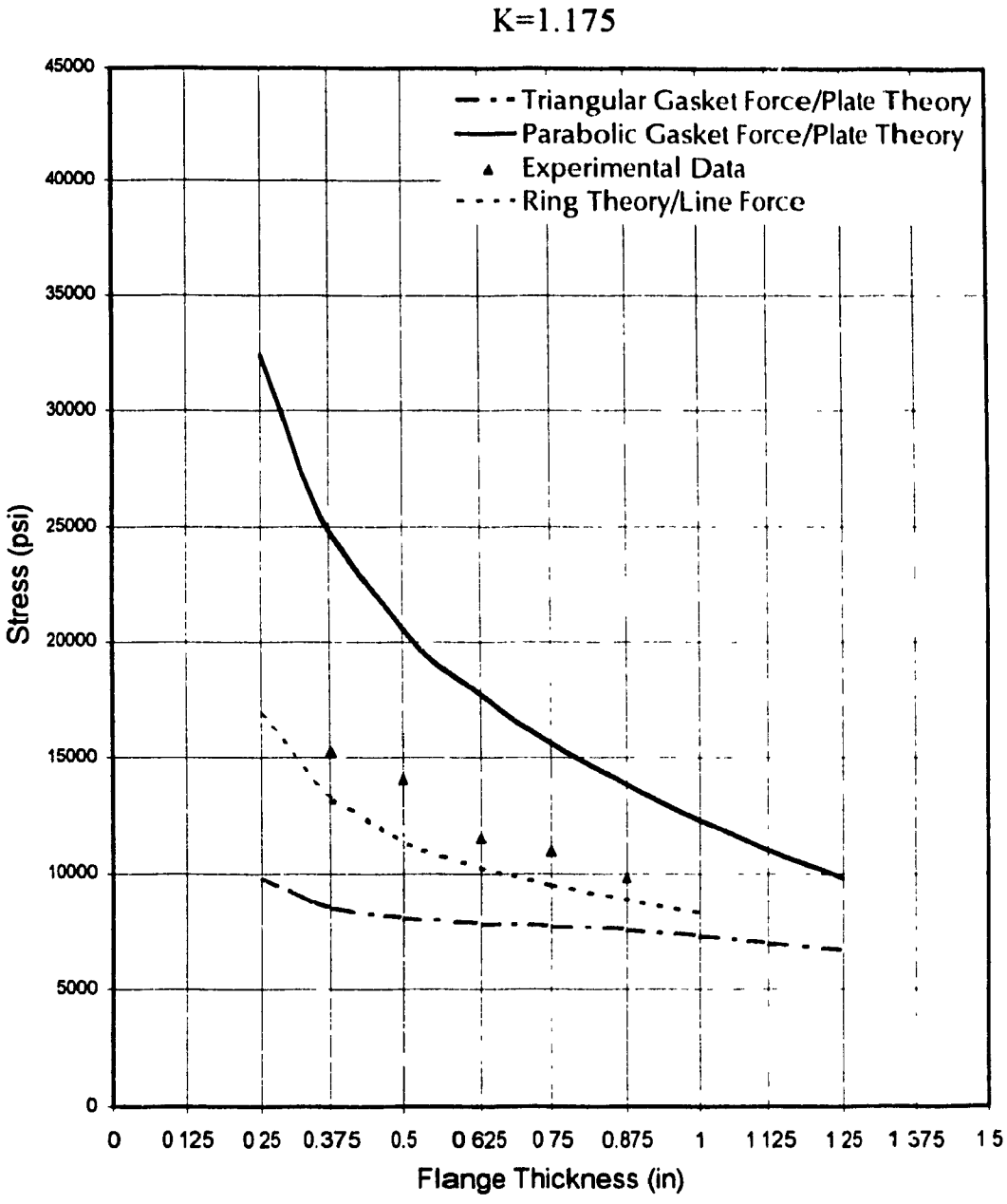

Figure 18: Maximum Tangential Flange Stress vs Flange Thickness Flange Connection With "1/16in" Full Face Rubber Gasket Results From Theoretical & Experimental Data

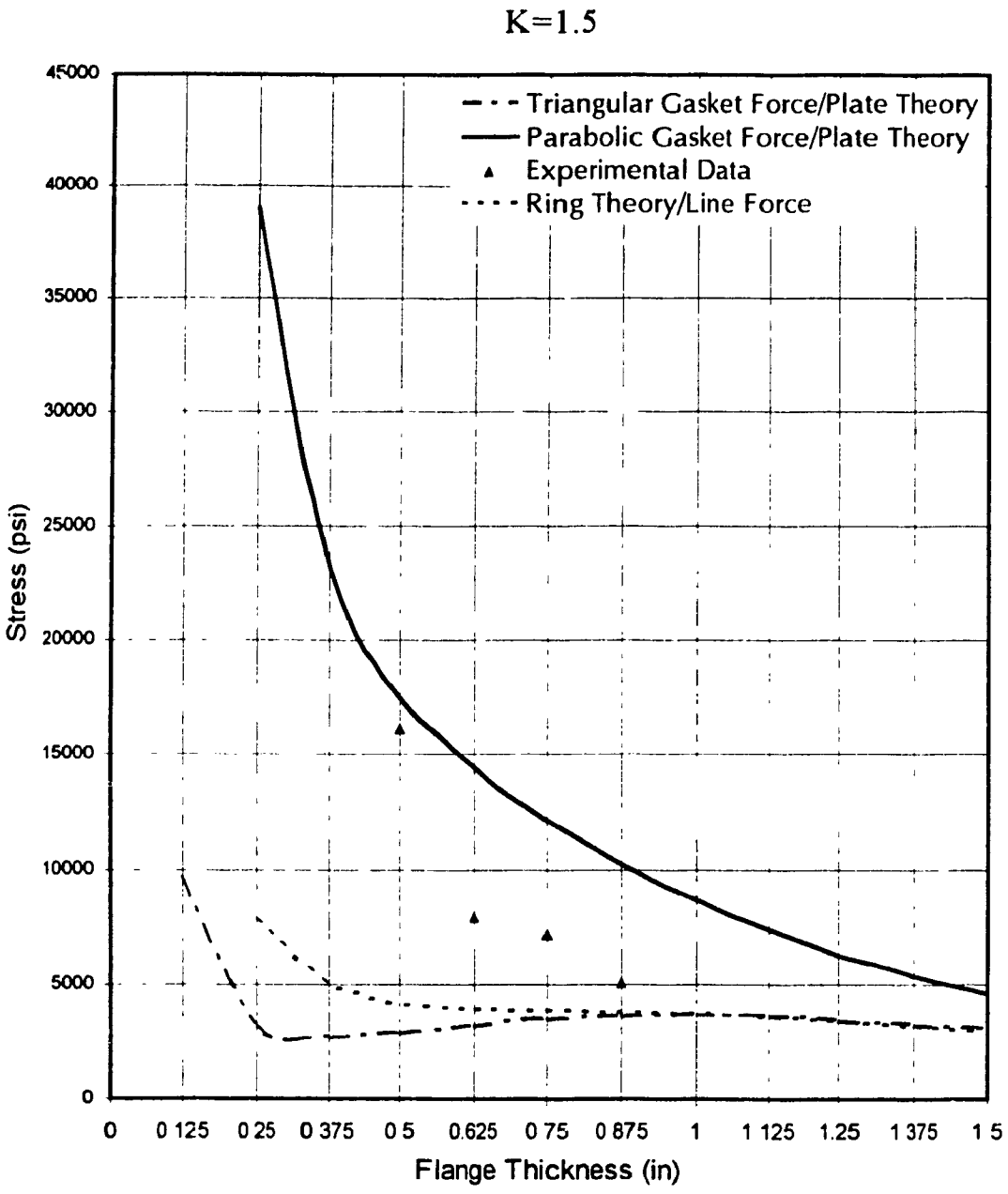

Figure 19: Maximum Tangential Flange Stress vs Flange Thickness Flange Connection With "1/8in" Full Face Rubber Gasket Results From Theoretical & experimental Data

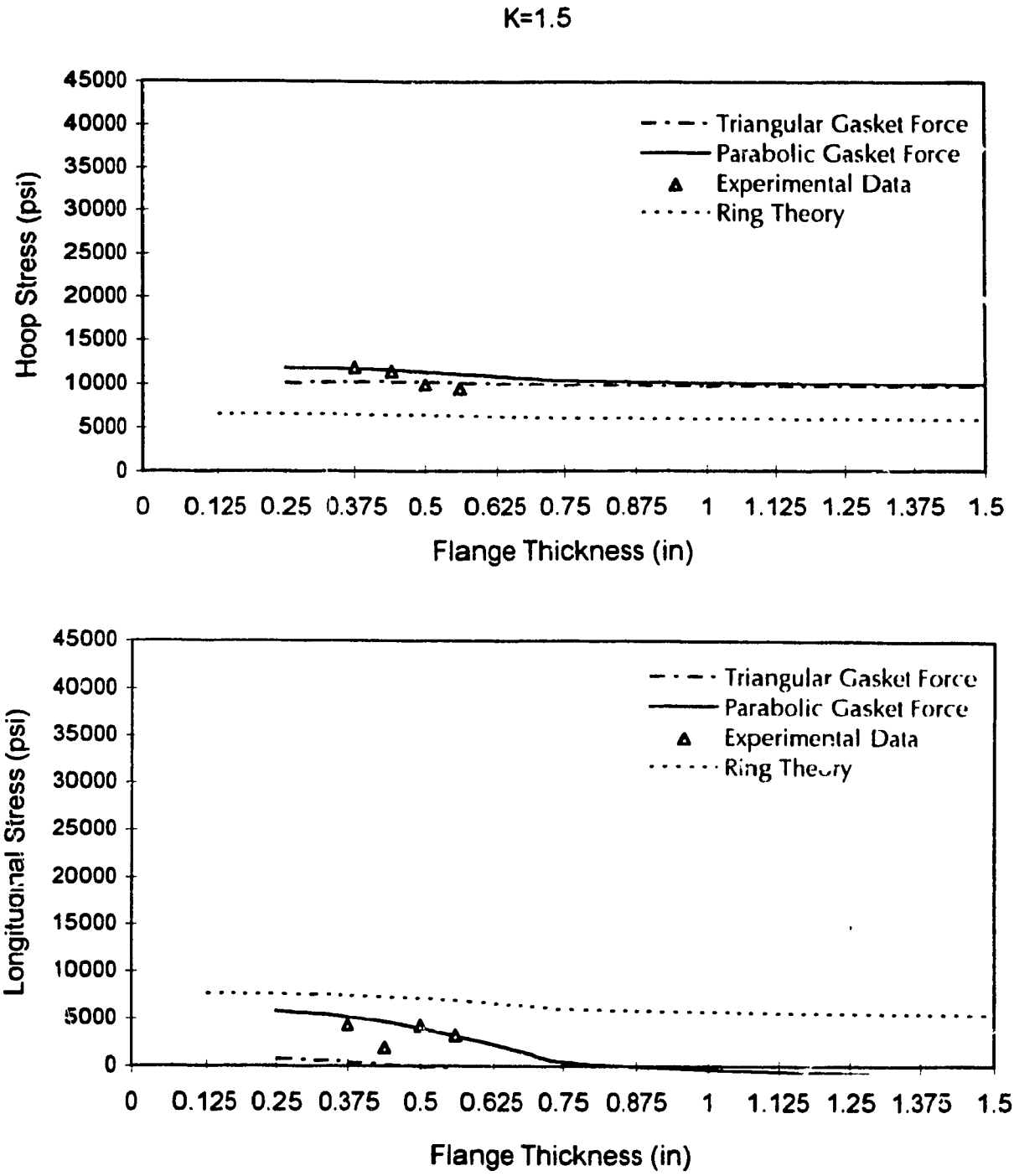

Figure 20: Hub Stress, 1/16 in Rubber Gasket, Vessel "B"

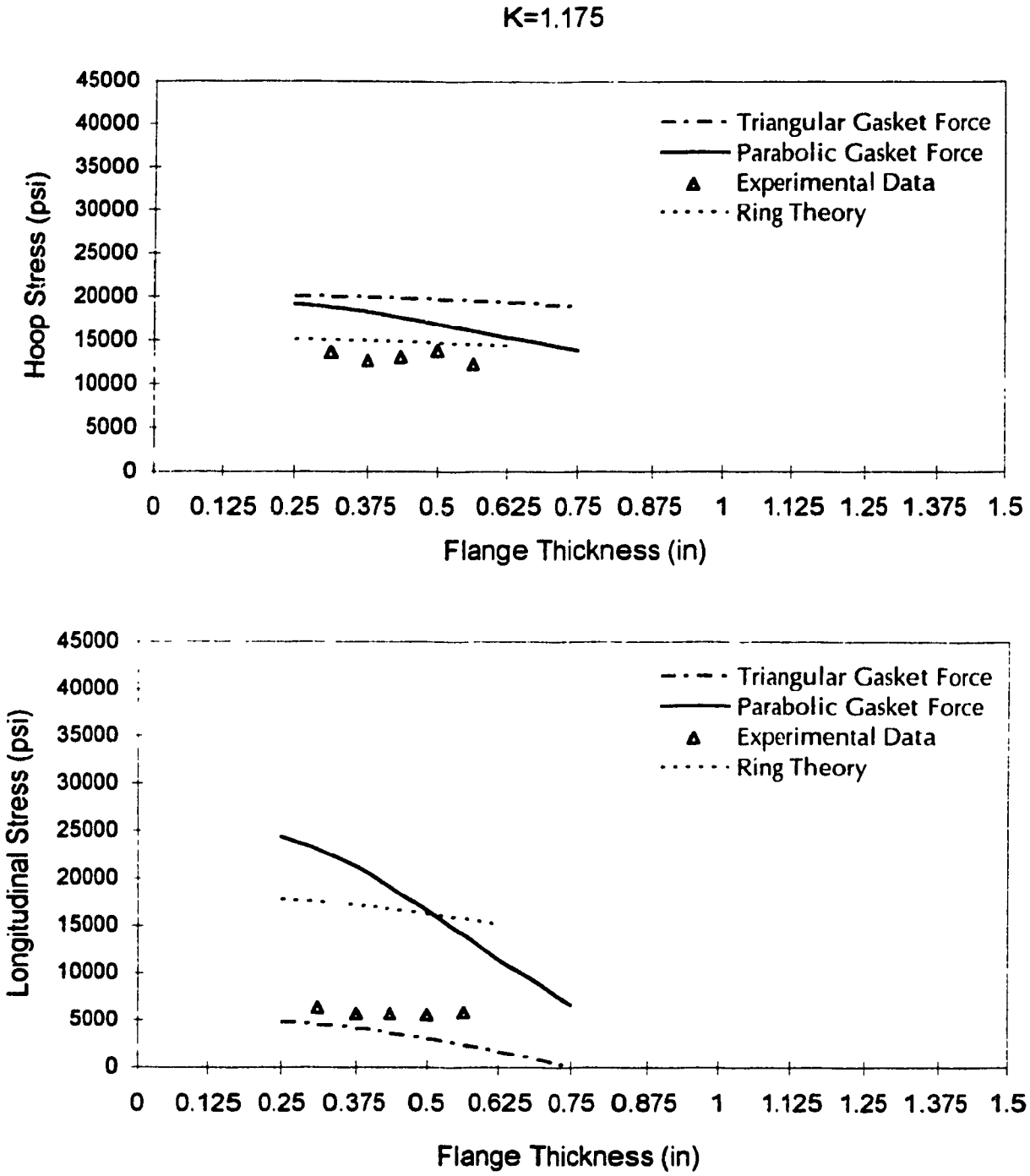

Figure 21: Hub Stress, 1/16 in Rubber Gasket, Vessel "A"

4.9 Summary

Equations to describe the flanged structure were developed and solved. The vessel wall is represented using shell equations. Flange equations are derived using two methods, plate theory and Timoshenko's ring theory, using both, linear and parabolic gasket force distributions. From continuity at the shell-flange junction a solution for the unknown discontinuity moment and force is obtained. Finally equations for stresses in shell and flange were developed. The flange tangential stress is based on the ASME Code "loose optional" type flange equations. Results from a parabolic gasket force distribution proved to be the safest, and the method is chosen for the design of bolted flat faced full face gasketed flange connections. In the next chapter stresses calculated from this method are compared with finite element and experimental results.

CHAPTER FIVE

FINITE ELEMENT ANALYSIS OF FLANGED STRUCTURE

5.1 General

To verify the analytical solution presented earlier, two approaches are undertaken. A finite element approach presented in this chapter is followed by an experimental work discussed in Chapter 6 .

The work that follows pertains to an axisymmetric finite element model based on a linear analysis of the flange. The gasket is modeled in two different ways. The first takes into account the gasket by replacing the contact gasket force by a parabolic force distribution, thus following the earlier analytical design work. The second incorporates the gasket into the model by representing it with nonlinear gap elements instead of the approximate parabolic force distribution.

5.2 Introduction

The Finite Element method [36] is a piece-wise approximation where the approximating function is formed by connecting simple functions, each defined over a small region called element, by interpolation from nodal values on the boundary to maintain inter-element continuity.

Finite element analysis has become popular with fast digital computers. The ability of computers to solve a large number of simultaneous equations in a relatively short period of time opted engineers to utilize numerical approximation methods for the analysis of complicated structures. The power of this method resides principally in its versatility. It can be applied to various physical problems with arbitrary shapes, loads and support conditions. A finite element analysis applied to a bolted flange connection can be a very helpful tool, because of its flexibility and ability to calculate strains and deflections anywere in the structure, unlike experimental verification, which can only measure surface strains at limited points, and is also costly and time consuming.

5.3 Finite Element Model of The Flanged Structure

Many satisfactory elements have been formulated and reside in popular programs. Properties of the structure, the finite element program, the purpose for the model and the computer working space and CPU time control the type of elements to be used in a specific model. For the purpose of verification of design of circular flat faced flanges with full face gaskets, 2-D linear axisymmetric elements are sufficient to accurately model flange and shell.

5.4 Structural Symmetry

Both, the cylindrical shell and the ring flange are solids of revolution that are generated by revolving a plane about an axis, that is most easily described in cylindrical coordinates r, θ and z [34] . Since this geometry is axially symmetric, it is called Axisymmetric Structure. In this case the material is isotropic and material properties, loads, and support conditions are axially symmetric, also displacements and stresses are independent of "θ" which means the circumferential displacement is zero and only radial and axial displacement components exist. This concludes that the flange-shell problem is mathematically two-dimensional. Taking advantage of this full

axial symmetry, the flanged structure can be modeled using 2-Dimensional (2D) axisymmetric elements.

5.5 **The ANSYS Finite Element Program** [35]

The ANSYS software, a production of Swanson Inc., is a large scale general purpose finite element program that has capabilities for linear and non-linear static and dynamic analysis. It can handle small and large displacements and solve elastic and plastic problems. It utilizes the matrix displacement method for the analysis and the wave front method for matrix reduction. Over a hundred different elements are available in its library.

Three phases are involved in the ANSYS finite element analysis. The pre-processing stage, where data such as geometry, materials and element types are provided, either interactively or through a batch file. The solution stage where the analysis type and options are defined, loads are applied and the program initiates the element solution. Post processing, where results can be reviewed through graphics displays and tabular listings.

5.6 Element Types used in Model

An assemblage of axisymmetric shell and plane elements are used for the shell and flange, respectively. In order to verify the analytical approach used earlier, the gasket is first replaced by a parabolic force distribution acting on the flange contact face. To test the effect of the gasket material on flange stresses, the gasket is included in the model using interface elements with a relative stiffness that is a function of the gasket material used.

5.6.1 Axisymmetric Shell and Plane Elements

Axisymmetric elements take advantage of the axial symmetry of the structure, thus reducing a complicated modelling task to one that is straight forward and easy to review. 2-D Axisymmetric elements, if they can be applied, give better results when compared with 3-D analysis [35].

For elements that are based on displacement fields, the general equation for the element stiffness matrix is given below,

$K = \int [B]^T [E] [B] . dv$ where

$[B] = [\delta] [N]$ where $[\delta]$ is the derivative

[E] : Is the material property matrix

[N] : Is the shape function matrix

5.6.2 **Three Dimensional Interface** [36]

This element represents two surfaces that may maintain or break physical contact and may slide relative to each other. The element is capable of supporting only compression in the direction normal to the surfaces and friction shear in the tangential direction, it has three degrees of freedom in x, y, z directions. When applied in the bolted flange connection, the element is only given a normal stiffness "K_n" that corresponds to the gasket material used. "K_n" will resist the flange compression only. This element has an advantage over using plane elements with different material properties for the gasket, because it allows possible separation along the gasket-flange contact area, common in flanged connections under pressure.

The stiffness matrix, also element properties for plane, shell and interface elements, are given in Appendix "B".

5.7 **Parameters Applied to the Model**

5.7.1 **Dimensional Parameters**

Dimensional parameters for the F.E. models are based on the dimensions of the pressure vessels used in the experiments described in Chapter 6.

In addition to the three different flanges tested with "K" values at 1.175, 1.416, 1.5, flanges with "K" values at 1.6 and 2 were also modeled. To find the effects of shell thickness on flange stresses, shells ranging in thickness from 1 to 4 times their basic thickness "g" were also modeled. Input parameters for the three vessels are given in Table (1).

5.7.2 Loading and Boundary Conditions

The bolt pre-loading is assumed to be uniformly distributed along the bolt circle which in an axisymmetric model is applied based on a 360° basis, that is the load value used is given in terms of the total load around the circumference, and applied at a node that lies on that bolt circle. Pressure load during operating conditions is applied uniformly on the shell elements representing the inside vessel walls. Parabolic gasket reaction force is applied on the flange surface elements in contact with the gasket. Boundary conditions are applied to prevent rigid body motion, they consist of constraints applied at the symmetry planes.

TABLE (1)

INPUT DIMENSIONAL PARAMETERS

VESSEL	Vessel A	Vessel C	Vessel B
K = A/B	K=1.175	K=1.416	K=1.50
A (in)	11.75	17.0	15.0
B (in)	10.0	12.0	10.0
C (in)	11.0	14.5	13.0
t (in)	0.25-1	0.25-1	0.25-1
g (in)	0.065	0.18	0.12
Bolt No.	16	16	12
P (psi)	200	200	200

5.7.3 **Material Properties**

Materials for the flange and vessel are made of crbon or stainless steel. The gasket materials used are either synthetic rubber or compressed asbestos.

SYMBOL	DESCRIPTION	VALUE
E	Modulus of easticity of flange and shell	$29x10^6$ psi (C.S) $28x10^6$ psi (S.S)
υ	Poisson's ratio of flange and shell	0.3

5.8 **Mesh Configuration**

The advantage of the 2-D axisymmetric model is its simplicity and ease of generation, where node points are cross sections of nodal circles. To build the model, a direct node and element generation approach is applied. After performing a number of initial analyses with various mesh refinements it was concluded that twelve (12) plane elements in two layers along the flange width and twenty four (24) axisymmetric shell elements along the shell length are sufficient to give good results.

5.9 Results of the Finite Element Analysis

5.9.1 Stress and Deflection Profiles In Operating Conditions

Under operating conditions the flanged structure is loaded with bolt load and pressure load. From input parameters given in Table (1), the results of the modeled structures, based on a parabolic gasket reaction force give certain deflection and stress profiles that are shown for the experimentally tested flanges in Figures 22 and 23. From the stress profiles it is observed that the maximum flange stress is the tangential stress located near the shell-flange junction. The maximum radial stress, located at the junction is lower. It is also observed that, as the flange thickness is reduced, the flange tangential and radial stresses tend to increase and, for very thin flanges, may exceed the tangential stress. This, however, is unrealistic for flat faced flanges where the flange thickness is always much greater than the shell thickness and only relatively soft gaskets are used.

In the shell, as the flange thickness increases, the longitudinal maximum stress tends to move away from the junction, exceeding the tangential stress at certain points. The tangential (hoop) stress is higher due to the membrane effect of the internal pressure, except at locations where the bending moment effects are high.

K=1.175

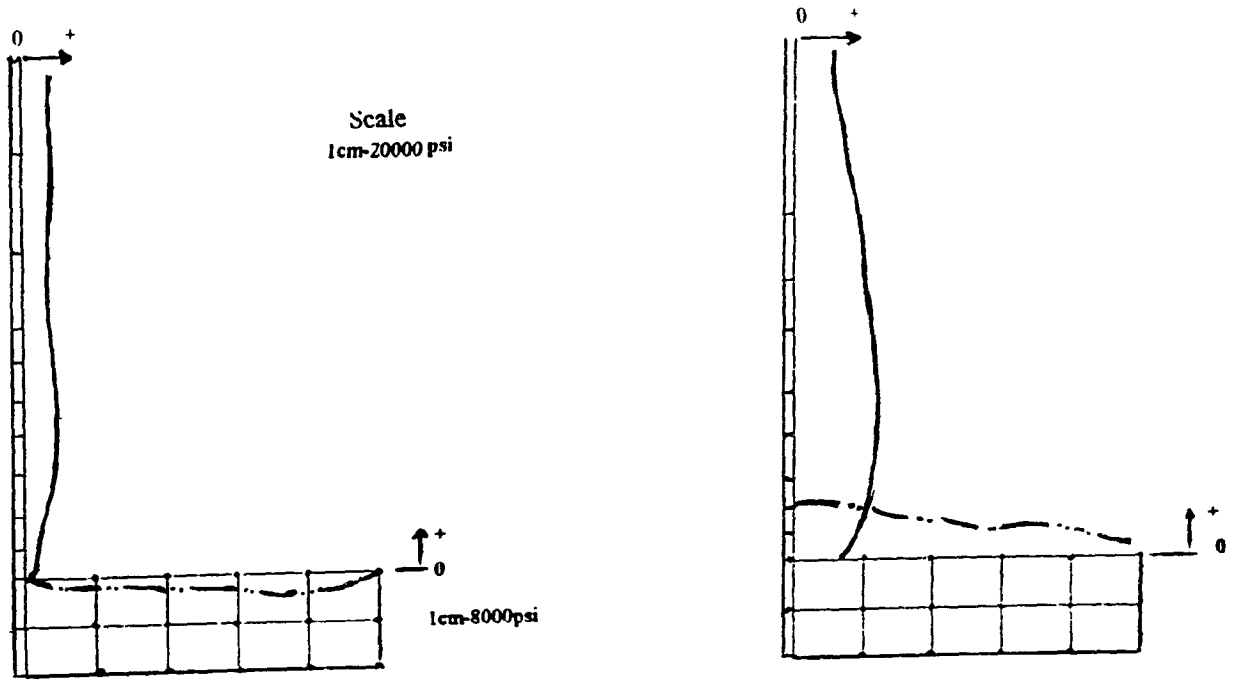

___Longitudinal Hub

___Tangential Hub Stress

_._._Radial Flange

_._._Tangential Flange Stress

Figure 22: Stress Profiles For Vessel "A"

K=1.5

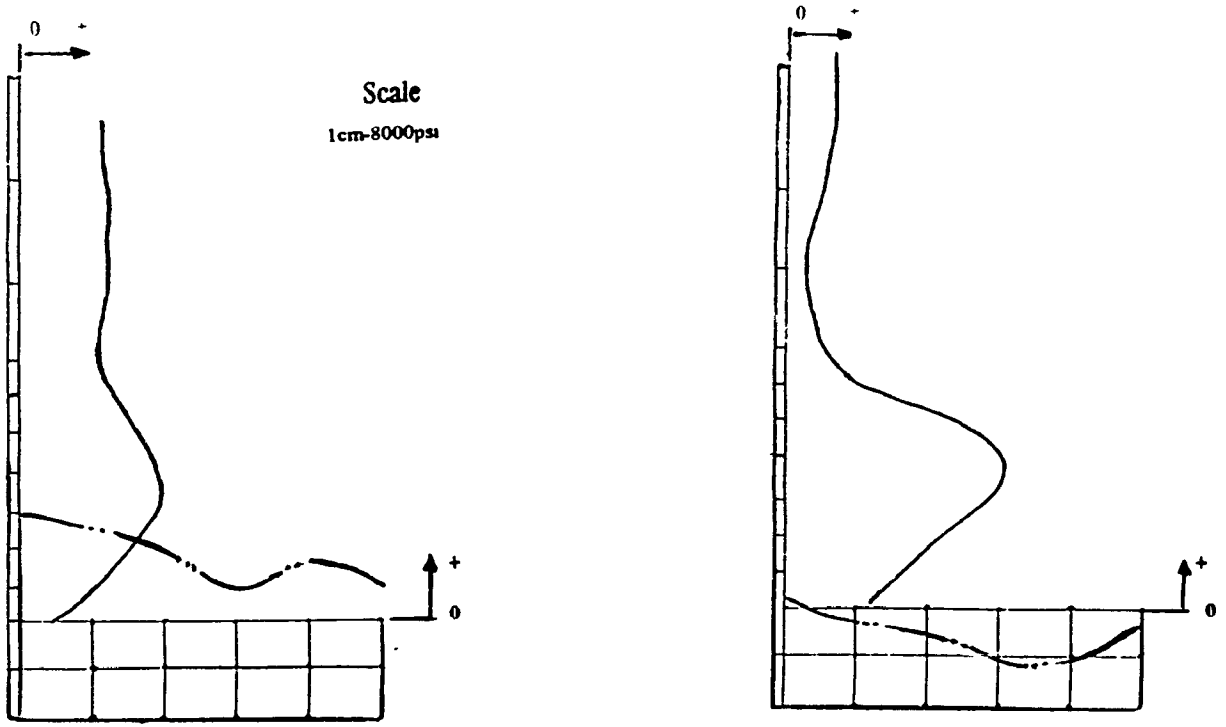

____Tangential Hub Stress

____Longitudinal Hub

_ . . _Tangential Flange Stress

_ . . _Radial Flange

Figure 23: Stress Profiles for Vessel "B"

5.9.2 Effects of Flange Thickness on Stresses

As mentioned earlier, the tangential stress increases in the flange as its thickness is reduced, which is shown in Figure 24, for a number of "K" values. The radial stress may become significant for thin flanges used with stiff gaskets, this however occurs when the flange deforms which can cause leakage. It is also clear that as the ratio (K=A/B) increases, the stresses also increase. This is also expected in circular flat plates with central holes subjected to a couple.

5.9.3 Effects of Hub Thickness on Flange Stresses

In order to completely understand the behaviour of the bolted flanged connection it is necessary to consider the effect of the hub thickness on the maximum stresses in the flange, it is after all the interaction between the shell and the flange that determines the amount of fixation at the shell-flange junction. In practical applications the ratio of flange to hub thickness usually exceeds 3. The model thus uses hub thicknesses that give ratios (t/g) ranging from 2 to 8. For a given flange thickness the maximum stress results are plotted in Figures 25 and 26, respectively, for two structures (K=1.175 and K=1.5), and for hub thicknesses ranging from .065 inch to .25 inch. These results indicate clearly that for the thick 1 inch flange the hub influence is

negligible. For the thinner .50 inch flange, though, the radial flange stress tends to increase as the hub thickness increases, while the tangential maximum stress goes down. This, however, does not become significant until the ratio (t/g) is less than three. In low pressure applications for flat face flanges higher ratios exist.

5.9.4 Gasket Materials

The most ambiguous part of a flanged joint is the contact area between the flange and the gasket; any non-linear behaviour of the gasket can only be speculated and incorporated into the flange design based on simplifying assumptions. To evaluate the effect of the gasket material on flange stresses, the gasket is included in the model as an interface element possessing normal stiffness in compression. The gasket is assumed to be elastic and to follow Hooke's law. Results indicate that, as the stiffness of the gasket is increased, the radial stress increases until a point is reached where the radial stress exceeds the tangential stress; at this stage the flange is deformed considerably and is expected to leak.

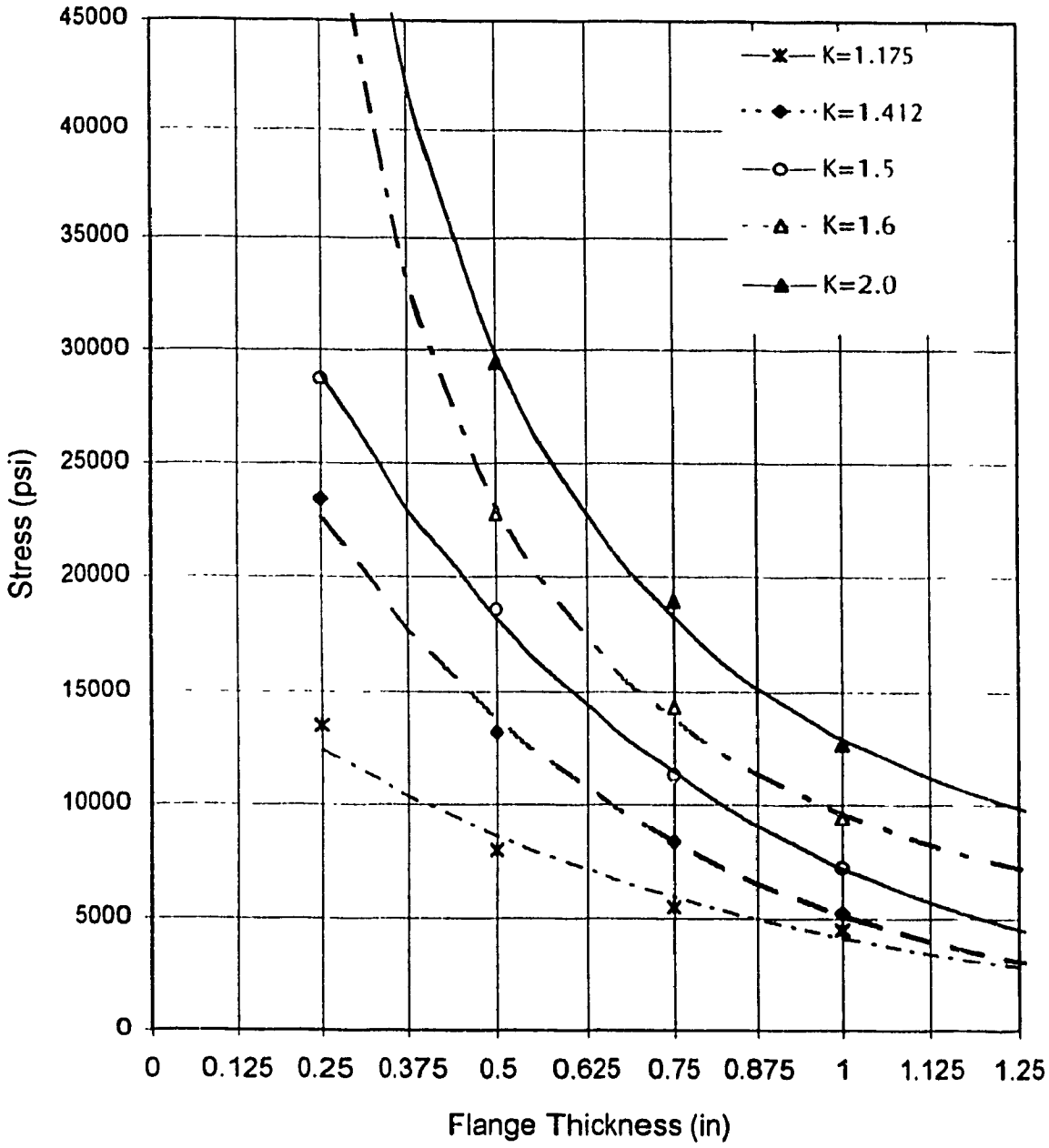

Figure 24: Effect of Flange Thickness on Tangential Stress For Different "K" Values

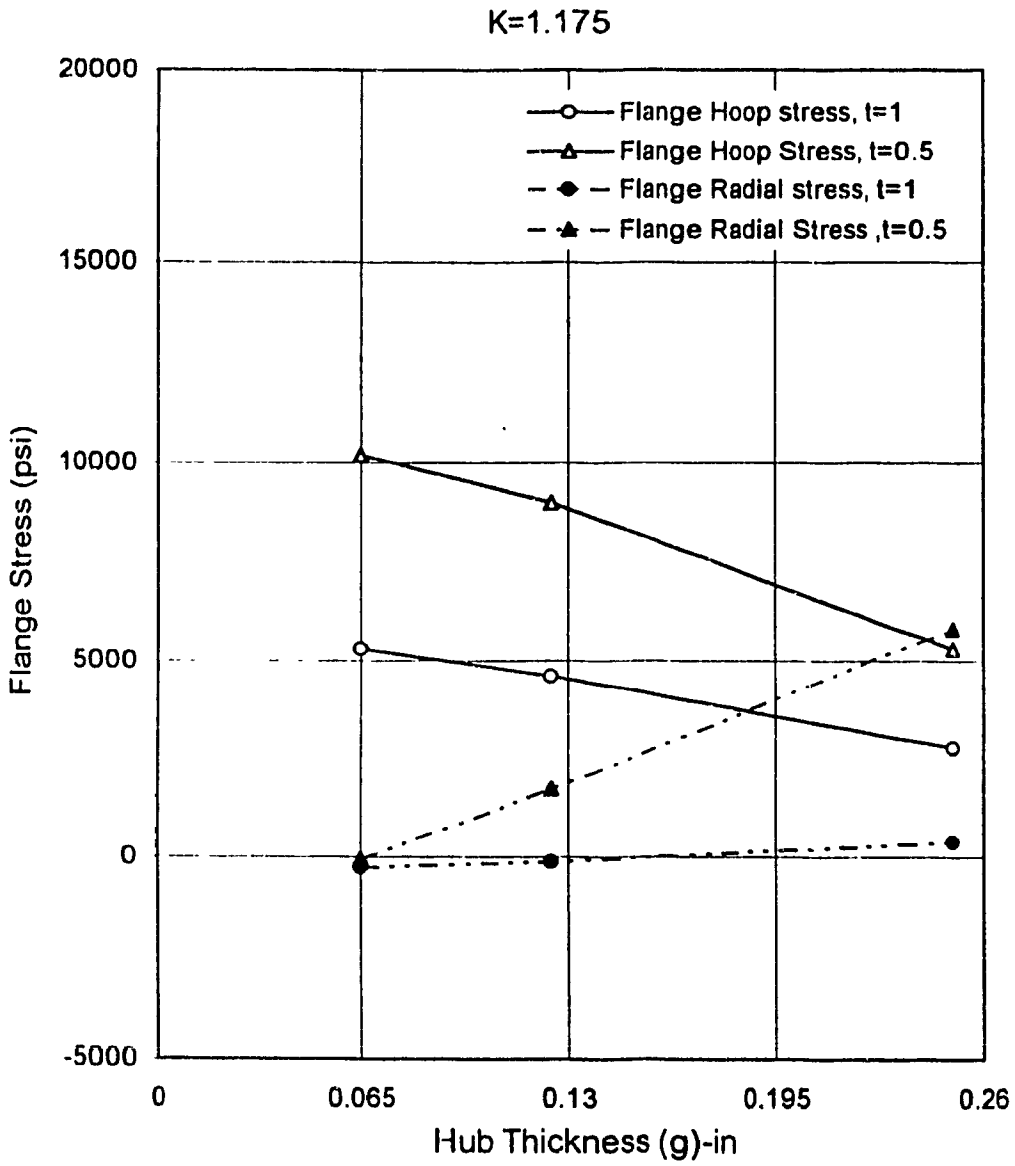

Figure 25: Effect of Hub Thickness on Flange Stresses

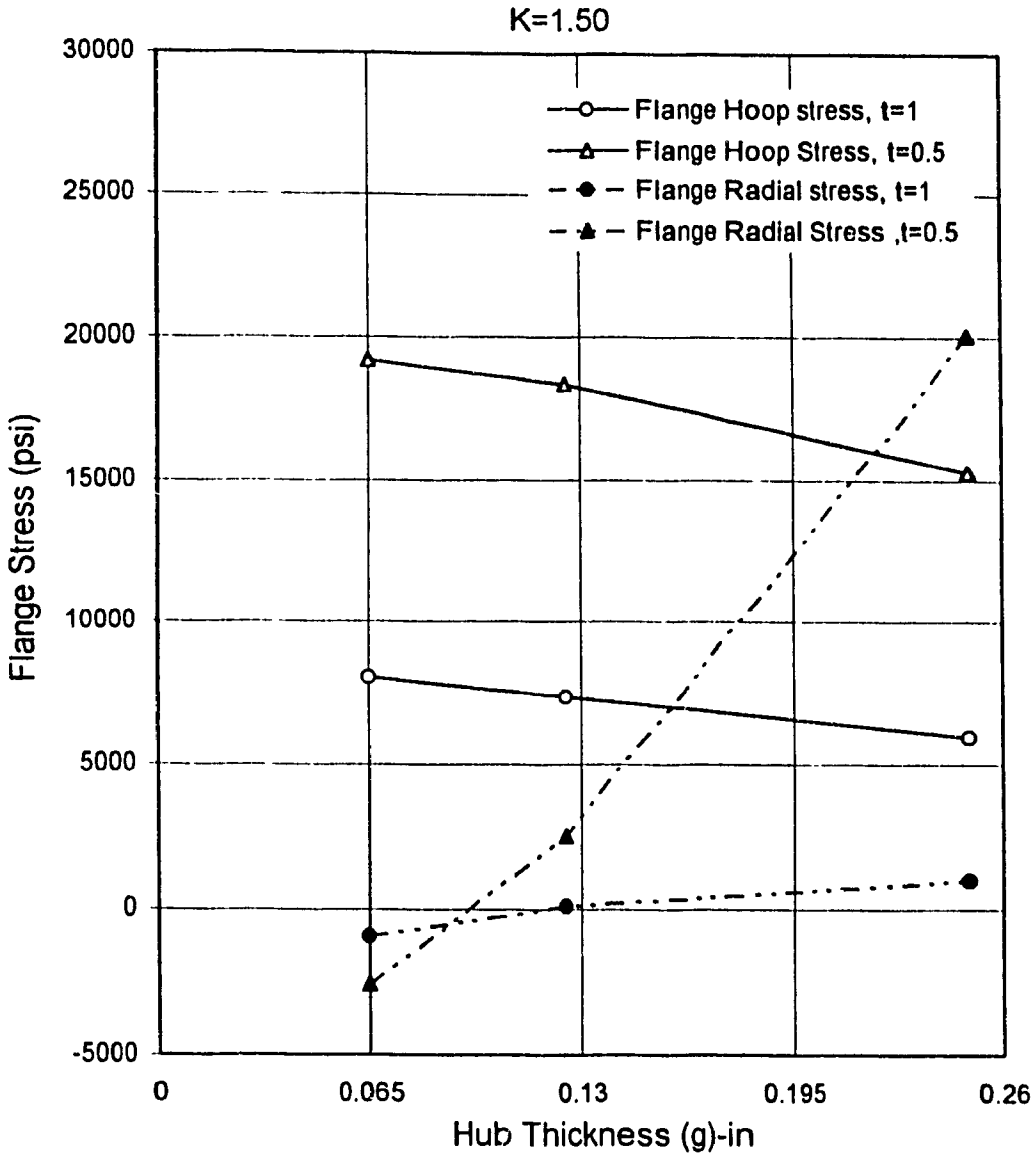

Figure 26: Effect of Hub Thickness on Flange Stresses

5.10 **Summary**

It is apparent that a simple finite element model like the one that was used can give results that experimental work will take a lot of time to accomplish. It is also clear that a flanged structure has many interrelated parts, the effect of which may be great or may not have much influence on the structural behaviour. Such a number of variables may confuse and even discourage many engineers from attempting to design a bolted flange. Results from finite element analysis can very much limit and clarify some of the ambiguity associated with analytical and experimental results. It is concluded that the tangential (hoop) stress is to a certain extent dominant in flat faced flanged connections under operating conditions. In pre-load conditions lower stress profiles exist and the tangential stress is not as significant as in operating conditions. The larger the "K" ratio, the larger the stresses become. The longitudinal hub stress is higher near the shell-flange junction, the maximum value tends to move away as the flange thickness is increased. Finally the hub thickness has little effect for t/g ratios more than three.

CHAPTER SIX

EXPERIMENTAL WORK

6.1 General

Experiments are the means by which analytical and numerical results can be verified. The objective of the experimental work is to find the actual behaviour of the bolted flat face flanged structure. From measurement of strains on the surface of the shell and flange, stresses are calculated.

6.2 Experimental Setup

6.2.1 Description of vessels

Three Pressure vessels are fabricated in accordance with the ASME Code, Section VIII, Division 1 design rules. Their dimensional and material specifications are given in Table 2, see Figures 27 through 31.

The required thicknesses are calculated based on the following ASME Code equations :

The shell as per, UG-27 (c)

$t=PR/(SE-0.6P)$

Flat heads as per UG-34(c)(2), with 100% joint efficiency;

$t= d(CP/SE)^5$ where "E" is the joint efficiency and "C" is a fixation factor.

TABLE -(2)
VESSEL SPECIFICATIONS

	Vessel A	Vessel B	Vessel C
Allowable P	200 psi	200psi	175psi
Design Temp.	200 F	200 F	200 F
Material	SA-240-304	SA-516-70	SA-516-70
Allowable stress	17800 psi	17500 psi	17500 psi
Bolts. Material	SA-193-B7	SA-193-B7	SA-193-B7
Bolt All. Stress	25000 psi	25000 psi	25000 psi

6.2.2 **Description of Flange**

Flanges are welded to the shell with full penetration welds which allow the gradual reduction of the flange thickness for different tests. A fillet weld along the back side of the flange reduces stress concentrations at the junction. Flanges for vessels "B" and "C" were fabricated, 1 inch thick; vessel B, however, was received with undersize flanges and was machined at Concordia to 0.875 inch thick. Vessel "A" was ordered 0.625 inch thick, and also received with rough surfaces, that required machining to 0.562 inch.

TABLE-(3)

FLANGE PARAMETERS

	VESSEL A	Vessel B	Vessel C
K value	1.175	1.50	1.416
Bolt Hole Dia.	7/16 in	7/8 in	7/8 in
No. Of Bolts	16	12	16
Bolt Diameter	3/8 in	3/4 in	3/4 in
Bolt Circle Dia.	10 in	13 in	15 in

6.2.3 **Description of Gasket**

1/8" Neoprene, 75 - 80 Durometer

1/16" Neoprene, 75 -80 Durometer

1/32" Neoprene, 75 -80 Durometer

1/8" Compressed Asbestos (anchor packing)

1/16" Compressed Asbestos (anchor packing)

1/32" Compressed Asbestos (anchor packing)

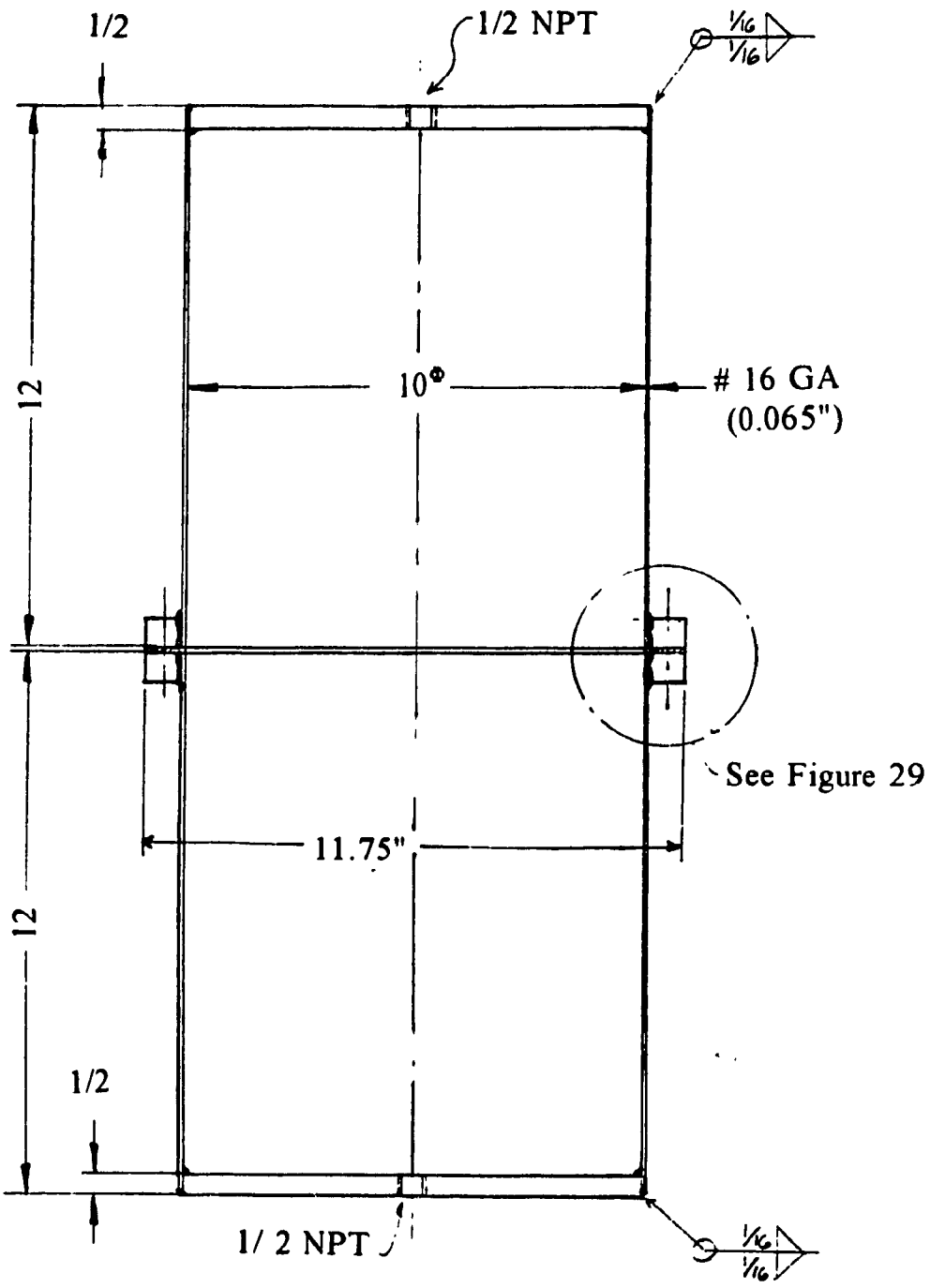

Scale: 3" - 1'-0"

Figure 27: Test Pressure Vessel "A", K = 1.175

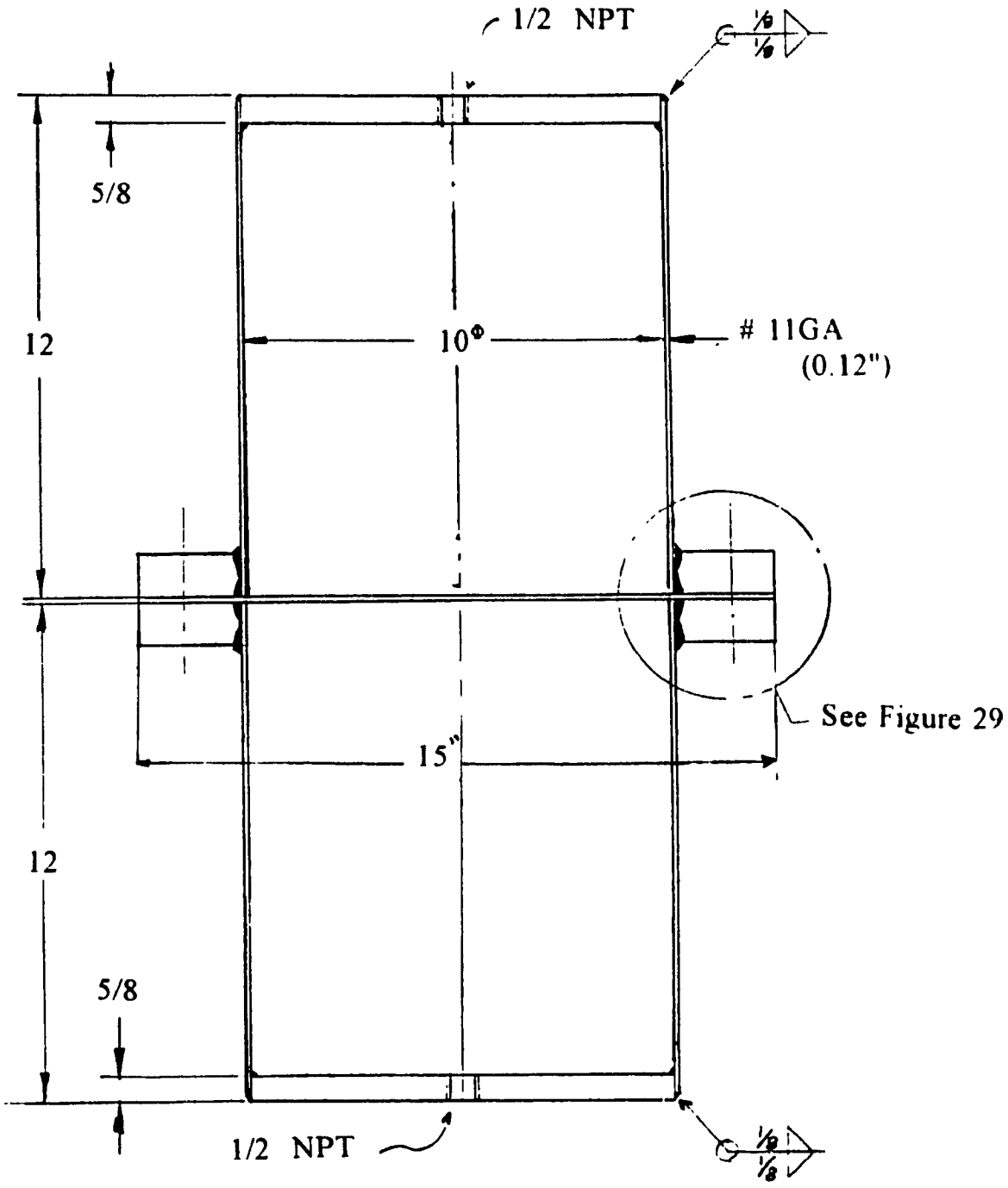

Scale: 3" - 1'-0"

Figure 28: Test Pressure Vessel "B", K = 1.5

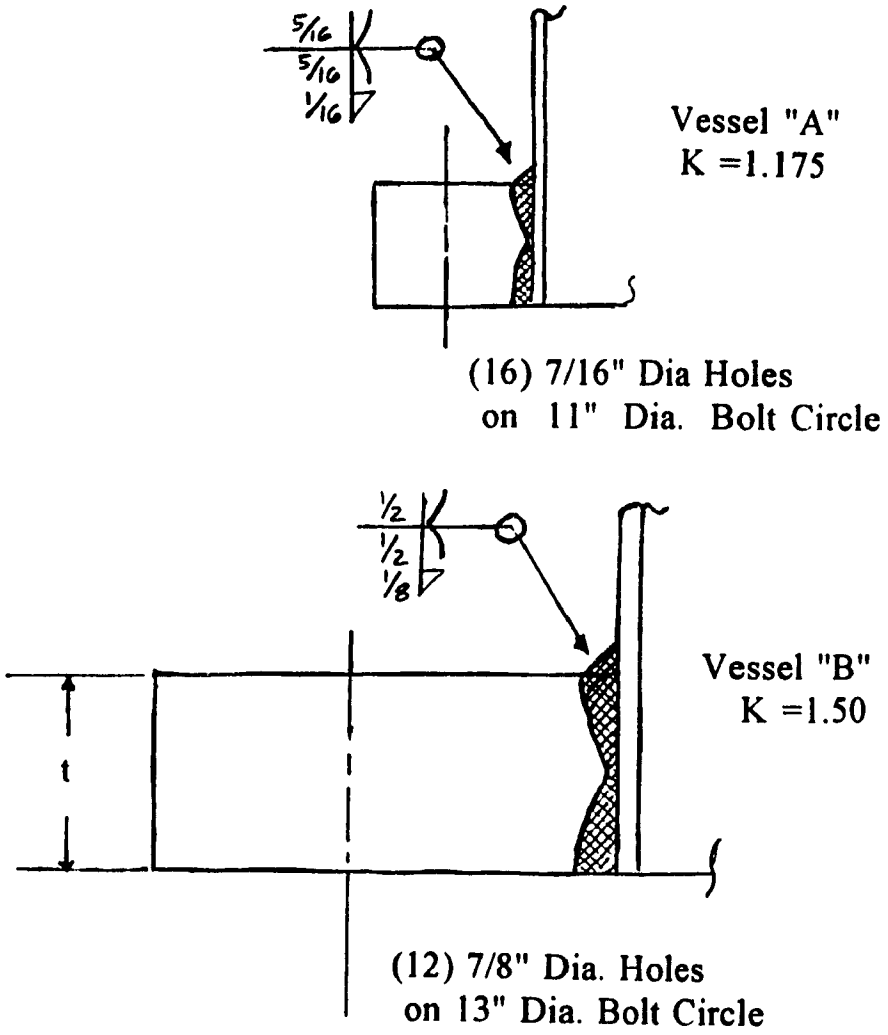

Figure 29: Test Pressure Vessel Flanges

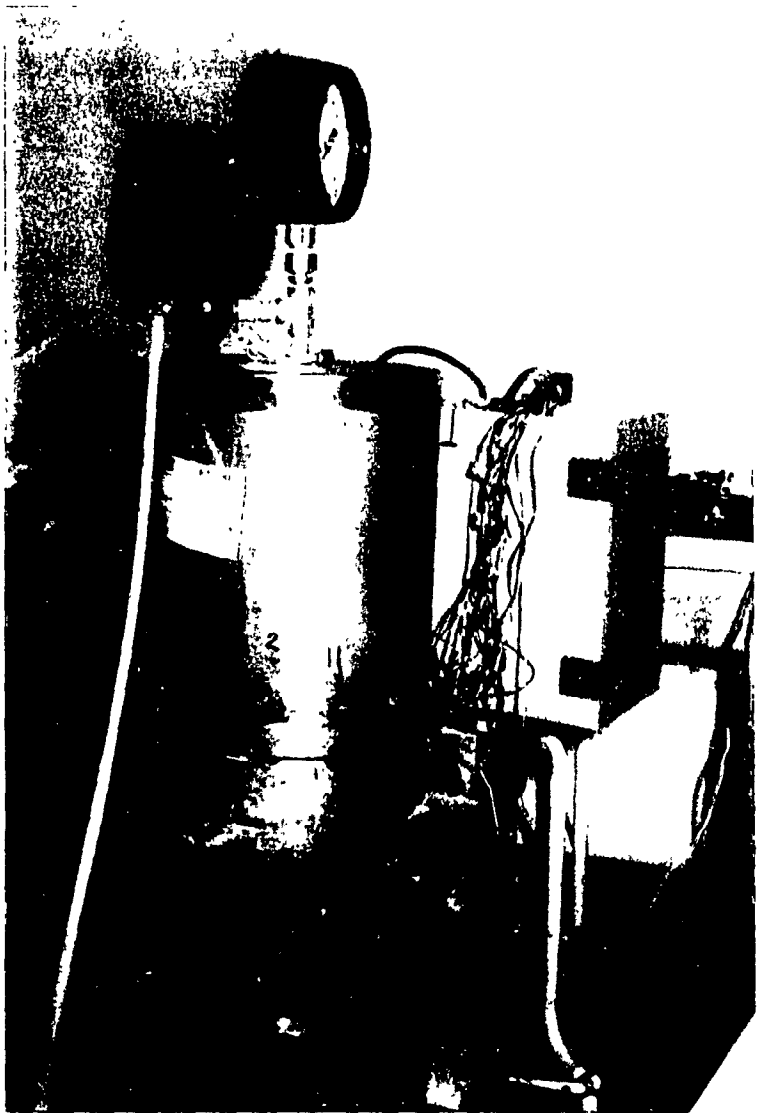

Figure 30: Photo of Test Vessel "A"

Figure 31: Photo of Test Vessel "B"

6.3 Data Measuring Equipment

The following instruments were used during the experiment:

1- Two Pressure Dial Gages up to 600 psi reading. One installed at the top of the vessel, the other at the discharge nozzle of the pump.

2- Computer: 486, 33 MHz Dx, IBM compatible, loaded with a data acquisition software from "MatLab".

3- Data acquisition instrument digital/ analog: Fluke, John Fluke MFG. Co.

The Fluke machine has 32 digital and analog input / output channels. The digital board receives electrical signals or voltage from the gages and converts conditioned signals into a digital machine format that is readable by the PC. A schematic diagram [38] is shown bellow, Figure 32.

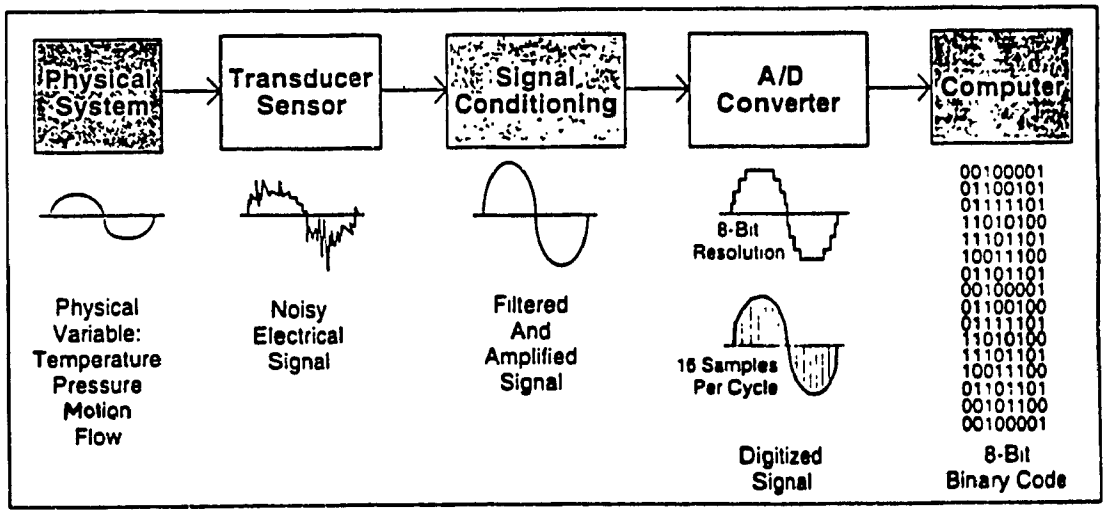

Figure 32 : Data Acquisition System

6.4 Strain Gages

Gage type selection depends on many factors, and the quality of the selection may effect the precision of the results considerably [37]. Thus following the guidelines and recommendation given by the manufacturer (M & M) the set of strain gages used were as follows :

	Vessel A	Vessel B
Shell :	EA-09-125TM-120	EA-06-125TM-120
Flange :	EA-09-062TT-120	EA-06-125TM-120
Bolts :	CEA-06-125-UN	CEA-06-125-UW

The difference in selection depends on the size of the gage and material type of the vessel. Thus, EA-09 is selected for Stainless Steel and EA-06 is selected for Carbon Steel, and all are selected based on room temperature operation.

6.4.1 Location of Strain Gages

Six strain gages are cemented to the outer pipe walls and the back faces of flanges, on a symmetry line that crosses the bolt circle at a point half way between two bolt holes. Since the vessel is symmetrical the location of the line is not important, and the measured strains are the principal strains.

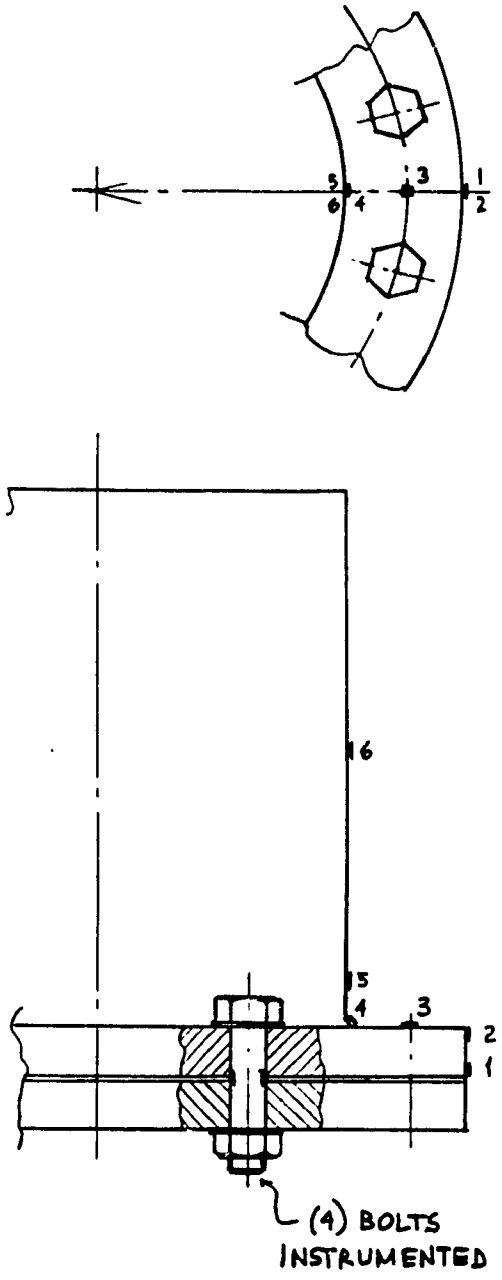

Figure 33: Pressure Vessel Strain Gage Layout

6.4.2 Instrumented Bolts

In order to insure uniform bolt loading each of the vessels was used with four bolts equipped with strain gages, on the unthreaded portion, mounted on opposite sides to average bending effects. The bolt diameters were machined down to the tensile stress area, holes drilled through the bolt head, and gages mounted with their wires passing through the drilled holes. The stress area of 3/4 inch bolts is .334 in^2, of 3/8 inch bolts it is .077 in^2. The instrumented bolts were installed at four opposite locations. A torque wrench was used to tighten the bolts to a predetermined stress, the torque level was adjusted according to the bolt strain gage readout. To reduce friction in the bolts, a spray lubricant was applied to bolts, threads, washers and nuts.

6.5 Test Procedure

A high pressure pump, capable of delivering up to 400 psi pressure, is connected through an opening at the bottom of the vessel. The vessel is mounted on a fabricated steel table 3 feet above ground level, the table is constructed so that it can hold the vessel in place during bolt-up and keep it aligned and levelled at all times. A pulley is installed directly above the centre line of the vessel, it is used to lift the top portion of the vessel,

allowing easy exchange of gaskets. After lifting the top portion of the vessel a gasket is installed and aligned with the bolt holes. The top portion is then lowered, bolts are inserted, and are tightened systematically until the required uniform torque (and stress) is reached. Strain readings are taken at 60 second intervals. Then the pump is operated and the vessel filled up while venting through an opening at the top. When the vessel is completely filled, the vent valve is closed, and pressure and strain gage readings are taken every 50 psi increments, until the flange leaks or the permissible design pressure of the vessel is reached (300 psig, including 50% over pressure for a hydrostatic test). The pump is then stopped and a discharge valve located at the bottom of the vessel is opened to drain the water. The process is repeated for all vessels with four different gasket types. Finally the vessel is dismantled and sent to the machine shop where the flange thicknesses are reduced for a new series of tests. Damaged strain gages are replaced and checked, and the whole procedure is repeated.

The following flange thicknesses were tested:

For Vessel "A": Flange thickness in inches tested are: 0.562, 0.50, 0.437, 0.375, 0.325 inch, each thickness tested with 1/16", 1/32" asbestos and rubber gaskets.

For Vessel "B": Flange thicknesses in inches tested are: 0.875, 0.75, 0.625, 0.50 inch, each thickness tested with 1/8", 1/16" asbestos and rubber gaskets.

For Vessel "C": The vessel was tested in earlier work, for flange thicknesses: 1", .75", .625", .5", with 1/8", 1/16" asbestos and rubber gaskets.

6.6 Experimental Data Results

Results from experiments are plotted in graphical form for the two vessels tested recently, "A" and" B". Data for vessel "C" are tabulated in [29]. Plots of experimental data results for K=1.175 and K=1.5 relate pressure, thickness and stress for the different gasket materials, The maximum tangential (hoop) stresses are shown in Figures 34 through 37, in the following order:

Vessel A (K=1.175):

1/32" and 1/16" Rubber Gasket.

1/32" and 1/16" Asbestos Gasket.

Vessel B (K=1.5):

1/16" and 1/8" Rubber Gasket.

1/16" and 1/8" Asbestos Gasket.

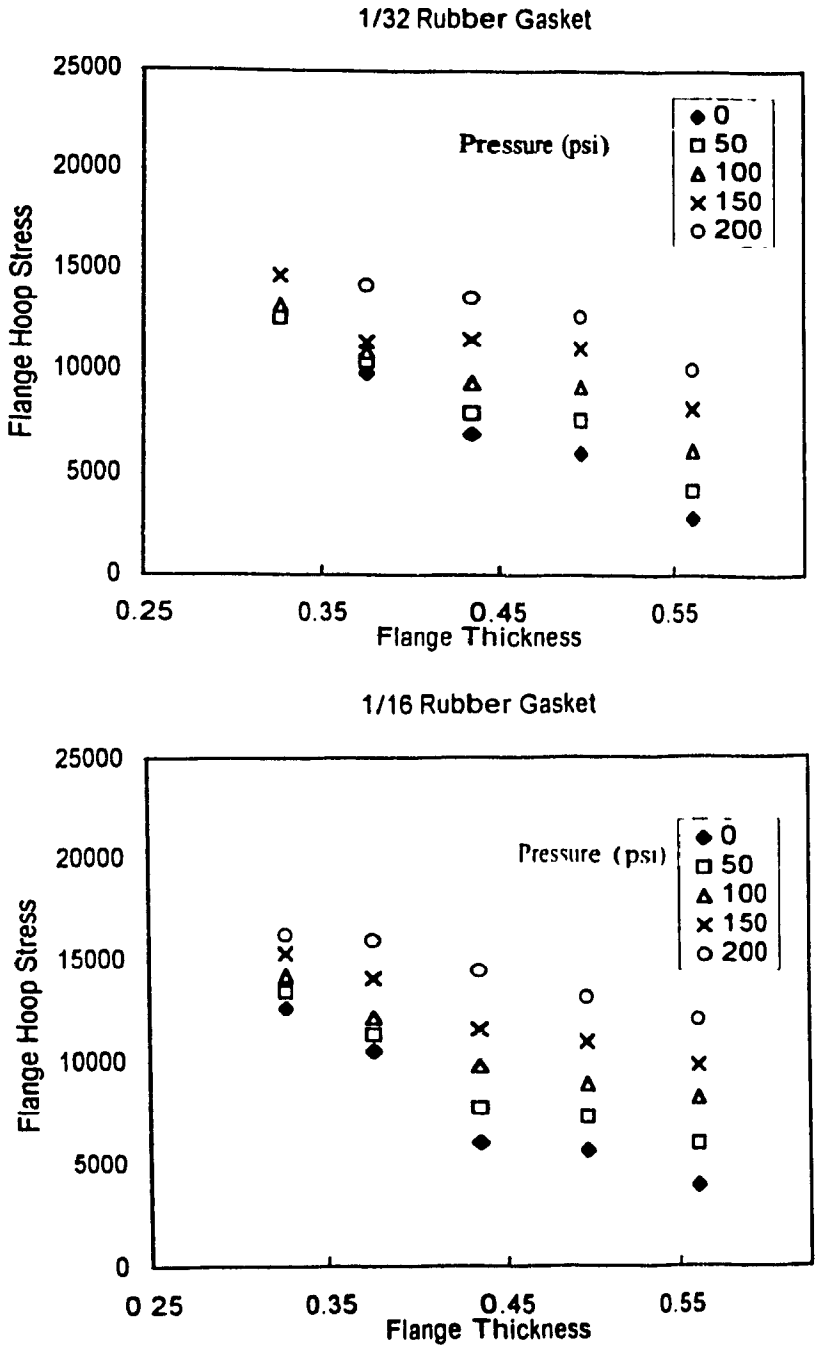

Figure 34: Experimental Stresss Data, Rubber Gasket For Vessel "A" (K=1.175)

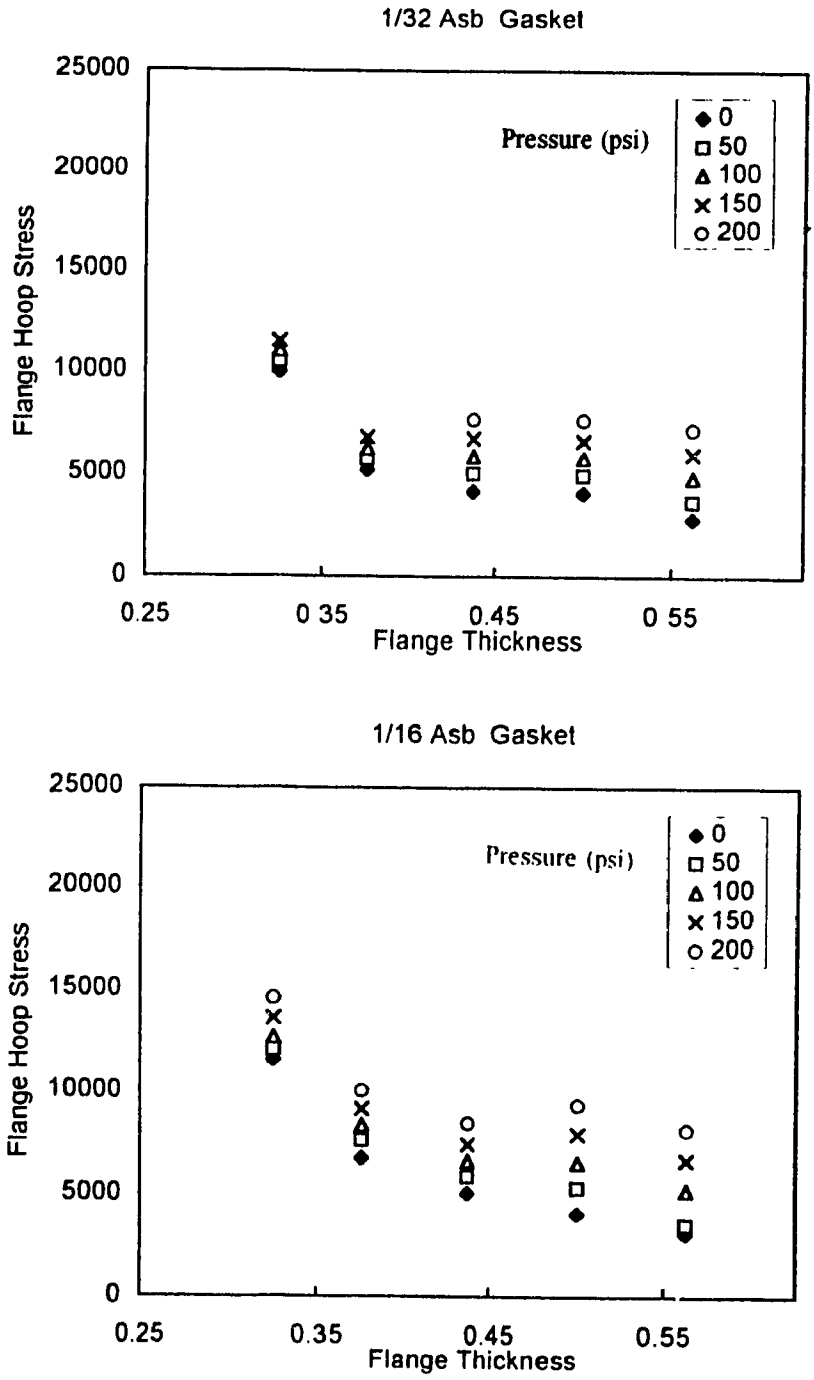

Figure 35: Experimental Stress Data, Asbestos Gasket For Vessel "A" (K=1.175)

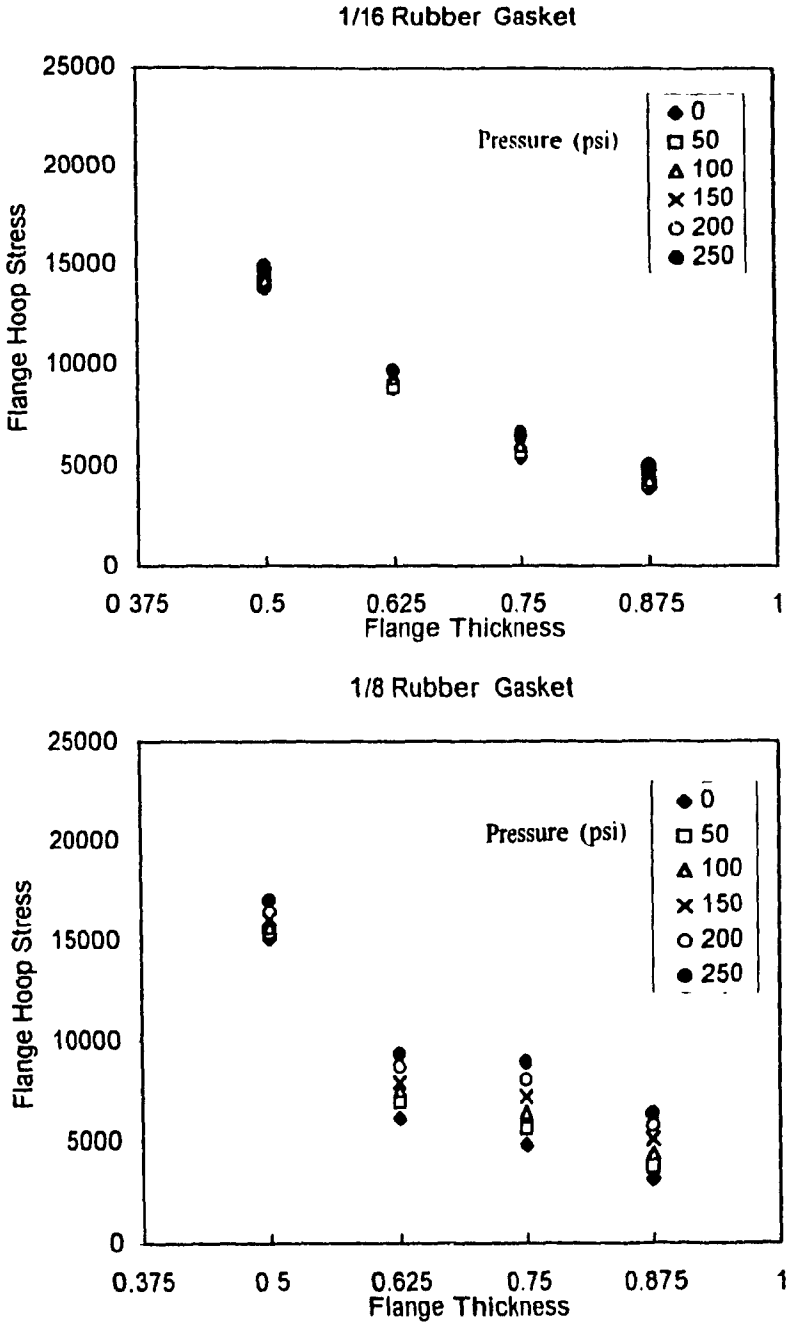

Figure 36: Experimental Stress Data, Rubber Gasket For Vessel "B" (K=1.50)

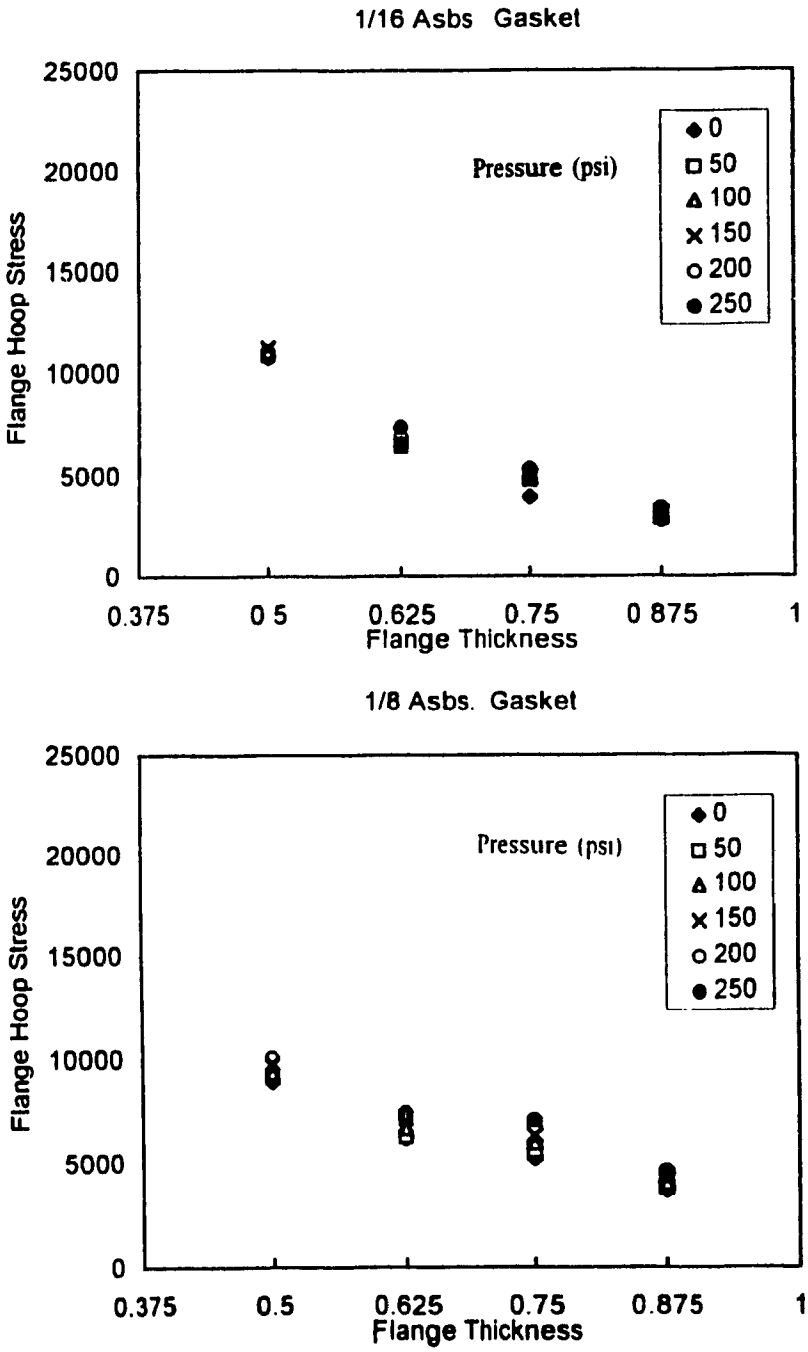

Figure 37: Experimental Stresss Data, Asbestos Gasket For Vessel "B" (K=1.5)

6.7 Concluding Remarks on Experimental Data

Measured data provide important clues to the behaviour of the flanged structure. The following conclusions are made.

6.7.1 Maximum Stresses

The maximum flange stress is observed to be the tangential stress located in most cases at gage number "3" (see Figure 33), which is halfway through the flange width. The radial flange stress is compressive and insignificant. In rubber gaskets (softer), stresses are higher and the location of the maximum tangential stress tends to move closer to the shell flange junction. In the shell the hoop stress is observed to dominate, with a maximum located at gage number "5". Stresses in the operating condition are higher than stresses during bolt-up and gasket seating for both, flange and hub. The operating pressure has more influence on stresses in flanges having small "K" values. For vessels "B" and "C" (K=1.5, 1.417) increases in pressure do not significantly affect the maximum tangential stress in the flange. For vessel "A"(K = 1.175), for the same pressure increases a greater influence on the tangential stress was observed.

6.8 SUMMARY

Strain gages were mounted on two pressure vessels which were tested, using a number of flange thicknesses, gasket types and varying pressures. From results of strain gage measurements, stresses were calculated and a stress profile was obtained. Based on these values, conclusions can be made about the behaviour of the flanged structure. In the next chapter the experimental data will be compared with results of analytical and finite element calculations.

CHAPTER SEVEN

PROPOSED NEW METHOD OF DESIGN

7.1 Introduction

The chapter starts by comparing the analytical, numerical and experimental results. It then leads to a simple method of design that is based on the numerical analysis described earlier. The favourable parabolic force profile is used to account for the gasket reaction force. Finally a numerical example is given based on the new developed method of design.

7.2 Comparison Between Results

Results from analytical solution, finite element and experimental data are compared for maximum tangential flange and hub stresses, in operating conditions. Calculated stresses from an analytical solution are based on plate theory using the parabolic force profile for the gasket reaction. Data is compared for the three pressure vessels A, B, C, using the maximum stresses obtained with rubber gaskets. The calculated stress values, compared with finite element and experimental values, are given in Figures 38, 39, 40, for K=1.175, 1.416, 1.5, respectively.

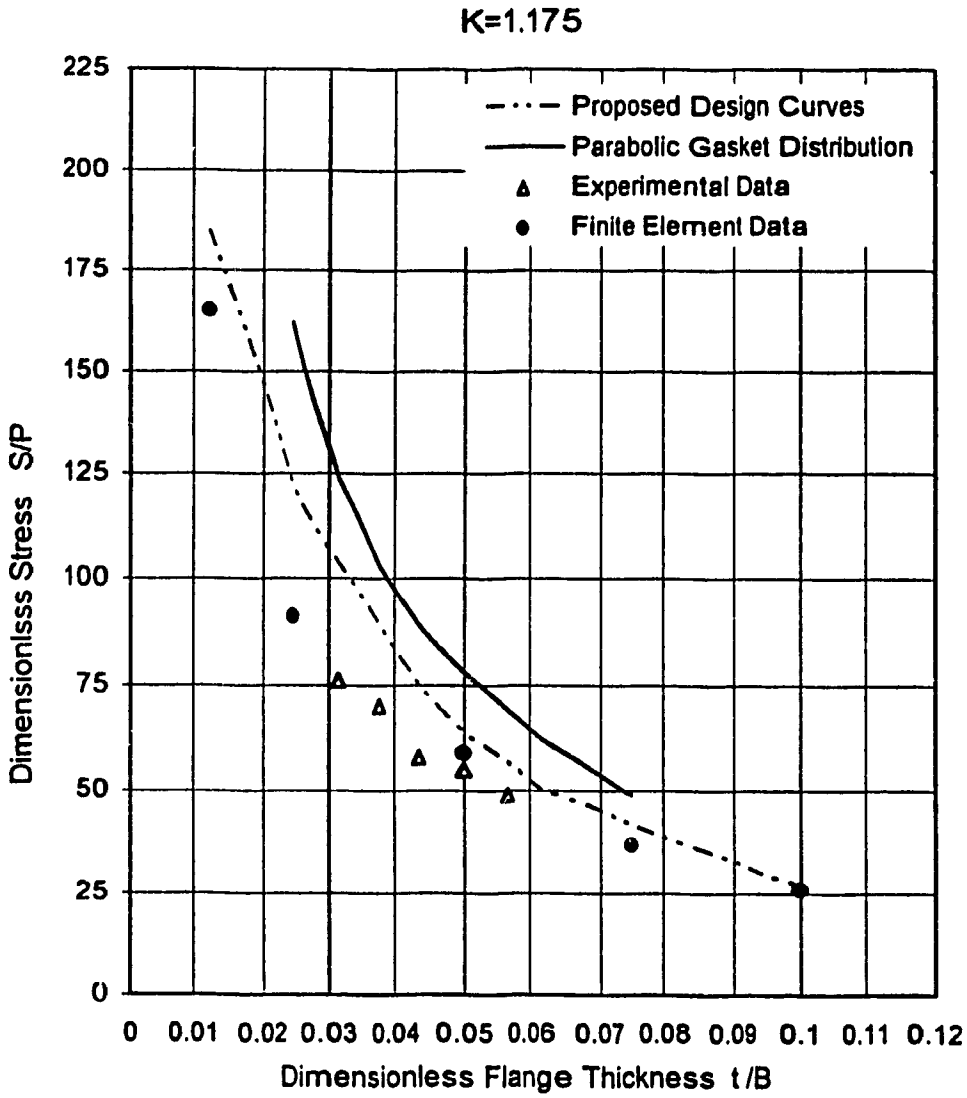

Figure 38: Stress Values For K = 1.175

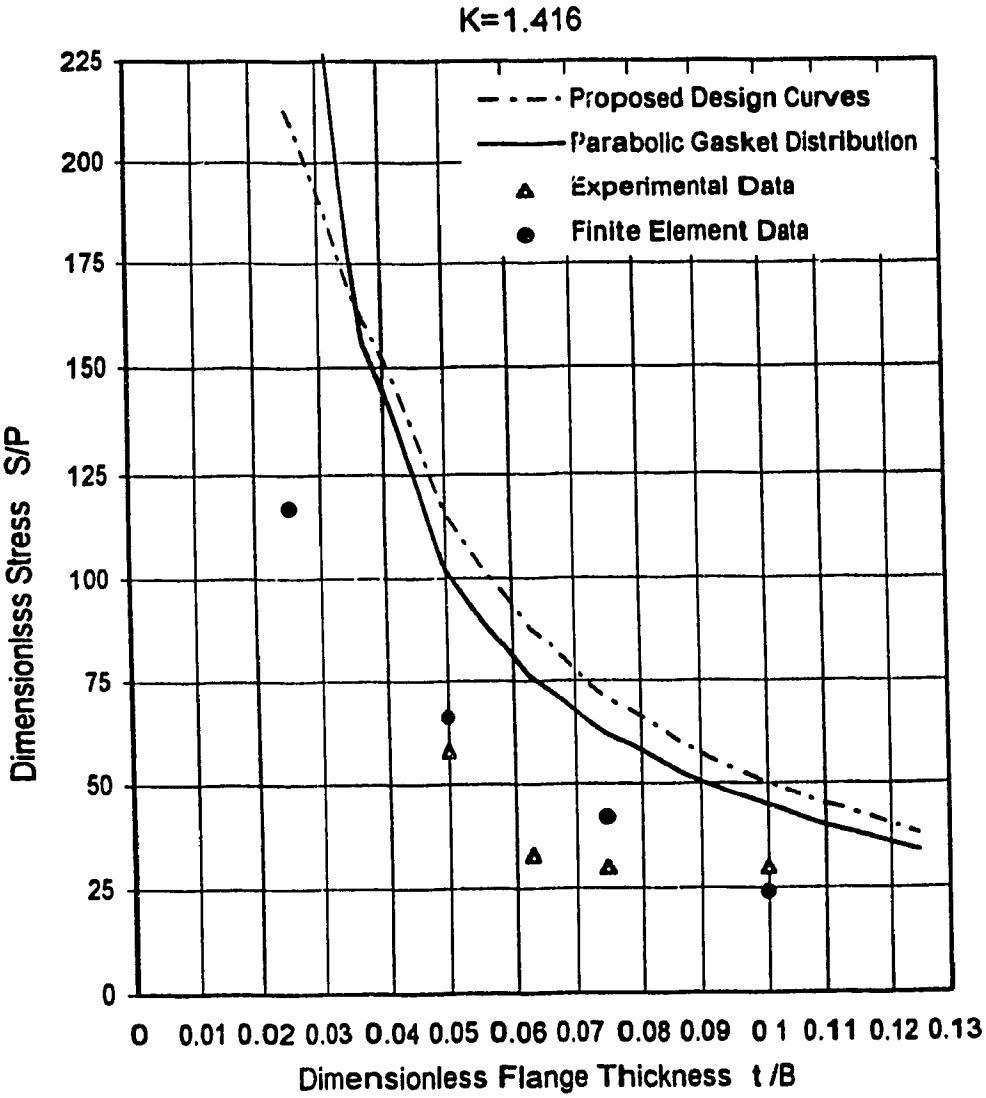

Figure 39: Stress Values For K = 1.416

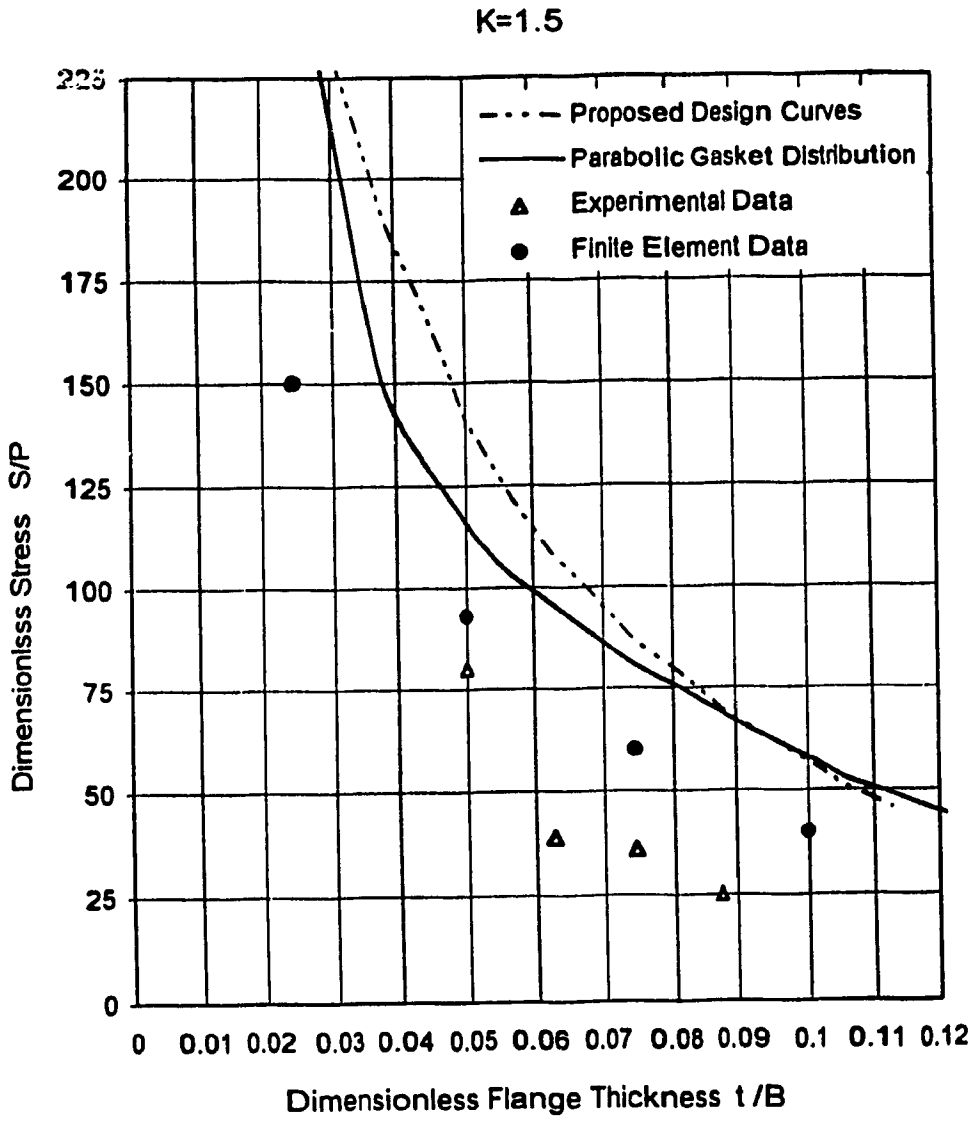

Figure 40: Stress Values For K = 1.50

From the above plotted data it can be seen that the analytical method is the safest. The finite element results follow the analytical method closely for thick flanges, they tend to deviate more as the flange thickness is decreased. This deviation is attributed to the effects of the shell, because the stresses calculated in the analytical method are based on a loose type flange where the contribution of the connecting shell is neglected. Finite element results have little difference when compared with experimental ones. It is thus concluded that the analytical method used with a parabolic gasket force distribution can safely be applied to the design of bolted flat faced flanges with full faced gaskets.

7.3 The New Design Method

Design of bolted flanges can be tedious and time consuming, often engineers tend to shy away from such work. Blach and Naser [30] devised a design procedure for flat faced flanges with full faced gasket that is simple and practical to apply for any engineer.

7.3.1 **Basis for the New Design**

The new design procedure is based on results of analytical and finite element analyses discussed earlier. Stresses calculated in the analytical method rest on the assumption that follows "loose optional" flange design rules, described in the ASME Code [27], which means that the effects of the shell are neglected and both flange radial stresses and hub longitudinal stresses are small and can be assumed to be zero. Finite element results in Article 5.9.3 reinforced this assumption for t/g ratios grater than 3, usually valid for low pressure applications used with flat faced flanges.

7.3.2 **Non-Dimensional Parameters**

The following non-dimensional parameters are defined:

K : outside to inside diameter ratio of the flange

t/B : flange thickness to inside diameter ratio of the flange

P/S: operating pressure to maximum tangential stress ratio

From the above parameters values are calculated for P/S and plotted, in Figure 41, for ranges of "K" from 1.1 to 2, and for t/B from .025 to .150. When plotted on log-log graph results yield straight lines, with little deviation attributed to the bolt loading.

7.3.3 **Design Procedure**

Design steps are based on design conditions available, so for a given inside diameter, a flange outside diameter is assumed based on expected bolt size from the pressure in question. The non-dimensional parameters are then calculated. From Figure 41, the parameter "t/B" is obtained and from it the required thickness. For a given flange thickness subjected to a certain pressure "A/B" and t/B are calculated and "P/S" is obtained. "S" is then compared with the allowable stress. To verify the adequacy of the bolt area provided, an assumption will have to be made based on the final flange geometry. From experience, it can be safely assumed that the gasket reaction force is accounted for by using (1.5) (H_d+H_t), for the total end flange force. For gasket seating conditions, the bolt area may be calculated, as for "ring flanges" based on the ASME Code [27].

7.3.4 **Verification of Design Curves**

Design curves are superimposed on analytical, finite element results and experimental data, shown earlier in Figures, 38, 39, 40, from which it can be seen that results using the proposed new method are in good agreement and on the safe side.

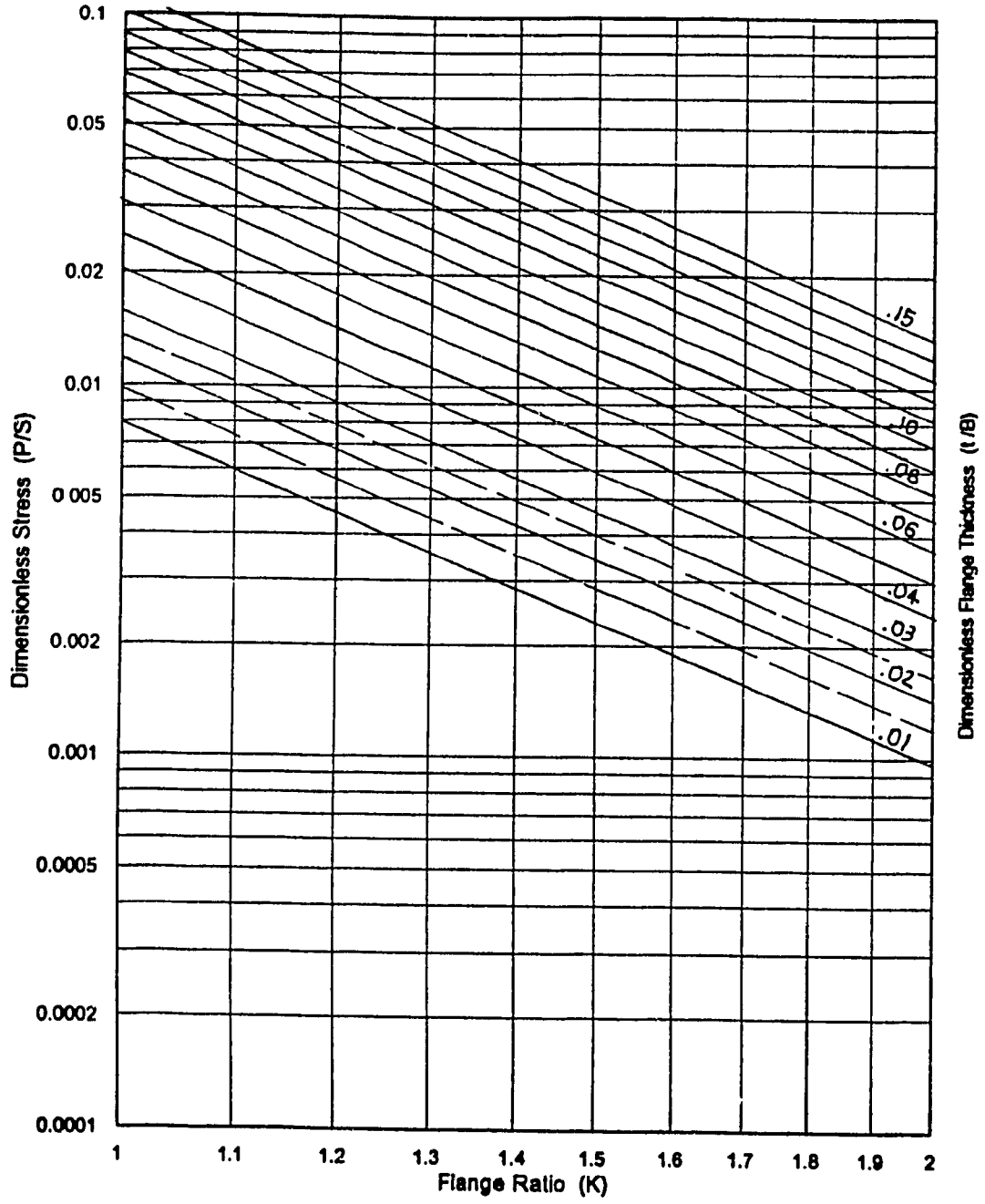

Figure 41 :Full Face gasketed flanges
Design Curves

7.3.5 NUMERICAL EXAMPLE [30]

A stainless steel pressure vessel is required with a full face flanged joint. A vessel inside diameter of 10 inches is required and, a design pressure of 200 psig and a temperature of 200° F are specified. A flange outside diameter of 11.75 inch is assumed to be used with 3/8 -16 UNC bolts. The allowable vessel stress is 18800 psi, the allowable bolt stress is 25000 psi.

Solution:

As a first step, a minimum flange thickness is obtained by calculating "K" and "P/S"; then from Figure 41, "t/B" is found which is then used to find "t".

K =A/B = 11.75/ 10.0 =1.175

P/S =200/18800 =.016

t = (0.035) (10) = 0.35 in

The minimum thickness is rounded off to 0.375 in and the stress is recalculated using Figure 41,

t/B = 0.375/10.0 = .0375

P/S= 0.011 [from Figure 41]

S =200 / .011 =18180 psi

This value compares well with experimentally calculated ones.

To check for bolt adequacy, the assumption given in Article 7.3.3 is applied. For a safe operating bolt load $W_{m1}= 1.5\ (H_d+H_t)$, may be used, [30].

7.4 Summary

The results of the analytical analysis are compared with both finite element and experimental data. It is concluded that they correlate well and that the analytical analysis is on the safe side. Thus a new design method is derived, which permits a simple analysis of full face gasketed bolted flanged connections. The method proposed determines only the maximum tangential stresses in the flange, in accordance with an "Optional Loose" classification of the ASME Code [27], Appendix 2-4(a)(3).

CHAPTER EIGHT

CONCLUSIONS

8.1 Concluding Remarks

The design method for full face gasketed bolted flanged connections presented in this thesis is based on analytical, numerical and experimental results. It includes a modified method of design that takes into account the possibility of bending of the flange face.

A new design procedure based on the modified design method was proposed. The procedure is a function of non-dimensional parameters and can easily be applied to other methods of solution. Due to the complexity of the problem, certain simplifying assumptions have been made to arrive at manageable equations. The effects of the assumptions on the confidence level of the method were shown to be within acceptable limits on the safe side. The method of design has shown good agreement with experimental and numerical analyses.

8.2 Recommendations For Future Work

The modified method presented thus far has shown much improvement when compared with the original work. The behaviour of flat face flanges with full face gaskets is a function of the gasket reaction force, and unless more information is obtained about it, the design will be incomplete. It is thus recommended that more experimental work be done for other flange geometries and also for the determination of more viable gasket properties.

REFERENCES

[1] Bach, C. "Deflections and Stresses of Circular, Square and Rectangular Plates", Springer Verlag, Berlin, Germany, 1891, 104 pages.

[2] Anonymous: "The Flanged Mouth-Piece Rings of Vulcanizers and Similar Vessels", The Locomotive, v 25, n 7, Jul 1905, pp 177-203.

[3] Crocker, S.: " The Crocker - Stanford Method " , Mech. Eng. v 49, n 12, Dec 1927, pp 1340 - 1342.

[4] Waters, E.O. & Taylor, J.H.: " The Strength of Pipe Flanges" Mech. Eng. v 49, n 5a, May 1927, pp 531 - 542.

[5] ASME Boiler Code Revisions: "Proposed Rules for Bolted Flanged Connections", Mech. Eng., v 56, n 5, May 1934, pp 309 - 313.

[6] Timoshenko, S.: "Flat Ring and Hubbed Flanges", Mech. Eng. v 49, n 12, Dec 1927, pp 1343 -1345.

[7] Wahl, A.M. & Lobo, G.: "Stresses and Deflections in Flat Circular Plates with Central Holes", ASME - Trans, Ser j, Appl. Mech., v 52, n 4, Apr 1930, pp 29 - 43.

[8] Holmberg, E.O. & Axelson, K.: "Analysis of Stresses in Circular Plates and Rings", ASME - Tran. Ser j, Appl. Mech., v 54, n 2, Jan 1932, pp 13 - 23.

[9] Water, E.O. -Wesstorm, D.B. -Rossheim, D.B. -Williams, F.S.G. "Formulas for Stresses in Bolted Flanged Connections", ASME -Trans, v 59, 1937, pp 161 - 169; Discussion: v 60, Apr 1938, pp 267 - 278.

[10] Water, E.O. -Wesstorm, D.B. -Rossheim, D.B. -Williams, F.S.G. "Development of General Formulas for Bolted Flanges", Taylor Forge & Pipe Works, Chicago, 1937.

[11] Rossheim, D.B. & Markl, A.R.C.: "Gasket Loading Constants", Mech. Eng., v 65 n 9, Sep 1943, pp647 - 648, Discussion Jan 1944,pp72 -73.

[12] Schwaigerer, S. Kobitzsch, R.: " Design Calculations For Gaskets and Flanges" -(translated), Technik, v 2, n 10 -11, Oct. 1947, pp 425 - 430, Nov 1947, pp 489 - 493.

[13] Wesstcrm, D.B. & Bergh, S.E .: "Effects of Internal Pressure on Stresses and Straines in Bolted Flanged Connections", ASME -Trans, v 73, n 5, Jul 1951, pp553 -568.

[14] Kraus, H. "Flexure of Circular Plate with a Ring of Holes", ASME Trans, Ser E, v 84, n 3, Sep 1962 , pp489 - 496.

[15] Kraus, H. - Rotondo, P. Haddon, W.D.: "Analysis of Radially Deformed Perforated Flanges", ASME - Trans, Ser B, vol 88, n 2, May 1966, pp 172 - 178.

[16] Lake, G.F. & Boyd, G.: "Design of Bolted Flanged Joints of Pressure Vessels", Inst'n Mech. Eng. Proc. v 171, 1957, pp 843 - 872.

[17] Schwaigerer, S. & Romer, F.: " Investigation on a Welded Hub Flange"- (translated), VGB-Mitteilungen, 1951, pp338 - 343.

[18] Siebel, E. & Schwaigerer, S. " Design Calculations for Flanges in High - Temperature Steam Piping", VGB-Merkblatter, n 4, 1951.

[19] Schwaigerer, S.: "Design Calculations for Flanged Joints for Pressure Vessels and Piping" -(translated), VDI-Z, v96, n 1, Jan 1954, pp7 - 12.

[20] Schwaigerer, S.: " Stress Calculations of Components used in Steam Boilers, Pressure Vessels and Piping" (translated), Springer Verlag, Berlin-Göttingen-Heidelberg, 1961.

[21] Schneider, R. W.: " Flat Face Flanges with Metal to Metal Contact Beyond the Bolt Circle" , ASME-Trans, Ser A, v 90, n 1, Jan 1968, pp 82- 88.

[22] Waters, E.O.: "Flat Face Flanges with Metal to Metal Contact Beyond the Bolt Circle", ASME-Trans, Ser A, v 90, n , Jan 1968, pp 82 - 88.

[23] Schneider, R. W. & Waters, E.O.: "ASME Code Case 1828 A simplified Method of Analyzing Part B Flanges", ASME-Trans, ser j, v 100, n 2, May 1978, pp 215-219.

[24] Anonymous: "Design of Flanges for Full Face Gaskets", Taylor Forge Inc.- Eng. Dept. Bulletin No. 45, Chicago, 1951.

[25] Blach A.E. & Bazergui & Baldur : " Bolted Flanged Connections with Full Faced Gaskets ", WRC Bulletin, No. 314, May 1986, pp 1 - 13.

[26] Blach A.E.: " Bolted Flange Connections for Non-Circular Pressure Vessels, Proceedings of the 6th International Conference on Pressure Vessel Technology, Beijing, China, Sept 1988, pp 267 - 280.

[27] "ASME Boiler and Pressure Vessel Code, Section VIII, Division 1, Pressure Vessels", The American Society of Mechanical Engineers, New York, 1992 Edition.

[28] Blick, R. G.: "Bending Moments and Leakage at Flanged Joints", Pet. Ref., v 29, n 2-6; Feb 1950, pp 101- 103; May 1950, pp 119 - 122; Jun 1950, pp 129 - 133.

[29] Blach A.E.: "Bolted Flanged Connections with Full Face Gaskets", Thesis for the Degree of Doctoral of Philosophy, University of Montreal, Montreal, Canada, Feb 1983.

[30] Blach A.E. & Naser K.: "Bolted Flanged Connection with Full Face Gasket-An Improved Design Method", ASME Pressure Vessel and Piping Conference, Hawaii, U.S.A, to be held in July 1995.

[31] Timoshenko S. & Woinowsky-Krieger : " Theory of Plates and Shells" McGraw-Hill, U.S.A, 1987, pp 51- 67 ; pp 466 - 485.

[32] J Roark & W. Young : " Formulas for Stress and Strain" Fifth Edition, McGraw-Hill, U.S.A., 1975, pp 324- 340.

[33] Timoshenko, S.: " Strength of Material, Part II", Van Nostrand, Princeton, N.J., 1930, pp 138 - 144.

[34] Cook, R. & Malkus D. & Plesha M.: "Concepts and Applications of Finite Element Analysis" , Third Edition, John Wiley & Sons Inc., Canada, 1989, pp 109 - 130 ; pp 293 - 298 ; pp 340- 358.

[35] Desalvo, G. J. & R.W. Gorman: " ANSYS Engineering Analysis System User's Manual", Swanson Analysis Systems Inc., Houston, U.S.A, 1990.

[36] Zahavi, E: "A Finite Element Analysis of Flange Connections", Journal of Pressure Vessel Technology, Aug 1993, vol 115, pp 327- 330.

[37] Budyans, R.: "Advanced Strength and Applied Stress Analysis", MaGraw-Hill Inc., 1977, U.S.A., pp 349- 411; Experimental Analysis.

[38] Cyber Reasearch Institute Inc., : " Data Acquisition", Volume one , CT, U.S.A, Publication , 1994.

Appendix A

DIMENSIONLESS COEFFICIENTS

Coefficients for Complete Solution using a Parabolic Gasket Force:

$$C1 = \frac{1 - \nu^2}{g^3 \cdot \beta^3}$$

$$C2 = \frac{B \cdot \gamma}{2 \cdot t} + 6 \cdot C1$$

$$C3 = \frac{Y \cdot B \cdot \pi}{6 \cdot \beta^2 \cdot t^3} + 2 \cdot C1$$

$$C4 = \frac{Y \cdot B \cdot \pi}{12 \cdot \beta \cdot t^2} - C1$$

$$C5 = \frac{Y}{6 \cdot \beta^3 \cdot t^3}$$

$$C6 = \frac{\beta \cdot B \cdot \gamma}{2} - \frac{(2 - \nu) \cdot \beta \cdot B^2}{8 \cdot g}$$

$$C7 = \frac{C2 \cdot C5}{6 \cdot C1 \cdot C4 + C2 \cdot C3}$$

$$C8 = \frac{C4 \cdot C6}{6 \cdot C1 \cdot C4 + C2 \cdot C3}$$

$$C9 = \frac{6 \cdot C1 \cdot C5}{C1 \cdot C4 \cdot 6 + C2 \cdot C3}$$

$$C10 = \frac{C3 \cdot C6}{6 \cdot C1 \cdot C4 + C2 \cdot C3}$$

$$C11 = \frac{1}{\beta \cdot B \cdot \pi} - C7 - \beta \cdot \frac{t}{2} \cdot C9$$

$$C12 = C8 - \beta \cdot t \cdot \frac{C10}{2}$$

$$C13 = \Gamma \cdot C11 + \frac{12}{3 + 5 \cdot K} \cdot E \cdot t^3 \cdot \frac{tg}{B \cdot G \cdot \pi^2 \cdot Y \cdot Eg \cdot b^2 \cdot hg \cdot \beta}$$

$$C14 = \frac{C11}{C13}$$

$$C15 = \frac{C12}{C13}$$

For a triangular gasket reaction force only C13 is adjusted to,

$$C13(t) = \Gamma \cdot C11(t) + \frac{3}{1 + 2 \cdot K} \cdot E \cdot t^3 \cdot \frac{tg}{B \cdot G \cdot \pi^2 \cdot Y \cdot Eg \cdot b^2 \cdot hg \cdot \beta}$$

Coeficients from simplifying assumptions given in Articles 4.5 & 4.51 are:

$$K1 = 1 + \beta \cdot \frac{t}{2}$$

$$K2 = 6 \cdot \frac{1 - \nu^2}{B \cdot \pi \cdot \beta \cdot Y} \cdot \left(\frac{t}{g}\right)^3$$

$$K3 = \frac{\alpha}{\pi \cdot Y \cdot hg} \cdot \frac{t^3}{b^2}$$

$$K4 = \left[\Gamma + K3 \cdot \left[(1) + \frac{K1}{K2} \right] \right]^{-1}$$

$$K5 = (1 + \beta \cdot t) \cdot K4 \cdot \beta^2 \cdot B^2 \cdot \left(\frac{\pi}{24} \right)$$

$$L1 = 1 + \beta \cdot \frac{t}{2}$$

$$L2 = 6 \cdot \frac{1 - \nu^2}{B \cdot \pi \cdot \beta \cdot Y} \cdot \left(\frac{t}{g} \right)^3$$

$$L3 = 8 \cdot \frac{\alpha}{\pi \cdot Y} \cdot \left(\frac{t}{b} \right)^3$$

$$L4 := \left[\Gamma + L3(t) \cdot \left[(1) + \frac{L1}{L2} \right] \right]^{1}$$

where,

$$\beta = \left(12 \cdot \frac{1 - \nu^2}{B^2 \cdot g^2} \right)^{.25} \quad \text{and} \quad \Gamma \quad 1 \quad \frac{hgs}{hg}$$

$$\alpha = \frac{12}{3 + 5 \cdot K} \cdot E \cdot \frac{tg}{Eg \cdot G}$$ For parabolic distribution

$$\alpha = \frac{3}{1 + 2 \cdot K} \cdot E \cdot \frac{tg}{Eg \cdot G}$$ For triangular distribution

APPENDIX B

STIFFNESS EQUATIONS OF FINITE ELEMENT

Stiffness matrix for plane axisymmetric elements;

Displacement Function:

$$a_i \quad \begin{pmatrix} u_i \\ v_i \end{pmatrix} \qquad a^e = \begin{bmatrix} a_i \\ a_j \\ a_l \\ a_k \end{bmatrix}$$

$$u \quad \begin{pmatrix} u \\ v \end{pmatrix} = \begin{bmatrix} IN_i & IN_j & IN_l & IN_k \end{bmatrix} \cdot a^e$$

with $$N_i = \frac{a_i + bi \cdot r + c_i \cdot z}{2 \cdot \Delta}$$,etc.

$$a_i = r_j \cdot z_m - r_m \cdot z_j$$

$$b_i = (z..i) - z_m = z_{jm}$$

$$c_i = r_m - r_j = r_{mj}$$

Where Δ is the area of the element.

N_i: The shape Function

a^e: Is the element displacement victor

Strains are:

$$\varepsilon = \begin{bmatrix} \varepsilon_z \\ \varepsilon_r \\ \varepsilon_\theta \\ \gamma_{rz} \end{bmatrix} \quad \begin{bmatrix} \frac{\delta v}{\delta z} \\ \frac{\delta u}{\delta r} \\ \frac{u}{r} \\ \frac{\delta u}{\delta z} + \frac{\delta v}{\delta r} \end{bmatrix}$$

$$\varepsilon \quad B \cdot a^e \qquad B_i \;\; B_j \;\; B_l \;\; B_k$$

$$B_i = \begin{bmatrix} 0 & \frac{\delta N_i}{\delta z} \\ \frac{\delta N_i}{\delta r} & 0 \\ \frac{1}{r} \cdot N_i & 0 \\ \frac{\delta N_i}{\delta z} & \frac{\delta N_i}{\delta r} \end{bmatrix}$$

Elasticity matrix, for an isotropic material;

$$\frac{G_2}{E_2} = \frac{G}{E} = m = \frac{1}{1\cdot(1+v)}$$

$$E = \frac{E(1-v)}{(1+v)\cdot(1-2\cdot v)}\cdot\begin{bmatrix} 1 & \frac{v}{1-v} & \frac{v}{1-v} & 0 \\ & 1 & \frac{v}{1-v} & 0 \\ & & 1 & 0 \\ & & & \frac{2-2\cdot v}{2\cdot(1-v)} \end{bmatrix}$$

From which the stiffness matrix is given by

$$\left(K^e\right)_{ij} = 2\cdot\pi\cdot\int B_i\cdot E\cdot B_j\cdot r\cdot dr\,dz$$

where, (r.dr.dz) is the volume